Stony Brook University

Class III phosphoinositide 3-kinase Vps34 in autophagy, endocytosis, and nutrient-induced signaling

A Dissertation Presented

by

Nadia Lane Jaber

to

The Graduate School

in Partial Fulfillment of the

Requirements

for the Degree of

Doctor of Philosophy

in

Molecular and Cellular Biology

(Immunology and Pathology)

Stony Brook University

August 2015

Stony Brook University

The Graduate School

Nadia Lane Jaber

We, the dissertation committee for the above candidate for the

Doctor of Philosophy degree, hereby recommend

acceptance of this dissertation.

Wei-Xing Zong – Dissertation Advisor
Professor, Department of Molecular Genetics and Microbiology

Deborah A. Brown - Chairperson of Defense
Professor, Department of Biochemistry and Cell Biology

Richard Lin
Professor, Department of Physiology and Biophysics

Kevin Czaplinski
Assistant Professor, Department of Biochemistry and Cell Biology

Zhenyu Yue
Professor, Department of Neurology and Neuroscience
Icahn School of Medicine at Mount Sinai, New York

This dissertation is accepted by the Graduate School

Charles Taber
Dean of the Graduate School

Abstract of the Dissertation

Class III phosphoinositide 3-kinase Vps34 in autophagy,

endocytosis, and nutrient-induced signaling

by

Nadia Lane Jaber

Doctor of Philosophy

in

Molecular and Cellular Biology

(Immunology and Pathology)

Stony Brook University

2015

Vps34 is the sole member of the Class III phosphoinositide 3-kinases (PI3Ks) identified in mammals thus far. It phosphorylates phosphatidylinositol (PI) to generate PI(3)P on intracellular membranes. Previous work has suggested that Vps34 is important for the protein degradation pathways of autophagy and endocytosis, as well as nutrient-induced mTOR signaling. However, due to the pluripotent nature of available PI3K inhibitors, a clear understanding of the functions of mammalian Vps34 remains to be illustrated. To investigate the precise role of Vps34 in these processes, I have generated and characterized mice with conditional genetic ablation of Vps34. Mice with liver or heart-specific deletion of Vps34 suffer from organ enlargement, excess lipid accumulation and organ dysfunction. Mice and embryonic fibroblasts (MEFs) lacking Vps34 are completely deficient in autophagy and instead accumulate intracellular aggregates. Vps34-deficient MEFs display a growth defect and dramatically reduced amino acid-induced mTOR signaling. In addition, while it is widely believed that Vps34 controls the early stages of endocytosis, I find that early endosome functions such as transferrin recycling and EEA1 recruitment are not affected by Vps34 knockout. This is attributed to a compensatory increase of Rab5-GTP which is sufficient to support these early endosome functions. Furthermore, I find that Vps34 is essential for late endocytic functions like cargo degradation and endosome morphology. Interestingly, the deletion of Vps34 leads to a dramatic increase in Rab7-GTP levels. In the absence of Vps34, the Rab7 GTPase activating protein Armus, which limits Rab7 activity, loses its correct intracellular localization. Increased Rab7-GTP levels in Vps34 knockout cells translate to increased effector RILP recruitment, which may enhance v-ATPase activity and cause intracellular vacuolization as well as failure of endosome-lysosome fusion. These results solidify our understanding of the role of mammalian Vps34 in autophagy and uncover a previously unappreciated role for Vps34 in maintaining late endosome functions via the regulation of Rab7.

Dedication Page

This thesis is dedicated to my grandfather, Ghareb Jaber, who truly valued education and hard work.

Table of Contents

List of Figures

List of Tables

List of Illustrations

List of Abbreviations

3-MA	3-methyladenine
4EBP1	Eukaryotic initiation factor 4E-binding protein 1
Baf A1	Bafilomycin A1
DFCP1	Double FYVE containing protein 1
EGF	Epidermal growth factor
EGFR	Epidermal growth factor receptor
ER	Endoplasmic reticulum
ESCRT	Endosomal sorting complex required for transport
FIP200	Focal adhesion kinase family interacting protein of 100 kD
GAP	GTPase activating protein
GEF	Guanine nucleotide exchange factor
GFP	Green fluorescent protein
GPCR	G protein coupled receptor
HOPS	Homotypic vacuole fusion and protein sorting complex
LC3	Microtubule-associated protein light chain 3
MEF	Mouse embryonic fibroblast
mTOR	Mammalian target of rapamycin
PE	Phosphatidylethanolamine
PH	Pleckstrin homology
PI3K	Phosphotinositide 3-kinase
PI	Phosphatidyltinositol
PI(3)P	Phosphatidyltinositol 3-phosphate
PX	Phox homology
RFP	Red fluorescent protein
S6K	p70 S6 kinase
SNARE	N-ethylmaleimide–sensitive factor attachment protein receptor
ULK1	Unc-51-like kinase 1
UVRAG	Ultraviolet radiation resistance-associated gene
Vps34	Vacuolar protein sorting 34
WIPI	WD-repeat protein interacting with phosphoinosides

Acknowledgments

I would like to acknowledge all of the scientists who contributed to this work: Zhixun Dou, JiAn Pan, Jennifer DeLeon, Juei-Suei Chen, Joseph Catanzaro, Namratha Sheshadri, Alex Bott, Ya-Ping Jiang, Lisa Ballou, Elzbieta Selinger, Xiaosen Ouyang, Jianhua Zhang, Noor Mohd-Naim, Jie Chen, Aimee Edinger, Vania Braga and Christopher Rocheleau.

I would also like to acknowledge my advisor Wei-Xing Zong, who guided this work, as well as the entire Zong lab, past and present, for their continuous support, entertainment and friendship: Jennifer DeLeon, JiAn Pan, Juei-Suei Chen, Alex Bott, Yu Sun, Zhixun Dou, Joseph Catanzaro, Namratha Sheshadri, Erica Ullman, Jennifer Guerriero, Yongjun Fan, and Jean Peng.

I thank my committee members for guiding this work and providing valuable feedback as well as reagents: Deborah Brown, Richard Lin, Kevin Czaplinski and Zhenyu Yue.

Finally I have to thank all of my friends and family for their encouragement while I completed this journey.

Vita

Education

Ph.D. candidate, Molecular and Cellular Biology — 2009 – 2015
Mentor: Wei-Xing Zong, Ph.D.
Stony Brook University, Stony Brook, NY

Advanced Graduate Certificate in Health Communications — 2013 - 2014
Stony Brook University, Stony Brook, NY

B.S., Biochemistry, *summa cum laude* — 2005 - 2009
Syracuse University, Syracuse, NY

Publications

Pan JA, Sun Y, Jiang YP, Jaber N, Dou Z, Yang B, Chen JS, Catanzaro JM, Ding WX, Moscat J, Ozato K, Lin RZ, and Zong WX. TRIM21 regulates redox homeostasis by ubiquitylating SQSTM1/p62. (Submitted)

Jaber N, Mohd-Naim N, DeLeon JL, Sheshadri N, Edinger AL, Braga VMM, and Zong WX. Class III PI 3-kinase Vps34 regulates Rab7 through recruitment of the GTPase activating protein Armus. (Submitted)

Naguib, A., Bencze G., Cho H., Zheng W., Tocilj A., Elkayam E., Faehnle C.R., Jaber N., Pratt C.P., Chen M., Zong W.X., Marks M.S., Joshua-Tor L., Pappin D.J., and Trotman L.C.. (2015) PTEN functions by recruitment to cytoplasmic vesicles. **Molecular cell**. 58:255-268.

Jaber N and Zong WX (2013) Class III PI3K Vps34: Its essential role in autophagy, endocytosis and heart and liver function. **Ann N Y Acad Sci**. 1280:48-51

Jaber N, Dou Z, Lin RZ, Zhang J and Zong WX. (2012) Mammalian PIK3C3/VPS34: The key to autophagic processing in liver and heart. **Autophagy**. 8(4):707-8

Jaber N, Dou Z, Chen JS, Catanzaro J, Jiang YP, Ballou LM, Selinger E, Ouyang X, Lin RZ, Zhang J and Zong WX. (2012) Class III PI3K Vps34 plays an essential role in autophagy and in heart and liver function. **Proc Natl Acad Sci USA**. 109(6):2003-8

Dufour A, Sampson NS, Li J, Kuscu C, Rizzo RC, Deleon JL, Zhi J, Jaber N, Liu E, Zucker S, and Cao J. (2011) Small-molecule anticancer compounds selectively target the hemopexin domain of matrix metalloproteinase-9. **Cancer Res**. 71(14):4977-88

Anwar K, Voloshyna I, Littlefield MJ, Carsons SE, Wirkowski PA, Jaber NL, Sohn A, Eapen S and Reiss AB. (2011) COX-2 inhibition and inhibition of cytosolic phospholipase A2 increase CD36 expression and foam cell formation in THP-1 cells. **Lipids** 46(2):131-42

Awards

NCI F31 Ruth L. Kirschstein NRSA (National Research Service Award) for Individual Predoctoral Fellows — 2013 - present

NIH T32 Training Grant, MCB Program, Stony Brook University — 2010 – 2012

Oral Presentations

"Vps34 Controls Rab7 to Regulate Endocytic Trafficking". PI 3-Kinase Signaling Pathways in Disease, Keystone Symposia, Vancouver, Canada (2015)

"Class III PI3K Vps34 Plays an Essential Role in Autophagy, Endocytosis, and Heart and Liver Function". Inositol Phospholipid Signaling in Physiology and Disease, New York Academy of Sciences, NY (2012)

1

Introduction

I. Phosphoinositide 3-kinases

i) General characteristics

Although yeast have only a single phosphoinositide 3-kinase (PI3K), *Drosophila* and mammals have evolved to encode multiple PI3Ks with differing functions. All PI3Ks phosphorylate phosphoinositides at the D-3 position of the inositol ring, but differ in their preferred phospholipid substrates. The resulting phosphoinositides recruit effector proteins with lipid-binding domains which carry out downstream functions. Mammalian PI3Ks are grouped into three classes based on their substrate specificity and sequence homology (Illustration 1)(Vanhaesebroeck et al., 2010).

ii) Class I PI3Ks

Class I consists of p110α, β, δ and γ, which utilize $PI(4,5)P_2$ as a substrate to produce $PI(3,4,5)P_3$ at the plasma membrane. All of the class I isoforms are expressed ubiquitously, but p110δ and γ are specifically enriched in B cells. p110α, β, and δ bind the regulatory subunit p85, while p110γ binds p101 and p87. The SH2 domain of p85 interacts with phospho-tyrosine residues of growth factor receptor tyrosine kinases at the plasma membrane. This interaction relieves p85 inhibition of p110 and brings the catalytic subunit to its substrate. Class I PI3Ks also contain Ras-binding domains, although the function of such is not completely understood (Vanhaesebroeck et al., 2010). p110β and γ can also receive input from G protein coupled receptors (GPCRs).

In addition, the class I PI3Ks regulate the GTPase activating proteins (GAPs) and guanine nucleotide exchange factors (GEFs) of small GTPases in the Rac, Ras and Arf families. For example, in the absence of serum p110β interacts directly with small GTPase Rab5 at the early endosome. This interaction relieves inhibition of Rab5 by p85α and thus enhances Rab5 activity (Dou et al., 2010; Dou et al., 2013).

Recruitment of the class I PI3Ks by these upstream factors will trigger the production of $PI(3,4,5)P_3$, which then recruits effector proteins containing pleckstrin homology (PH) domains. Effectors include Akt, which activates mTOR to regulate growth and proliferation. As such, activating mutations in p110α or inactivating mutations in the $PI(3,4,5)P_3$ phosphatase PTEN are often found in human cancers.

iii) Class II PI3Ks

The class II PI3Ks C2α, β, and γ are able to phosphorylate PI and PI(4)P *in vitro*, thereby producing PI(3)P, and PI(3,4)P_2 (Vanhaesebroeck et al., 2010). However, PI is predicted to be the preferred substrate. C2α is ubiquitously expressed, whereas β and γ have a more restricted expression. Like the class I PI3Ks, class II PI3Ks contain Ras binding, C2, helical, and catalytic domains. Unlike class I, however, the class II kinases do not bind to any regulatory subunits and instead contain a Phox homology (PX) domain and second C2 domain at their N termini (Falasca and Maffucci, 2012).

PI3K-C2α is found in clathrin coated vesicles and its activity is stimulated by clathrin (Posor et al., 2015). Other studies show that C2α kinase activity is stimulated by insulin, chemokines and cytokines. Insulin induces the translocation of C2α to the plasma membrane, although the functional relevance of this translocation is unknown. C2α is known to play a role in the plasma membrane targeting or secretion of multiple molecules such as GLUT4, neurosecretory granules and insulin (Falasca and Maffucci, 2012). In addition, C2α was recently discovered to be required for angiogenesis, through the regulation of transforming growth factor β (TGFβ) signaling (Aki et al., 2015).

The C2β isoform is activated by growth factors like epidermal growth factor (EGF), and plays a role in cell migration, K+ channel activation and cell survival. C2β regulation of RhoA mediates the actin skeleton to control cell morphology (Blajecka et al., 2012). Being the least studied PI3K, there are no known biological roles for C2γ (Falasca and Maffucci, 2012).

iv) Class III PI3Ks

a) General characteristics

Vps34 is the sole member of class III, which phosphorylates PI to produce PI(3)P. In 1988 a screen for genes involved in vacuolar protein sorting in *Saccharomyces cerevisiae* identified Vps34 (Robinson et al., 1988). The subsequent cloning and characterization of Vps34p revealed that it indeed is necessary for the sorting of vacuolar proteins, and possesses both phosphatidylinositol 3-kinase and protein kinase activity in *S. cerevisiae* (Herman and Emr, 1990; Stack and Emr, 1994). Identification of Vps34 homologues in other organisms affirmed that it is conserved from yeast to humans (Backer, 2008).

Vps34 forms a heterodimer with its regulatory subunit Vps15, which is myristoylated, allowing it to bind to intracellular membranes. Unlike the class I and II PI3Ks, Vps34 lacks a Ras-binding domain (Vanhaesebroeck et al., 2010). Interestingly, Vps15 also contains a putative Ser/Thr kinase domain, and although its function or targets are unknown it was shown to be important for G protein coupled receptor (GPCR) signaling in yeast (Heenan et al., 2009; Miller et al., 2010). Vps34 also interacts with Beclin 1, which acts as a scaffold to regulate the interaction of Vps34 with multiple proteins (Funderburk et al., 2010; McKnight and Zhenyu, 2013; McKnight et al., 2014).

Vps34 produces PI(3)P on endosome, autophagosome and phagosome membranes to recruit effectors with FYVE or Phox homology (PX) domains, many of which are involved in vesicle trafficking and membrane remodeling. The role of Vps34 in endocytosis, autophagy and nutrient-induced mTOR signaling will be discussed in detail below. In addition to these functions, Vps34 also plays a role in phagosome maturation and endosome-to-Golgi retrograde trafficking.

b) Inhibitors

Much of the previous work establishing Vps34 in these cellular functions came from studies in yeast, where Vps34 is the only PI3K, or utilized chemical inhibitors wortmannin or 3-methyladenine (3-MA) (Blommaart et al., 1997; Petiot et al., 2000; Seglen and Gordon, 1982). Since mammals have multiple PI3Ks with overlapping or more intricate functions than the primordial yeast Vps34, it is difficult to translate studies in yeast to those in mammals. In addition, the fungal metabolite wortmannin not only inhibits all three classes of PI3Ks, but also inhibits various other kinases such as mammalian target of rapamycin (mTOR) and myosin light chain kinase (MLCK), complicating the interpretation of these results (Mizushima et al., 2010). 3-MA also has varying effects on autophagy and inhibits class I PI3Ks as well (Bago et al., 2014; Wu et al., 2010).

c) Animal models

Only during the past few years have genetic manipulation studies of Vps34 been carried out. Whole body deletion of Vps34 in mice is embryonic lethal, effecting embryonic development and cell proliferation (Zhou et al., 2011). Conditional deletion of Vps34 in sensory

neurons revealed that it is integral for neuronal health and stability. The authors suggest this is mainly through Vps34's role in endocytic traffic, as conditional deletion of autophagy protein Atg7 generates a distinct phenotype, and because LC3-II is detectable in the knockout tissue (Zhou et al., 2010).

II. Macroautophagy

i) General characteristics

Autophagy, which means self-eating, is a term used to describe the lysosomal degradation of intracellular materials. It is an integral process that is conserved from yeast to mammals, and serves to rid the cell of unwanted or unused material such as long lived proteins, damaged organelles, protein aggregates or pathogens (Yang and Klionsky, 2010). An important aspect of autophagy is that its completion results in the production of macromolecules, which can be reused or metabolized, thus providing the cell with an internal nutrient source. As such, autophagy is especially important for cells during periods of nutrient deprivation and stress. However, a basal level of autophagy is carried out in all cells to maintain protein homeostasis and support normal cell functioning.

Three types of autophagy have been identified thus far, namely, chaperone-mediated autophagy, microautophagy, and macroautophagy. Chaperone-mediated autophagy involves the delivery of specific substrates directly to the lysosome lumen via chaperone complexes. Microautophagy is the degradation of cellular materials via invagination of the lysosome membrane (Majeski and Dice, 2004). Macroautophagy involves the *de novo* formation of a double-membraned organelle termed the autophagosome, which sequesters intracellular debris and delivers them to the lysosome via vesicular trafficking (Illustration 2). Macroautophagy, hereto referred to as autophagy, is the most well studied form of autophagy and will be the focus of this work.

ii) Molecular mechanisms

Autophagy can be considered in two stages: the early stage, which involves autophagosome formation; and the late stage, which involves maturation and degradation. The formation stage can be further separated into the nucleation, elongation and closure steps. The

molecular machinery of each step in mammalian autophagy will be introduced here (yeast contain homologous proteins, which will not be discussed).

a) Nucleation

Autophagosome formation begins with nucleation of a membrane structure termed the isolation membrane or phagophore, which resides on the endoplasmic reticulum (ER) (Axe et al., 2008). The most upstream complex in autophagosome formation consists of ULK1/2, FIP200 and mAtg13 (Itakura and Mizushima, 2010). This complex couples the nutrient-dependent regulation of mTORC1 to recruitment of the Vps34 complex (Hosokawa et al., 2009; Itakura and Mizushima, 2010; Yang and Klionsky, 2010).

Vps34 forms a complex with Vps15, Beclin 1 and Atg14L or UVRAG. Atg14L stimulates the kinase activity of Vps34 (Zhong et al., 2009), while UVRAG interacts with multiple proteins including Bif-1, HOPS and Rubicon. Bif-1 is required for autophagy and may provide a membrane bending force during phagophore formation. HOPS plays a role in autophagosome maturation, while Rubicon acts as a negative regulator of Vps34 activity (Yang and Klionsky, 2010). Vps34 also interacts with the small GTPase Rab5 via Vps15 (Christoforidis et al., 1999b), and Rab5 has been shown to be essential for autophagy (Ravikumar et al., 2008). The Rab5-Vps34 interaction and Vps34 activity are positively regulated by class I PI3K p110β (Dou et al., 2010; Dou et al., 2013).

Two autophagy-related PI(3)P-interacting proteins, DFCP1 and the WIPI family, have been identified thus far, and their localization is dependent on Vps34 (Itakura and Mizushima, 2010). DFCP1 localizes to the ER via an ER-targeting domain in full nutrients, but under starvation conditions localizes to structures termed omegasomes in a PI(3)P dependent manner. Omegasomes are characterized as ER-associated PI(3)P-positive structures from which the LC3-positive autophagosome is generated (Axe et al., 2008). Axe *et al*. also demonstrate that Vps34 is localized to Lamp2-positive structures which almost always associate with the ER, and suggest that Vps34 dictates the site of autophagosome nucleation via PI(3)P production (Axe et al., 2008).

The WIPI family consists of four members (WIPI-1, -2, -3, and -4), each containing multiple WD-repeats that mediate protein-protein interactions. Interestingly, WIPI-1 was shown to localize to cup-shaped structures reminiscent of omegasomes in a Vps34-dependent manner

(Proikas-Cezanne et al., 2004). In addition, both WIPI-2 and -4 regulate the formation of autophagosomes from omegasomes in a PI(3)P dependent manner. WIPI-2 also regulates LC3 lipidation, which is essential for the elongation step of autophagosome biogenesis (Lu et al., 2011; Polson et al., 2010).

b) Elongation and closure

Two ubiquitin-like systems are required for phagophore elongation, the Atg5/12 system and the LC3 system. Atg7 and Atg10 act as the E1 and E2-like enzymes to conjugate Atg12 to Atg5. The Atg5-12 conjugate then associates with Atg16L. In the LC3 system, Atg4 cleaves the C-terminal arginine residue of LC3, exposing a critical glycine residue. The E1-like Atg7 then activates LC3 and transfers it to the E2-like Atg3, which finally transfers it to phosphatidylethanolamine (PE) on both the inner and outer autophagosome membranes (Ichimura et al., 2004). Interestingly, the Atg5-12-16L complex may act as an E3-like enzyme for LC3 lipidation (Fujita et al., 2008). LC3 has been implicated in autophagosome membrane expansion and closure although the mechanism is still under debate (Nair and Klionsky, 2005; Nakatogawa et al., 2007; Sou et al., 2008; Weidberg et al., 2010). The lipidation of LC3 onto PE (termed LC3-II) changes its mobility on SDS-PAGE, allowing easy detection. In addition, LC3-II appears as puncta via microscopy assays, and as a result, LC3 lipidation is the most widely used indicator of autophagy. However, there are many caveats to this method including the fact that LC3 is prone to aggregation and can be lipidated by other mechanisms (Florey et al., 2015; Mizushima et al., 2010).

Expansion of the double-membraned autophagosome requires a discrete membrane source. Mammalian Atg9 is a transmembrane protein which localizes to LC3-positive autophagosomes upon starvation, in a ULK1-dependent manner (Webber et al., 2007; Yang and Klionsky, 2010). More recent work has shown that Atg9 and Atg16L1-positive vesicles originate from the plasma membrane and fuse to provide a membrane source for the growing phagophore (Puri et al., 2014). The formation of these vesicles is dependent on clathrin-mediated endocytosis, and their fusion depends on various SNARE proteins (Moreau et al., 2015).

While the phagophore is expanding and before its closure, autophagic cargoes are delivered into its lumen. In some cases cargo consists of bulk cytoplasm, and in other cases cargo is more specifically regulated, such as ubiquitinated protein aggregates and damaged organelles.

Specific autophagic degradation of whole organelles such as mitochondria (mitophagy), ribosomes (ribophagy), peroxisomes (pexophagy), pathogens (xenophagy) and endoplasmic reticulum (reticulophagy) has been observed. p62 and NBR1 act as chaperones for selective autophagy, binding both ubiquitinated cargo and LC3 for efficient delivery (He and Klionsky, 2009; Kirkin et al., 2009).

c) Maturation

A fully formed autophagosome is defined as a double-membraned organelle with intraluminal content, sometimes including whole mitochondria. Completed autophagosomes undergo a maturation phase, which involves fusion with early and/or late endosomes (forming an amphisome) and eventually lysosomes (forming an autolysosome). The outer membrane of the autophagosome fuses with the lysosome membrane, while the inner membrane and its contents are degraded by lysosomal hydrolases. LC3 lipidated to the inner membrane will be degraded, while LC3 lipidated to the outer membrane will be un-lipidated by Atg4, returning to its cytosolic LC3-I form.

Fusion of autophagosomes with endosomes and lysosomes requires the typical endocytic machinery, including the ESCRT and HOPS complexes, UVRAG, Rab7, Lamp2 and the SNARE protein Vti1b (Eskelinen, 2005; Liang et al., 2008a; Simonsen and Tooze, 2009). Degradation of the enclosed autophagic cargo by hydrolases (such as cathepsins D, B and L) produce macromolecules which are transported out of the autolysosome via nutrient transporters and into the cytoplasm for reuse. Nutrients produced by autophagy can reactivate mTOR during prolonged periods of starvation (Yu et al., 2010). Nutrient regulation of mTOR will be discussed in detail in section 1.IV.

iii) Regulation

The most well known regulator of autophagy is nutrient and growth factor availability. The autophagic machinery senses nutrient status in multiple ways. For example, Beclin 1 is bound and sequestered by Bcl-2 under nutrient-rich conditions, but released from Bcl-2 during starvation. In addition, mTORC1 binds, phosphorylates, and inhibits ULK1 in the ULK1-Atg13-FIP200 complex under nutrient-rich conditions. Upon nutrient starvation or growth factor withdrawal, mTORC1 dissociates from the complex and ULK1 is dephosphorylated, allowing

autophagy initiation (Hosokawa et al., 2009). Furthermore, low ATP/AMP ratios activate AMP-activated protein kinase (AMPK) which then inhibits mTORC1 via phosphorylation (Yang and Klionsky, 2010). In addition, AMPK directly phosphorylates and activates ULK1 to promote autophagy (Kim et al., 2011). p53 can also induce autophagy in response to DNA damage or oncogene activation via the AMPK/mTORC1 pathway (Yang and Klionsky, 2010).

Various stress conditions are also known to induce autophagy, including ER stress, hypoxia, oxidative stress and infection (He and Klionsky, 2009). Furthermore, Vps34 is phosphorylated and inhibited by Cdk1 during mitosis and by the neuron-specific Cdk5, suggesting that autophagy may be inhibited during cell proliferation and neuron development (Furuya et al., 2010). Importantly, a genome-wide screen identified multiple growth factors and cytokines, such as MAPK and Stat3, which inhibit Vps34 to regulate autophagy under nutrient-rich conditions in an mTORC1-independent manner (Lipinski et al., 2010a). More work is needed to fully understand how basal mTORC1-independent autophagy is regulated.

iv) Physiological relevance

Basal autophagy is constitutive in all cells, which helps maintain protein homeostasis and proper cell functioning. This basal autophagy is especially important for quiescent cells such as neurons and muscle cells, which are not able to divide to dilute harmful protein aggregates or damaged organelles (Mizushima et al., 2008). Not surprisingly then, the disruption of various autophagy genes in multiple tissues in mice often leads to organ dysfunction and death (Jaber et al., 2012; Komatsu et al., 2005; McKnight et al., 2014; Nakai et al., 2007; Yue et al., 2003). In addition, autophagy was shown to have a critical role in survival of the neonatal starvation period immediately following birth (Kuma et al., 2004).

A specialized form of autophagy termed xenophagy functions to eliminate intracellular pathogens including bacteria, parasites, and viruses, and many pathogens have evolved mechanisms to inhibit autophagy for their survival (Mizushima et al., 2008). In addition, autophagic degradation of bulk cytoplasm provides peptides for MHC II presentation (Deretic, 2006). Thus, autophagy plays an integral role in immune functions.

Consistent with its role in promoting homeostasis, autophagy has been attributed to many disease states. Plentiful evidence show that autophagy is a protective factor against neurodegeneration (Komatsu et al., 2006), and may be disrupted in Alzheimer's (Lipinski et al.,

2010b) and Huntington disease (Ravikumar et al., 2004), as well as cancer (Mizushima et al., 2008). The disruption of autophagy by Beclin 1 or Atg5 deletion was shown to accelerate DNA damage and chromosomal instability, leading to tumor formation. However, established solid tumors can reactivate autophagy to promote cancer cell survival in the face of nutrient limitation, hypoxia and cell damage due to drug treatment (Mathew and White, 2007).

III. Endocytosis

i) General characteristics

Like autophagy, endocytosis is a protein degradation pathway which serves to promote normal homeostasis by internalizing and trafficking proteins and signaling molecules from the extracellular space, plasma membrane, and Golgi (Illustration 3). Also quite similar to autophagy, the endocytic pathway is extremely dynamic, such that the precise identity of organelles and stages has been difficult to define. In general, however, the endocytic pathway can be considered in terms of three organelles: the early endosome (EE), the late endosome (LE), and the lysosome. The term endocytosis also encompasses the internalization of fluid, solutes and proteins at the plasma membrane, which is in and of itself a highly complicated process and will not be discussed in detail here. Vesicular trafficking and fusion events between these three organelles (EE, LE and lysosome) mediate the process of endocytosis, which (unlike autophagy) includes more than one fate for the cargo proteins involved (Huotari and Helenius, 2011).

ii) Molecular mechanics

a) Early endosome

Transmembrane receptors at the plasma membrane, such as growth factor receptors and nutrient transporters, constantly bind ligands and transmit signaling cascades into the cytoplasm. The precise timing of initiation and termination for these signaling cascades is extremely critical for normal homeostasis. To regulate these signaling pathways, plasma membrane proteins are ubiquitinated and internalized via clathrin-dependent or -independent mechanisms into small vesicles, and delivered to the early endosome. The early endosome serves as a sorting station for the enclosed cargo, deciding and manifesting their fates. Cargoes can be recycled back to the plasma membrane for re-use, sent to the *trans*-Golgi, or delivered to the lysosome for degradation. The slightly acidic pH of early endosomes (6.3-6.78) allows internalized ligand-

receptor complexes to dissociate and undergo separate trafficking patterns; some receptors are recycled while their ligands are degraded (Jovic et al., 2010).

The major molecular players of the early endosome are the small GTPase Rab5 and the class III PI3K Vps34. Active Rab5-GTP is maintained at the early endosome via its guanine nucleotide exchange factor (GEF) Rabex-5. An interaction between Vps15 and Rab5 targets the Vps34-Vps15-Beclin 1-UVRAG complex to early endosomes (Christoforidis et al., 1999b). PI(3)P generation on the early endosome will recruit downstream effector proteins containing FYVE or PX domains, which bind PI(3)P. Interestingly, a subset of these effectors also contain Rab5-binding domains, and as such their recruitment is thought to depend on a double signal from both PI(3)P and Rab5-GTP. One such effector, EEA1, tethers opposing vesicles to mediate docking, and assembles SNAREs to mediate fusion (Christoforidis et al., 1999a; Lindmo and Stenmark, 2006). The CORVET complex, which is recruited via Rab5, is also believed to tether endosomes and interact with SNAREs to promote fusion (Balderhaar and Ungermann, 2013). Tethering and fusion is required for vesicle delivery to early endosomes as well as homotypic fusion of early endosomes. Other effectors, such as Rabenosyn5 and Rabankyrin5, regulate recycling events (Jovic et al., 2010).

Another PI(3)P and Rab5 effector is the ESCRT-0 factor Hrs, which binds to ubiquitin and clathrin. This allows Hrs to cluster cargoes destined for degradation in a unique microdomain of the early endosome. Hrs also recruits the ESCRT-I complex, which sequentially recruits complexes II and III, to regulate intraluminal vesicle (ILV) formation (Lindmo and Stenmark, 2006). The inward budding of the endosome membrane to form ILVs serves to sequester membrane proteins from the cytoplasm, abrogating signaling cascades and making them more accessible to lysosomal hydrolases (Eden et al., 2009; Huotari and Helenius, 2011; Katzmann et al., 2002). On the other hand, cargoes destined for recycling will accumulate in separate microdomains on early endosome tubules that will eventually bud off and fuse with the Rab4- and Rab11-positive recycling endosome. Cargoes destined for retrograde traffic to the *trans*-Golgi network will be sequestered into tubules by the retromer complex (Woodman, 2000).

Although it is generally assumed that Vps34 produces PI(3)P to support early endosome functions, PI(3)P may be generated by various mechanisms and a direct requirement for Vps34 at the early endosome has not been clarified. The PI3K inhibitor wortmannin blocks homotypic fusion, and anti-hVps34 antibodies block both heterotypic and homotypic fusion of early

endosomes (Christoforidis et al., 1999b; Li et al., 1995). Wortmannin also causes EEA1 to dissociate from early endosomes (Simonsen et al., 1998); however, gene silencing of hVps34 in human glioblastoma cells by siRNA did not affect EEA1 localization (Johnson et al., 2006). Likewise, targeting MTM1 phosphatase, which de-phosphorylates PI(3)P, to the endosome does not affect EEA1 localization (Fili et al., 2006). As the class II PI3Ks can produce PI(3)P and have roles in clathrin-mediated endocytosis (Gaidarov et al., 2001; Posor et al., 2013), their involvement at the early endosome has been speculated (Johnson et al., 2006). Indeed, phospholipid measurements in cells with PI3K-C2α and -β deletion showed a 15-20% reduction in PI(3)P (Devereaux et al., 2013). In addition, the sequential dephosphorylation of PI(3,4,5)P_3 into PI(3)P has been suggested as another viable route for Vps34-independent PI(3)P at the early endosome (Shin et al., 2005).

b) Late endosome

Although early and late endosomes are often considered as separate organelles, early endosomes undergo a maturation process to become late endosomes. The maturation of early endosomes to late endosomes allows the silencing of early endosome functions and acquisition of late endosome functions, including the ability to fuse with lysosomes. This is mediated by the shedding of Rab5-GTP and the simultaneous acquisition of Rab7-GTP on endosome membranes (Rink et al., 2005). The activity of Rab7, like other small GTPases, is modulated by GTPase activating proteins (GAPs) and guanine nucleotide exchange factors (GEFs). GAPs activate the intrinsic GTP hydrolysis activity of Rabs, promoting their GDP-bound off state, while GEFs promote the exchange of GTP for GDP, facilitating the active state. GDP-dissociation inhibitors (GDIs) lock Rabs in their GDP-bound off state, while GDI-displacement factors (GDFs) free Rabs from inhibition by these GDIs. While the HOPS complex subunit mVps39 is often cited as a Rab7 GEF based on its homology to the yeast Ypt7 GEF, mVps39 does not regulate Rab7 activity, but does promote lysosome clustering. TBC1D15 was confirmed as a Rab7 GAP, however (Peralta et al., 2010). Another Rab7 GAP, Armus, was also recently confirmed (Frasa et al., 2010) and was shown to play a role in autophagosome maturation (Carroll et al., 2013).

A mechanism for this “Rab switch” during endosome maturation has been proposed, whereby Rab5-GTP recruits the Mon1-Ccz1 complex, which displaces the Rab5 GEF, Rabex5, and recruits Rab7 (Poteryaev et al., 2010). The Mon1-Ccz1 complex then acts as a GDI-

displacement factor for Rab7, thereby activating Rab7 (Bohdanowicz and Grinstein, 2010). The recruitment or activation of Rab7 is also thought to depend on the C VPS/HOPS complex, but its precise function in this process is unknown (Peralta et al., 2010; Poteryaev et al., 2010). Interestingly, Mon1 and its homolog interact with PI(3)P in *C. elegans* and yeast, and its recruitment to endosomes is inhibited by wortmannin, suggesting that Vps34 may play a role in the Rab switch (Cabrera et al., 2014; Lawrence et al., 2014; Poteryaev et al., 2010).

In addition to a switch in Rab proteins, endosome maturation also involves a switch in phosphotinositides from PI(3)P to PI(3,5)P_2. The PI 5-kinase PIKfyve is recruited to endosomes via its FYVE domain, where it phosphorylates PI(3)P to generate PI(3,5)P_2. This phospholipid regulates ILV formation and endosome size (Ikonomov et al., 2003; Ikonomov et al., 2015). Interestingly, the ESCRT-III subunit Vps24 interacts with PI(3,5)P_2, which may aid the increase in ILV formation associated with endosome maturation (Lindmo and Stenmark, 2006). In addition, PI(3,5)P_2 activates the Ca^{+2} channel TRPML1 (Dong et al., 2010) and the Na^{+} channels TPC1 and TPC2 (Wang et al., 2012). As Ca^{+2} flux is required for fusion reactions, these findings may explain how PIKfyve regulates endosome size (Luzio et al., 2007a). Consistent with this idea, overexpression of TRMPL1 in Vac14 knockout (a positive regulator of PIKfyve) rescues the enlarged late endosome phenotype (Dong et al., 2010).

The recruitment and activation of Rab7 on late endosomes allows the subsequent recruitment of Rab7 effectors such as RILP, retromer, HOPS, Rabring7 and Rubicon. RILP mediates minus-end motility by recruiting dynein-dynactin motors, mobilizing endosomes towards the nucleus where they can interact with lysosomes. LEs also exhibit plus-end motility, and bidirectional transport may be necessary for proper functioning (Lebrand et al., 2002). The retromer complex regulates retrograde traffic from the endosome to the *trans*-Golgi. The HOPS complex is important for endosome tethering and SNARE pairing prior to fusion, and may also play a role in the Rab switch (Liang et al., 2008b; Starai et al., 2008; Sun et al., 2010). Interestingly, the HOPS complex in yeast binds to multiple phospholipids including PI(3)P and PI(3,5)P_2 (Stroupe et al., 2006). The Rab7 effector Rubicon negatively regulates endosome maturation by sequestering UVRAG away from the HOPS complex, preventing its activation (Sun et al., 2010). Another Rab7 effector, Rabring7, is an E3 ligase which may help sort ubiquitinated cargo (Huotari and Helenius, 2011).

c) Lysosome

The lysosome is considered the "cell stomach" for its major role of digesting cellular material. They are characterized as electron-dense organelles via electron microscopy and their membranes are positive for glycoproteins Lamp1 and 2, but negative for mannose-6-phosphate receptors (M6PRs) (Huotari and Helenius, 2011). Lysosomes contain catabolic enzymes such as proteases, glycosidases, nucleases, phosphatases and lipases (Platt et al., 2012). Late endosomes fuse with lysosomes by "kissing" (short contact between organelles) or direct fusion (Bright et al., 2005; Luzio et al., 2000)

Mechanistically, membrane fusion requires three steps: 1) tethering, 2) *trans*-SNARE complex formation, and 3) membrane fusion. The *trans*-SNARE complex for endosome fusion consists of syntaxin-7, VTI1B and syntaxin-8, complexed with Vamp8 for homotypic LE-LE fusion and Vamp7 for LE-lysosome fusion (Luzio et al., 2007b; Pryor et al., 2004). Interestingly, Vamp8 but not Vamp7 interacts with PI(3)P *in vitro* (Dai et al., 2007). A GDI inhibitor, as well as the PI3K inhibitors wortmannin, LY294002 and 3-MA were all able to inhibit content mixing in a late endosome-lysosome fusion assay, suggesting the involvement of a PI3K and a Rab protein in LE-lysosome fusion (Mullock et al., 1998). Furthermore, syntaxin-7, VTI1B, syntaxin-8, and Vamp7 are integral for fusion of autophagosome precursor vesicles and fusion of autophagosomes with lysosomes (Moreau et al., 2011; Moreau et al., 2013).

Fusion of late endosomes and lysosomes produces a hybrid organelle from which lysosomes are then regenerated (Mullock et al., 1998; Pryor et al., 2000). Interestingly, wortmannin treatment also leads to a dramatic reduction in the overall number of lysosomes, suggesting that a PI3K may have a role in lysosome reformation (Mousavi et al., 2003).

Lysosomes depend on the delivery of acid hydrolases from late endosomes. Cathepsins are delivered from the *trans*-Golgi to the late endosome via mannose-6-phosphate receptors. In the late endosome the receptors dissociate and return to the Golgi via retrograde trafficking. Endosomes deliver cathepsins by fusing with lysosomes, where some cathepsins like cathepsin D undergo proteolytic cleavage into their active forms (Zaidi et al., 2008). Without continual fusion with endosomes, lysosomes lose their acidity and degradative capacity (Huotari and Helenius, 2011).

The pH of lysosomes falls around 4.5, which is integral for the optimal activity of lysosome enzymes (Huotari and Helenius, 2011). The acidic pH of endosomes and lysosomes (as

well as other organelles and tissues) is regulated by the multi-subunit complex v-ATPase, which uses ATP hydrolysis to drive proton transport across membranes. v-ATPase consists of the V0 transmembrane holoenzyme complex and the V1 cytosolic complex. V1 facilitates ATP hydrolysis while V0 forms a pore to transport protons. The activity of v-ATPase is regulated by multiple mechanisms including expression of subunits, subcellular localization of the complex and association/dissociation of V1 and V0 (Breton and Brown, 2007). The lysosome membrane also contains Ca^{+2}, Na^{+}, K^{+} and Cl^{-} transporters, and the activities of these enzymes may be interlinked with v-ATPase (Huotari and Helenius, 2011). In addition, certain symporters and antiporters require a proton gradient for efficient functioning (Beyenbach and Wieczorek, 2006). The role of v-ATPase in LE/lysosome fusion remains controversial (Baars et al., 2007; Kawai et al., 2007; Klionsky et al., 2008; Peters et al., 2001; van Weert et al., 1995).

iii) Physiological relevance

Like autophagy, endocytosis is an integral process for cellular homeostasis, and its disruption or deregulation is implicated in various disease states. Genetic defects in multiple aspects of vesicular trafficking and endocytosis have been identified as causative factors in various diseases, especially those involving neurodegeneration. It is speculated that neurons are particularly susceptible to trafficking defects due to their long axons, which require vesicle trafficking for long distances to achieve homeostasis (Olkkonen and Ikonen, 2006). For example, activating mutations in the Rab7 gene have been identified as the causative factor in Charcot-Marie-Tooth (CMT) type 2B disease, an inherited disease which affects motor and sensory nerves (Cogli et al., 2009). Furthermore, a subset of diseases termed lysosomal storage disorders are caused by genetic defects in lysosome biology, mostly due to defects in the lysosomal acid hydrolases. The resulting accumulation of macromolecules can have deleterious consequences (Platt et al., 2012). For example, mutant Niemann-Pick type C (NPC1) protein leads to cholesterol overload in late endosomes which leads to their paralysis, ultimately leading to liver dysfunction, ataxia and dementia (Lebrand et al., 2002). Genetic ablation of both Vps34 and Beclin 1 in neurons leads to neurodegeneration, which has been attributed to defects in endocytosis rather than autophagy, though it is likely a result of defects in both (McKnight et al., 2014; Zhou et al., 2010).

IV. Nutrient induced mTOR signaling

i) General characteristics

mTOR complex 1 (mTORC1) senses the availability of amino acids, glucose, energy, and growth factors to act as the master regulator of cell growth and proliferation. mTORC1 regulates cellular responses to these inputs by phosphorylating eukaryotic initiation factor 4E-binding protein 1 (4EBP1) and ribosomal p70 S6 kinase 1 and 2 to enable cap-dependent protein translation and translation of ribosomal proteins (Laplante and Sabatini, 2009; Wiczer and Thomas, 2012). Activation of mTORC1 thus promotes protein synthesis, cell proliferation and cell growth (Byfield et al., 2005). mTORC1 is directly regulated by the GTPase Rheb which is in turn regulated by its GAP, the TSC1/2 complex.

ii) Role of Vps34

Vps34 has been implicated in amino acid-induced mTORC1 activity (Backer 2008). Amino acid and glucose starvation inhibit Vps34 kinase activity, and siRNA against Vps34 blocks insulin-induced and amino acid-induced phosphorylation of S6K and 4EBP1 by mTORC1 (Byfield et al., 2005; Nobukuni et al., 2005). This is contradictory to the role of Vps34 in autophagy, which is activated upon nutrient starvation. One possibility is that distinct Vps34 complexes with separate subcellular localizations are regulated differentially by nutrients (Ktistakis et al., 2012).

Vps34 may regulate amino acid-induced mTOR activity via phospholipase D1. Amino acid-stimulated production of PI(3)P activates PLD1 via its PX domain, and causes it to translocate to the lysosome (Yoon et al., 2011). Generation of phosphatidic acid by PLD1 can activate mTORC1 (Fang et al., 2001). However, exogenous phosphatidic acid cannot activate mTORC1 in the absence of amino acids, suggesting the involvement of another parallel pathway (Sun et al., 2008). Indeed, it was discovered that amino acids are also sensed by the Rag GTPases. Amino acids promote GTP loading of RagB, which interacts with and recruits mTORC1 to the lysosome where it is activated by Rheb (Sancak et al., 2010; Sancak et al., 2008).

iii) Role of the lysosome

The lysosome and amino acid-induced mTORC1 signaling are intimately linked in both directions. For example, amino acid-stimulated mTORC1 activity is blocked by a perturbation of the late endosomal/lysosomal compartment via constitutive active Rab5 expression or knockdown of HOPS subunit hVps39, which interrupts endosome maturation and leads to enlarged EE-LE hybrid organelles. However, overexpression of Rheb rescues mTORC1 signaling in cells expressing constitutive active Rab5, suggesting that a characteristic of endocytic maturation (the authors suggest luminal pH or lipid composition) may be required for proper localization of Rheb (Flinn et al., 2010). Furthermore, the v-ATPase complex is required for mTORC1 to sense amino acids in the lysosome lumen (Zoncu et al., 2011).

On the other hand, mTORC1 controls lysosome integrity and biogenesis. mTORC1 becomes activated on lysosomes after prolonged periods of stimulation, which attenuates the autophagic response and promotes lysosome reformation from autolysosomes (Yu et al., 2010). Consistent with these findings, mTORC1 phosphorylates and promotes nuclear localization of the transcription factor TFEB, which regulates lysosome biogenesis by increasing the transcription of various lysosomal genes, including the v-ATPase subunits (Pena-Llopis and Brugarolas, 2011). Likewise, the subcellular positioning and pH of lysosomes is regulated by amino acid availability and mTORC1 activity (Korolchuk et al., 2011). Finally, overexpression of wild-type or constitutive active Rheb induces late endosome swelling, suggesting that Rheb may regulate late endosome integrity as well (Saito et al., 2005).

2

Rationale and Aims

I. Rationale and Aims

Prior to the identification of specific Vps34 inhibitors (Bago et al., 2014; Dowdle et al., 2014; Pasquier et al., 2015; Ronan et al., 2014), the roles of class III PI3K Vps34 in autophagy, endocytosis and amino acid-induced mTORC1 signaling were gathered mainly by studies using the plieotropic inhibitors wortmannin and 3-MA. Thus, I sought to clarify these roles via specific deletion of Vps34 in mouse liver and heart, and to utilize mouse embryonic fibroblasts (MEFs) to investigate these roles at the molecular level. In addition, as kinase-independent roles for other PI3Ks have been identified (Dou et al., 2010), I sought to determine the requirement for lipid kinase activity in these proposed functions.

The following aims were defined for this dissertation:

1) Investigate the role of Vps34 in mammalian autophagy
2) Investigate the role of Vps34 in nutrient-induced mTOR signaling
3) Investigate the role of Vps34 in Rab5-mediated early endocytosis
4) Investigate the role of Vps34 in Rab7-mediated late endocytosis
5) Investigate the role of PI 3-kinase activity in Vps34 functions

3

Results

I. Vps34 is essential for mammalian autophagy

i) Generation and characterization of Vps34 knockout mice and MEFs

Vps34 conditional knockout mice ($Vps34^{f/f}$) were generated by flanking exon 4 of the Vps34 gene with loxP sites (Fig. 1A). When exposed to Cre recombinase, exon 4 is excised, producing a premature stop codon and leading to the deletion of 755 of the 887 amino acids of Vps34. Mouse embryonic fibroblasts (MEFs) were generated from day 13-16 embryos of $Vps34^{+/f}$ matings. MEFs with each of the possible genotypes were immortalized with SV40 large T antigen (Fig. 1B). Infection with adenovirus containing Cre recombinase (hereafter referred to as knockout/KO) resulted in complete loss of Vps34 protein as early as 4 days post-infection (Fig. 6A). $Vps34^{+/+}$ MEFs infected with adenoviral Cre or $Vps34^{f/f}$ MEFs infected with control adenovirus were used as controls for possible effects of flox or Cre expression (referred to as wild-type/WT).

Vps34 KO MEFs accumulate large translucent vacuoles by day 6 after Cre addition (Fig. 1C), and display a drastic proliferative defect compared to wild-type (Fig. 1D). In wild-type cells, stable expression of GFP-2xFYVE (the PI(3)P binding domain FYVE conjugated to GFP) leads to GFP^+ puncta, which represent PI(3)P-positive organelles (Fig. 1E). In sharp contrast, no GFP-2xFYVE puncta were observed in Vps34 KO MEFs (Fig. 1E), indicating a loss of PI(3)P. In addition, the Vps34 and Beclin 1-associated PI 3-kinase activities were drastically reduced upon Vps34 deletion (Fig. 1F). Together these data indicate that our Vps34 knockout strategy was successful.

The $Vps34^{f/f}$ mice were bred to muscle creatinine kinase (Mck)-Cre or albumin (Alb)-Cre mice to generate tissue-specific knockouts in heart and liver, respectively, to study the effect of Vps34 loss in these organs. Expression of Cre recombinase under control of the albumin promoter results in deletion of floxed genes specifically in the liver by 6 weeks of age. Successful deletion of Vps34 was confirmed in hepatocytes isolated from 8-week old mice (Fig. 2A). Littermates with either $Vps34^{f/f}$;Alb-Cre^- or $Vps34^{+/+}$;Alb-Cre^+ genotypes were used as controls for the possible effect of either floxed Vps34 or Cre, and did not show apparent difference, hence are both referred to as wild-type mice. In addition, heterozygous $Vps34^{+/f}$;Alb-Cre^+ mice were indistinguishable from wild-type mice. Noticeably, liver-specific $Vps34^{-/-}$ mice were smaller than wild-type mice, and exhibited enlarged and pale livers (Fig. 2B). Both liver mass and liver protein content of $Vps34^{f/f}$;Alb-Cre^+ mice were significantly higher than that of

wild-type mice (Fig. 2C). Histological analysis revealed the presence of intracellular vacuolization, and an accumulation of lipids (hepatic steatosis) indicated by Oil Red O staining in the livers of $Vps34^{-/-}$ mice (Fig. 2D). Additionally, Periodic Acid Schiff (PAS) staining revealed a lack of glycogen deposits (Fig. 2D). The majority of the $Vps34^{f/f}$;Alb-Cre^{+} mice died within a year (Fig. 2E).

Autophagy also plays an important role in the heart. As such, $Vps34^{f/f}$ mice were bred to Mck-Cre mice to delete Vps34 in cardiomyocytes. Gross anatomical analysis of $Vps34^{f/f}$;Mck-Cre hearts revealed marked cardiomegaly (Fig. 3A) and increased heart to body weight ratio (Fig. 3B). Echocardiogram of the animals *in vivo* demonstrated an increase in left ventricular wall thickness and mass, as well as decreased cardiac contractility with lower ejection fraction and fractional shortening (Fig. 3C and Table 1). Although they appeared normal at birth, $Vps34^{f/f}$;Mck-Cre mice died between 5-13 weeks of age (Fig. 3D). Electron microscopy revealed disorganized mitochondria and Z-lines in $Vps34^{-/-}$ hearts, as well as increased small mitochondria and enlarged vacuoles (Fig. 3E).

ii) Autophagy is compromised by Vps34 deletion in the liver and heart

We first examined the effect of Vps34 deletion on autophagy *in vivo*. Increased levels of p62, LC3-I/II, and poly-ubiquitinated proteins were observed in Vps34 knockout hepatocytes (Fig. 2A) and total liver lysates (Fig. 4A). To further study the involvement of Vps34 in liver autophagy, $Vps34^{f/f}$ mice were bred with GFP-LC3 transgenic mice, then with Alb-Cre mice. As expected, a diffuse pattern of GFP-LC3 was observed in the wild-type liver of fed mice. A 24 h fasting resulted in the formation of GFP-LC3 puncta in the wild-type liver, representative of starvation-induced autophagy (Fig. 4B). However, large GFP-LC3 aggregates were observed in the $Vps34^{-/-}$ livers and the amount and pattern of aggregates appeared unaffected by fasting (Fig. 4B).

Moreover, while a 24 h fasting induced autophagosomes in wild-type liver, Vps34-null liver displayed virtually no autophagosomes and extremely enlarged mitochondria as visualized by electron microscopy (Fig. 4C). In addition, the electron microscopy revealed deficient hyaloplasmic glycogen deposits and the presence of large lipid droplets in Vps34-null livers (Fig. 4C), consistent with the PAS and Oil Red O staining results (Fig. 2D). Upon fasting, liver mass of wild-type mice decreased by approximately 30%, whereas no significant weight change was

detected in $Vps34^{f/f}$;$Alb\text{-}Cre^{+}$ mice (Fig. 2E), suggesting that the starvation response is compromised in Vps34-null livers.

Consistent with the phenotypes observed in Vps34-null livers, $Vps34^{-/-}$ hearts and cardiomyocytes displayed elevated levels of p62, LC3-I/II, and poly-ubiquitinated proteins (Fig. 5A, B), as well as the presence of large GFP-LC3 aggregates (Fig. 5C). Together these results suggest that autophagy is blocked by the deletion of Vps34 in both liver and heart.

iii) Autophagy is impaired but LC3 lipidation is preserved in Vps34 knockout MEFs

To investigate the autophagy phenotype in molecular detail, we turned to the Vps34 knockout MEFs. As infection of adenoviral Cre led to a progressive abolishment of Vps34 expression, a reciprocal accumulation of LC3-I/II and p62 was observed (Fig. 6A). Because autophagy is a dynamic process involving both autophagosome formation and degradation, these changes can be indicative of either increased induction or decreased degradation (Mizushima et al., 2010). To clarify this, WT and KO MEFs were serum starved in the presence or absence of lysosomal protease inhibitors E64D and pepstatin A (PepA). E64D and PepA treatment led to increased levels of LC3-II in wild-type MEFs at the basal state and upon serum starvation, indicating autophagic degradation, termed *flux* (Fig. 6B). In sharp contrast, the level of LC3-II was high in Vps34-null MEFs at the basal state, and was not further increased upon serum starvation and/or E64D plus PepA treatment (Fig. 6B), indicating that while LC3 conjugation to phosphatidylethanolamine (PE) still occurs, autophagy flux is impaired in Vps34-null MEFs. Compromised autophagic flux was also indicated in the long-lived protein degradation assay, at both basal and serum-starved conditions (Fig. 6C). The remaining protein degradation activity in Vps34-null MEFs is likely due to alternative forms of protein degradation such as chaperone-mediated autophagy and proteasomal degradation (Kaushik et al., 2008).

One of the most definitive assays for autophagy is observing autophagosomes by electron microscopy. While we observe a strong induction of characteristic double membraned autophagosomes in serum starved WT cells, we find very few autophagosomes in KO cells (Fig. 6D). Instead we observe single membraned organelles devoid of intraluminal content at both fed and starved states in the KO cells, representing the vacuoles observed by phase microscopy (Fig. 1C). GFP-DFCP1, which localizes to the site of autophagosome nucleation (Axe et al., 2008), was expressed in the MEFs its colocalization with another autophagic marker, Atg12, was

observed to investigate phagophore formation. In WT cells we observe few DFCP1 or Atg12 puncta in full media, but an increase in both under serum starvation (Fig. 6E). In KO cells we observe a diffuse signal for both DFCP1 and Atg12, which does not change upon serum starvation (Fig. 6E). Together, these data suggest that phagophore formation, autophagosome formation, and functional autophagy flux are blocked by Vps34 deletion.

To further visualize autophagy, we stably expressed GFP-LC3 and observed puncta formation under nutrient starvation conditions. WT cells displayed a characteristic punctate pattern upon nutrient deprivation, indicating the formation of autophagosomes (Fig. 7A). In contrast, large LC3 structures were observed in KO MEFs even at the basal state. These large structures are morphologically distinct from autophagic puncta. Importantly, the quantity of the LC3 aggregates did not appear to change upon nutrient starvation, consistently indicating that Vps34 KO cells have impaired autophagic flux (i.e. are not induced or degraded). As the overexpression of LC3 can lead to aggregation (Mizushima et al., 2010), we tried visualizing LC3 at the endogenous level. To this end, MEFs were cultured in serum-free medium and subjected to immunofluorescence for endogenous LC3. Consistent with our GFP-LC3 data, LC3 puncta are formed in starved WT cells while large LC3 aggregates are observed in both fed and starved KO cells (Fig. 7B).

Vps34 has been implicated in regulating Atg5-Atg12 conjugation (Ravikumar et al., 2008), which complexes with Atg16L and serves as an E3-like enzyme for LC3 conjugation to PE. Although an increase of free Atg5 was observed, the conjugated Atg5-Atg12 form was not significantly affected in Vps34 KO cells (Fig. 7C). This finding is consistent with the observation that LC3 lipidation occurs in the absence of Vps34, and also indicates that Atg5-Atg12 conjugation is independent of Vps34.

Although we do not observe any autophagosomes by EM (Fig. 6D), we wanted to investigate the nature of the LC3 aggregates observed in Vps34 KO cells. To this end tandemly tagged mCherry-GFP-LC3 was expressed in the MEFs. Autophagosomes decorated with mCherry-GFP-LC3 will appear yellow, while the degradation of GFP but not RFP in lysosomes will make autolysosomes appear red. In wild-type MEFs, a number of red puncta are observed under fed conditions, representing basal level autophagy (Fig. 8A). Upon nutrient starvation, the numbers of both yellow and red puncta increased, indicating an increase in autophagosomes and autolysosomes, respectively. In contrast, the LC3 aggregates observed in both fed and starved

conditions in Vps34 KO MEFs appeared yellow, and few red puncta were observed under either fed or starved conditions (Fig. 8A), suggesting that the aggregates do not represent functional autophagosomes. To confirm this, we performed immuno-electron microscopy against GFP-LC3 in the MEFs. While we observe LC3 decorating the inner and outer autophagosome membranes in WT cells, we find LC3 in large intracellular aggregates which are not associated with any membrane structures in KO cells (Fig. 8B).

iv) Conclusions

Taken together, these results indicate that autophagy flux is blocked in Vps34-deficient livers and hearts. The appearance of hepatomegaly, hepatic steatosis, increased liver protein content, lack of glycogen deposition, and increased fatality are highly consistent with the phenotype observed in the autophagy-deficient $Atg7^{-/-}$ and $Atg5^{-/-}$ livers (Komatsu et al., 2005; Takamura et al., 2011). These results confirm that autophagy has an integral role in promoting homeostasis for normal organ functions.

Using multiple approaches, we thoroughly investigated autophagy in the Vps34 knockout MEFs, and conclude that Vps34 deletion severely disrupts phagophore and mature autophagosome formation, as well as autophagy flux. Interestingly, our data indicate that Vps34 is not required for Atg5-12 or LC3-PE conjugation *in vitro* and *in vivo*, but perhaps regulates the site of LC3 lipidation.

II. Vps34 is required for nutrient-induced mTOR signaling

i) Amino acid-induced but not steady state mTORC1 signaling is impaired in Vps34 knockout mice and MEFs

Using chemical inhibition or siRNA, Vps34 has been implicated in amino acid-induced mTORC1 activity (Backer, 2008). To confirm these observations we examined mTORC1 activation in Vps34 knockout MEFs upon amino acid stimulation. As assessed by phospho-S6 and phospho-4EBP1, amino acid-induced activation of mTORC1 was severely compromised in Vps34 KO MEFs (Fig. 9A). Importantly, this did not represent slower mTORC1 activation, as even prolonged stimulation with amino acids did not induce phosphorylation of downstream

target S6 (Fig. 9B). However, we noticed that the steady state level of mTORC1 activation in complete media was not affected by Vps34 deletion (Fig. 9A, B).

Likewise, no apparent difference in mTORC1 signaling was observed in the Vps34-null liver under either fed or fasted condition (Fig. 8C). Similarly, basal mTORC1 activation was not affected by Vps34 deletion in isolated cardiomyocytes cultured in complete media (Fig. 8D).

ii) Conclusions

In agreement with previous findings, these data indicate that Vps34 indeed plays an essential role in mediating amino acid activation of mTORC1. However, Vps34 is dispensable for steady state mTORC1 signaling in complete media, suggesting that mTORC1 activation by serum and other nutrients can compensate for defective amino acid-stimulation in Vps34 knockout cells.

III. Vps34 deletion enhances Rab5 activity but does not compromise early endosome functions

i) Transferrin recycling is not affected by Vps34 deletion

Vps34 localizes to the early endosome where it helps to recruit effector proteins that contain PI(3)P and Rab5 binding domains, such as EEA1, thereby regulating the delivery and sorting of endocytic cargo (Sato et al., 2001). The iron-binding molecule transferrin and its receptor are internalized to early endosomes, where the iron will dissociate, allowing the receptor and ligand to be recycled back to the plasma membrane (Spiro et al., 1996). Although some evidence indicates that wortmannin reduces the rate of transferrin recycling (Martys et al., 1996; Spiro et al., 1996), surprisingly no defect was observed in the rate of transferrin recycling in Vps34 knockout cells (Fig. 10A). As in wild-type, biotinylated-transferrin is lost from the intracellular space and accumulates in the media, indicating normal recycling. To ensure that transferrin is delivered to early endosomes in Vps34 knockout cells, we used transferrin tagged with Alexa-Fluor-594 to track its movement. Internalized transferrin colocalized with EEA1 in both WT and KO cells (Fig. 10B).

ii) EEA1 recruitment to endosomes is not affected by Vps34 deletion

Since we observed no effect of Vps34 deletion on the early endosome function of recycling, we investigated EEA1 recruitment. EEA1 is thought to be recruited to early endosomes via dual signals from Rab5-GTP and PI(3)P (Simonsen et al., 1998). To investigate whether Vps34 is responsible for PI(3)P production and EEA1 recruitment to early endosomes, we performed a Rab5 immunoprecipitation. Surprisingly, EEA1 interacted with Rab5 to a similar extent in both wild-type and Vps34 knockout cells (Fig. 10C). These findings suggest two possible scenarios: 1) PI(3)P may be produced by alternative sources such as the Class II PI3Ks (Devereaux et al., 2013; Falasca and Maffucci, 2012; Posor et al., 2013); and/or 2) a compensatory mechanism is triggered to cope with the loss of Vps34.

To investigate the role of class II PI3Ks in Vps34 knockout cells we used the pharmacological inhibitor wortmannin, which inhibits all classes of PI3Ks at high concentrations and decreases EEA1 membrane localization (Simonsen et al., 1998). Indeed, treatment with a high concentration of wortmannin led to decreased EEA1 membrane localization in wild-type cells, but not knockout cells (Fig. 9D). Likewise, endogenous Rab5 and EEA1 colocalized on small punctate structures in untreated wild-type cells, which became disperse with wortmannin treatement (70.3% of EEA1 colocalized with Rab5 in DMSO treatment; 39.1% colocalized in wortmannin treatment) (Fig. 10E). In contrast, Rab5 and EEA1 colocalized on enlarged endosomes in Vps34-deficient cells (as previously described (Johnson et al., 2006; Morel et al., 2013)), and this localization was only marginally affected by wortmannin (75.9% of EEA1 colocalized with Rab5 in DMSO treatment; 64.2% colocalized in wortmannin treatment) (Fig. 10E). This trend was observed with more clarity and in more detail by structured illumination microscopy (SIM) (Fig. 10F).

iii) Rab5 activity is elevated in Vps34 knockout MEFs

Previous reports indicate that expression of the constitutively active mutant of Rab5 can bypass the loss of EEA1 membrane localization upon wortmannin treatment (Li et al., 1995; Simonsen et al., 1998). Indeed, a GST-tagged Rab5-binding domain (GST-R5BD) that binds active Rab5-GTP revealed that Rab5-GTP levels were enhanced in Vps34 knockout cells (Fig. 10G).

iv) Conclusions

We were surprised to discover that Vps34 deletion had no effect on transferrin recycling or EEA1 recruitment to $Rab5^{+}$ early endosomes. Although others have found that the class II PI3Ks contribute to PI(3)P production, we do not find evidence that they play a role in the context of VPs34 deletion. Instead we find an increase in Rab5-GTP levels, which may compensate for the absence of Vps34 and allow efficient cargo delivery and sorting.

IV. Vps34 controls late endosome morphology and functions, and Rab7 activity

i) Late endosome morphology is dramatically altered by Vps34 deletion

We observe a dramatic accumulation of single membraned, phase-lucent vacuoles upon Vps34 deletion (Fig 1C, 6D), which others have identified as swollen late endosomes (Johnson et al., 2006). To confirm this phenotype, we incubated WT and KO MEFs with Acridine Orange, which emits green fluorescence at neutral pH and red fluorescence at acidic pH. We confirmed that the vacuoles caused by Vps34 deletion are indeed acidic (Fig. 11A). We also immunostained for early endosome protein Rab5 and late endosome/lysosome proteins Rab7 and Lamp1, and found that the vacuoles are decorated with Rab7 and Lamp1 but not Rab5 (Fig. 11B). These data confirm that the vacuoles caused by Vps34 deletion are indeed swollen late endosomes.

ii) EGFR degradation and ILV formation are abrogated in Vps34 knockout MEFs

In contrast to transferrin and its receptor, the epidermal growth factor receptor (EGFR) is internalized and degraded in lysosomes following stimulation with its ligand EGF. We therefore used EGFR degradation as a readout for endocytic trafficking through the late endosome and lysosomal degradation. While EGFR is completely degraded following 3 hours of stimulation with EGF in WT cells, we see a marked reduction in EGFR degradation in KO cells (Fig. 12A), suggesting a major defect in trafficking through the late endosome/lysosome.

To determine where the undegraded EGF and its receptor accumulate in KO cells, we utilized a GFP-EGFR construct. After overnight serum starvation, we observe GFP-EGFR localized to the plasma membrane in both wild-type and knockout cells. After stimulation with EGF for 1 or 3 hours, we observe GFP-EGFR on intracellular puncta in WT cells, but in large ring-shaped structures in KO cells (Fig. 12B). Likewise, Alexa-Fluor-647 EGF localizes to punctate Rab7+ Lamp1+ endosomes in wild-type cells, but to the limiting membrane of enlarged

Rab7+ Lamp1+ endosomes in knockout cells (Fig. 12C). These data suggest that EGF and its receptor are not being sequestered into intraluminal vesicles, an important feature of endosome maturation, which primes endocytic cargo for degradation (Huotari and Helenius, 2011).

iii) Lysosomal degradative capacity is abrogated by Vps34 deletion

The decreased EGFR degradation we observe in KO cells could be due to a failure of cargo delivery or a failure of proteolytic capacity in lysosomes. To determine the degradative capacity of lysosomes in KO MEFs, we utilized DQ BSA which is trafficked through the late endosome and fluoresces upon proteolytic cleavage in the lysosome. In WT cells we observe DQ BSA fluorescence which partially colocalizes with an internalization control marker, Dextran Oregon Green (Fig. 12D). On the other hand, we do not detect any DQ BSA fluorescence in Vps34 knockout cells, reflecting a marked reduction in lysosomal proteolytic capacity. We also observe slightly lower uptake of Dextran Oregon Green in knockout cells.

To further investigate the degradative capacity of Vps34 knockout cells, we examined the steady state level of cathepsin D maturation. Immature cathepsin D is trafficked from the ER to the Golgi before reaching the late endosome/lysosome, where it is cleaved into its intermediate and then mature form by other cathepsins (Zaidi et al., 2008). Compared to wild-type, we find a large increase in immature and intermediate forms coupled with a decrease in mature cathepsin D in KO cells (Fig. 12E). These data could represent a defect in either the delivery of cathepsin D to the late endosome/lysosome, or a defect in the final proteolytic cleavage step. Regardless, it is clear that the deletion of Vps34 leads to severe defects in lysosomal degradative activity.

iv) Rab7 activity is elevated by Vps34 deletion

Rab7 is a small GTPase which regulates membrane fusion and fission reactions of the late endosome, including fusion of the late endosome with lysosomes. Since we observe obvious defects in late endocytic functions in Vps34 knockout cells, we sought to investigate the Rab7 activity level in these cells. Using a GST-tagged Rab7 binding domain (GST-R7BD (Peralta et al., 2010)) pull down, we were surprised to find elevated levels of Rab7-GTP in Vps34 knockout cells (Fig. 13A), which is refractory to serum starvation or EGF stimulation (Fig. 13B).

Rab7 regulates late endosome functions through the recruitment of effector proteins such as RILP. To determine if Rab7 is able to recruit its effectors in Vps34 KO cells, we expressed

GFP-RILP and observed its colocalization with endogenous Rab7. As expected, overexpression of GFP-RILP causes clustering of $Rab7^+$ late endosomes near the microtubule organizing center in wild-type cells (Harrison et al., 2003), and imaging with structured illumination microscopy revealed the spherical nature of these clustered endosomes (Fig. 13C). We also observe colocalization between GFP-RILP and Rab7 in Vps34 knockout cells, though in contrast, they both reside on the membrane of swollen late endosomes (Fig. 13C). These data suggest that Rab7 is GTP-bound and able to recruit its effector RILP despite the loss of Vps34.

v) Vps34 controls Rab7 activity through Armus

We were intrigued by the finding that Vps34 deletion leads to elevated Rab7 activity, and decided to investigate further. The activity of Rab GTPases is modulated by GTPase activating proteins (GAPs) and guanine nucleotide exchange factors (GEFs). Although no mammalian Rab7 GEFs have been identified so far, Armus was recently confirmed as a Rab7 GAP (Carroll et al., 2013). Expression of Armus was sufficient to reduce Rab7-GTP levels in both wild-type and knockout cells (Fig. 14A).

We therefore sought to determine if Vps34 regulates Rab7 activity through Armus recruitment. Armus was described to have varying localizations in epithelial cells, one of which being intracellular puncta (Frasa et al., 2010). To determine the role of Vps34 in Armus localization, we created a stable Vps34 knockdown in HeLa cells (Fig. 14B). Similar to Vps34 knockout MEFs, shVps34 HeLa cells acquired a vacuolated morphology, presumably representing swollen late endosomes (Fig. 14C). Expression of RFP-Armus in shScramble control cells revealed a punctate localization which is almost completely lost with Vps34 knockdown (Fig. 14D). These data suggest that Vps34 may play a role in the regulating the localization of Rab7 GAP Armus.

We hypothesized that Vps34 may regulate the localization of Armus by recruiting it to $PI(3)P^+$ membranes. Indeed, Armus has a predicted PH domain which could mediate PI(3)P binding (Lemmon, 2003). It has been previously reported that overexpression of GFP-2xFYVE can sequester PI(3)P, thereby displacing other PI(3)P binding proteins (Carpentier et al., 2013). Therefore, to investigate the interaction of Armus with PI(3)P we co-expressed RFP-Armus with GFP-2xFYVE. We find that the expression of GFP-2xFYVE abolishes RFP-Armus puncta in

non-targeting control cells (Fig. 14E). Importantly, GFP-2xFYVE does not form puncta in shVps34 cells, confirming the loss of PI(3)P in these cells (Fig. 14E).

In collaboration with Vania Braga from Imperial College of London, we sought to investigate the interaction of Armus with PI(3)P more directly. To this end, a protein-lipid overlay using the PH domain of Armus (GST-Armus-PH) was performed. A positive interaction between Armus-PH and PI(3)P, as well as PI(4)P, and phosphatidic acid was detected (Fig. 14F). GST-PLC-δ1-PH binding to PI(4,5)P2 was used as a positive control.

vi) Rab7 and v-ATPase mediate vacuolization in Vps34 knockout cells

Intracellular vacuolization has been observed upon inhibition of Vps34 (Jaber et al., 2012; Johnson et al., 2006; Reaves et al., 1996; Ronan et al., 2014). In addition, Rab7 activation has been reported to be essential for vacuolization in several conditions such as in yeast and in *Helicobacter pylori* infection (Genisset et al., 2007; Haas et al., 1995; Papini et al., 1997; Schimmoller and Riezman, 1993). Since we observed Rab7 hyperactivation in Vps34 knockout cells, we tested whether the vacuolization in Vps34-deficient cells was due to reduced Armus recruitment and Rab7 hyperactivation. Indeed, silencing Rab7 or ectopic expression of Armus in Vps34 knockout MEFs led to a complete reversal of vacuolization (Fig. 15A-C).

The vacuolar H^+ v-ATPase mediates the acidic pH of endosomes and lysosomes, which is essential for normal degradative functions and may also be required for fusion (Baars et al., 2007; Kawai et al., 2007; Klionsky et al., 2008; Peters et al., 2001; van Weert et al., 1995). In addition, hyperactivation of v-ATPase via *H. pylori* toxin VacA produces vacuolization. It is speculated that the influx of protons by v-ATPase triggers osmotic swelling of endosomes, leading to vacuolization (Genisset et al., 2007; Papini et al., 1996; Papini et al., 1997). Interestingly, Rab7 can modulate the activity of v-ATPase via its effector RILP, which recruits the v-ATPase subunit V1G1 to endosome membranes to positively regulate v-ATPase activity (De Luca et al., 2014). Since we observed a dramatic increase in Rab7 activity in Vps34 knockout cells, we reasoned that v-ATPase activity may contribute to vacuolization in Vps34 KO cells. Indeed, treatment with the v-ATPase inhibitors bafilomycin A1 (BafA1) or concanamycin A led to a dramatic reversal of the vacuolization in Vps34 knockout cells (Fig. 15D). This effect was not observed with other lysosome inhibitors such as E64D and pepstatin

A, chloroquine, or calcium chloride (Fig. 15E). Moreover, vacuolization was also inhibited by silencing V1G1 (a subunit of v-ATPase) in HeLa cells with Vps34 knockdown (Fig. 15F, G).

vii) Conclusions

These data suggest that Vps34 may recruit Rab7 GAP Armus to endosomes via PI(3)P production to modulate Rab7 activity and regulate late endosome and lysosome functions. In the absence of Vps34, defective Armus recruitment leads to Rab7 hyperactivation. We also find that Rab7 and v-ATPase contribute to the vacuolization of late endosomes in Vps34-deficient cells, suggesting that v-ATPase may also be hyperactivated by Vps34 deletion.

V. The functions of Vps34 are dependent on its catalytic activity

i) Reconstitution of wild-type and kinase-dead Vps34

To determine whether the defects we observed in $Vps34^{f/f}$ MEFs are specific consequences of the loss of Vps34 kinase activity, we expressed HA-tagged Vps34 wild-type or a kinase-dead (KD) mutant, K771A, that fails to interact with the PI substrate (Miller et al., 2010) in Vps34-deficient MEFs. The stability of the Vps34-Vps15-Beclin 1 complex is inter-dependent, meaning loss of one complex member leads to degradation of the others (Itakura et al., 2008). Indeed, we observe a decrease in the levels of Beclin 1 in Vps34 knockout cells (Fig. 16A). Reconstitution with either wild-type or Vps34 KD in the Vps34 knockout MEFs rescued the protein levels of Beclin 1, indicating that the Vps34 KD mutant is capable of forming the complex (Fig. 16A). We and others observe a large increase in the protein level of Rubicon, a negative regulator of autophagy, in Vps34 knockout cells (Devereaux et al., 2013). Interestingly, reconstitution with wild-type, but not KD Vps34 rescues the expression of Rubicon. This may reflect the regulation of Rubicon by autophagic degradation (Fig. 16A).

ii) Characterization of wild-type and kinase-dead reconstituted MEFs

Consistently, wild-type but not Vps34 KD rescued the block in autophagy flux in Vps34 knockout cells (Fig. 16B). Moreover, Vps34 wild-type but not the KD mutant rescued the vacuolization phenotype (Fig. 16C), EGFR degradation (Fig. 16D), and abrogated mTOR signaling as measured by the phosphorylation of S6 (Fig. 16E).

iii) Conclusions

These data indicate that the defective autophagy, endocytosis, and mTOR signaling in Vps34 knockout MEFs are specifically due to Vps34 ablation and that these functions are dependent on Vps34 catalytic activity. We can also reasonably conclude that the effects of Vps34 deletion cannot be attributed to loss of binding partners such as Beclin 1.

4

Discussion

I. The role of Vps34 in mammalian autophagy

Although it is well accepted that Vps34 plays an essential role in autophagy in yeast, Vps34 is the only PI 3-kinase in yeast while mammals have a large PI3K gene family. Attempts to clarify the role of mammalian Vps34 with the plieotropic inhibitors wortmannin or 3-MA cannot distinguish the contributions of individual PI 3-kinases. Thus the role of Vps34 in mammalian autophagy has not been clearly defined. While whole body knockout is embryonic lethal in mice (Zhou et al., 2011), genetic deletion of Vps34 in sensory neurons produced dramatic neurodegeneration but surprisingly did not affect LC3-II levels, leading the authors to conclude that Vps34-independent mechanisms of autophagy exist in mammals (Zhou et al., 2010).

In an effort to confirm these observations and potentially characterize Vps34-independent autophagy, we created mouse models with specific deletion of Vps34 in the heart or liver (Fig. 1A). We observe many severe physiological effects of Vps34 deletion, such as hepatomegaly (Fig. 2B, C), hepatic steatosis (Fig. 2D), cardiac hypertrophy (Fig. 3A) and defective contractility (Fig. 3C and Table 1), which ultimately leads to death (Fig. 2E, 3D). These phenotypes can be at least partially explained by defective autophagy, since they are also observed in $Atg7^{-/-}$ and $Atg5^{-/-}$ animals (Komatsu et al., 2005; Nakai et al., 2007; Singh et al., 2009). However, we cannot rule out the possibility that these phenotypes are caused by defects in other pathways, such as endocytosis.

In addition, we isolated MEFs to investigate the effect of Vps34 deletion on autophagy at the molecular level. Although we also detect higher levels of LC3-II in the MEFs as well as the knockout mice (Fig. 2A, 4A, 5A-B, 6A-B), steady state levels of LC3-II are not a good representation of dynamic autophagic flux. Indeed, multiple assays for autophagy flux indicate a major deficiency in Vps34-null mice and MEFs (Fig. 4B-D, 6B-D, 7A-B), indicating that the increased LC3-II represents blocked autophagic flux in KO. Thus, although Vps34-independent mechanisms of autophagy may exist (Codogno et al., 2012; Devereaux et al., 2013), our data suggests that Vps34 is a master regulator of mammalian autophagy.

We briefly investigated the precise molecular mechanism of Vps34 in autophagy regulation. DFCP1 and the WIPI family (WIPI1-4) have been identified as PI(3)P binding proteins which localize to the omegasome, although their exact functions in phagophore formation are unclear. We find a complete absence of DFCP1 and Atg12 puncta in Vps34 KO

cells (Fig. 6E), which suggests that Vps34 regulates phagophore formation. However, further characterization of phagophore formation in the Vps34 KO cells is warranted, such as immunofluorescence for WIPI1/2 and electron microscopy for phagophore structures.

In addition, Vps34 is known to regulate vesicle fusion reactions via interactions with Rab GTPases and tethering complexes such as HOPs and EEA1, which also regulate SNARE pairing (Lindmo and Stenmark, 2006; Starai et al., 2008). Interestingly, Atg9- and Atg16L1-positive vesicles fuse to generate the phagophore, and their fusion depends on various SNARE proteins (Moreau et al., 2015; Puri et al., 2014). Interestingly, the SNARE Vamp8 interacts with PI(3)P in vitro (Dai et al., 2007), and although Vamp8 has not been implicated in autophagosomes formation, the interaction of other SNAREs with PI(3)P has not been investigated.Thus, an attractive hypothesis is that Vps34 may also regulate phagophore formation by regulating Atg9- and Atg16L1-positive vesicle docking and fusion. Further work, such as immunofluorescence of Atg9 or Atg16L, or an investigation of SNARE pairing, will be needed to concretely affirm this hypothesis.

In light of the lack of phagophores and autophagosomes in Vps34 KO mice and MEFs, we were quite surprised to detect the lipidated form of LC3 (LC3-II). LC3 is thought to be lipidated on the growing phagophore membrane, hence its use as an indicator for autophagosome formation (Ichimura et al., 2004). Although PI3K inhibitors wortmannin and 3-MA have been shown to inhibit starvation-induced LC3 lipidation (Wu et al., 2010), LC3-II is detectable in Vps34Δ yeast (Obara et al., 2008). Interestingly, this suggests that another wortmannin and 3-MA sensitive kinase is responsible for the regulation of LC3 lipidation. In addition, LC3 is lipidated in Atg14L or Beclin 1 siRNA treated cells, and FIP200$^{-/-}$ MEFs (Hosokawa et al., 2009; Zhong et al., 2009). Together with our data, this suggests that LC3 lipidation may not be regulated by the Vps34 or ULK1 complexes, and instead may occur in parallel. Since LC3 is accumulated in large intracellular aggregates in the KO cells (Fig. 7A-B, 8A-B), it is possible that Vps34 dictates the proper site for LC3 lipidation on phagophores/autophagosomes via PI(3)P production (Axe et al., 2008). An interesting experiment would be to target Vps34 to an ectopic membrane via addition of a tag, and investigate whether LC3 lipidation occurs at this ectopic site.

II. The role of Vps34 in nutrient-induced mTOR signaling

Vps34 has been implicated in amino acid-induced mTORC1 signaling *in vitro* and *in vivo*. Consistent with previous work, we find that amino acid-induced mTORC1 signaling is severely reduced in Vps34 KO cells (Fig. 9A-B). However, we find that steady state mTORC1 signaling is not affected, suggesting that input from serum and other nutrients are not dependent on Vps34, and are able to support basal levels of mTORC1 activity (Fig. 9A-D). This also suggests that the growth defect we observe in Vps34 KO MEFs cannot be attributed to mTORC1 signaling (Fig. 1D).

While some evidence suggests that Vps34 has a direct role in amino acid-induced mTORC1 activation via phospholipase D1 (PLD1) activation (Yoon et al., 2011), another possibility is that Vps34 regulates mTORC1 activation indirectly by controlling late endosome/lysosome integrity (Flinn et al., 2010). Because we find severe defects in late endosome/lysosome functions in Vps34 KO cells, the latter hypothesis is a definite possibility. Preliminary efforts to clarify mTOR localization to lysosomes in KO cells were unsuccessful in my hands (data not shown). However, it would be interesting to determine if PLD1, mTORC1, and Rheb are properly localized to the late endosome/lysosome in Vps34 KO cells.

As we have uncovered a previously unappreciated role for Vps34 in regulating v-ATPase activity, another possible angle for Vps34 regulation of mTORC1 is through v-ATPase. Amino acid-stimulated mTORC1 activity is dependent on the amino acid transporter PAT1 (Zoncu et al., 2011), and protons supplied by v-ATPase provide a driving force for PAT1 (Boll et al., 2004). Indeed, we find that Bafilomycin A1 treatment to reduce v-ATPase hyperactivity in Vps34 KO cells partially rescues amino acid-induced mTORC1 activity (data not shown). Further work will be needed to characterize v-ATPase activity and the effect on PAT1 and mTORC1 in Vps34 KO cells.

III. The role of Vps34 in Rab5-mediated early endocytosis

Various lines of evidence suggest that Vps34 has a major role at the early endosome by interacting with Rab5 and co-recruiting effectors containing PI(3)P and Rab5 binding domains. Thus, we were surprised to find no effect of Vps34 deletion on transferrin recycling (Fig. 10 A,B) or EEA1 recruitment to $Rab5^{+}$ endosomes, although they were enlarged (Fig. 10 C-F).

Based on the existing literature, we hypothesized that class II PI3Ks could produce PI(3)P at the early endosome. However, treatment with a high dose of wortmannin which inhibits all three classes of PI3Ks did not reduce EEA1 localization in Vps34 KO cells, suggesting that the class II PI3Ks are not responsible for early endosome functions in Vps34 KO cells (Fig. 10D-F). However, since wortmannin is very pleiotropic and likely has unidentified targets, it is not the optimal mechanism for testing the involvement of class II PI3Ks. Unfortunately, efforts to knockdown class II PI3K-C2α and C2β were unsuccessful in my hands. Recent work demonstrated that PI3K-C2α and -β are responsible for 15-20% of PI(3)P levels (Devereaux et al., 2013). In addition, C2α-mediated production of $PI(3,4)P_2$ is essential for the scission of clathrin coated pits at the plasma membrane and for the clathrin-mediated endocytosis of transferrin (Posor et al., 2013). Thus, we cannot rule out a possible role for these enzymes at the early endosome. In addition, the sequential dephosphorylation of $PI(3,4,5)P_3$ into PI(3)P has been suggested as another viable route for Vps34-independent PI(3)P at the early endosome (Shin et al., 2005), which has not been explored in the context of Vps34 deletion.

Expression of the constitutive active mutant of Rab5 can bypass wortmannin inhibition of EEA1 localization (Li et al., 1995; Simonsen et al., 1998), suggesting that an increase in Rab5 activity may be able to sustain EEA1 recruitment despite the loss of Vps34. Indeed, we discovered that Rab5-GTP levels are elevated in Vps34 knockout cells (Fig. 10G). This increase in Rab5 activity may be sufficient to recruit EEA1 to endosomes and thus support early endosome functions such as vesicle docking and fusion, cargo sorting, and recycling. Consistent with this idea, both EEA1 and Rabenosyn-5 contain two Rab5 binding domains, suggesting that they could potentially bind two molecules of Rab5-GTP to mediate membrane tethering (Kummel and Ungermann, 2014). In order to support our hypothesis it will be important to demonstrate that reducing Rab5 activity in knockout cells abolishes EEA1 localization and transferrin recycling. Efforts to reduce Rab5 activity through overexpression of a Rab5 GAP were unsuccessful (data not shown).

While we find elevated Rab5-GTP levels in Vps34 KO cells, we do not yet know how Vps34 mechanistically regulates Rab5 activity. Because Mon1 binds PI(3)P and displaces the Rab5 GEF Rabex5 to reduce Rab5-GTP (Poteryaev et al., 2010), an attractive hypothesis is that Vps34 may recruit Mon1 to early endosomes. In addition, TBC-2 acts as a Rab5 GAP in *C. elegans* (Chotard et al., 2010), and its recruitment to endosomes is regulated by Vps34 (Law *et*

al., in submission). Interestingly, there are two TBC-2 homolog in mammals, Armus and TBC1D2B. Since we have shown that Armus localization is inhibited by Vps34 deletion (Fig. 14D-F), it will be very interesting to determine if the loss of Armus also contributes to the increase in Rab5-GTP we observe in Vps34 knockout cells. However, the increase in Rab5 activity could represent a compensation mechanism, rather than a direct effect of Vps34 deletion, due to the fact that short term PI3K inhibition by wortmannin reduces EEA1 membrane localization, while permanent Vps34 deletion does not (Fig. 10D-F). It may be difficult to tease apart these different scenarios in future work.

IV. The role of Vps34 in Rab7-mediated late endocytosis

In contrast to the preservation of early endosome functions, we find severe defects in late endosome functions in Vps34 knockout cells, such as late endosome morphology (Fig. 11 A-B), EGFR degradation (Fig. 12A-C), protease activity (Fig. 12D) and cathepsin maturation (Fig. 12E). These results are consistent with previous observations using other methods to inhibit Vps34, and suggest that Vps34 has a major role in regulating late endosome functions.

Importantly, we find that the loss of Vps34 is associated with a dramatic increase in Rab7-GTP levels (Fig. 13A-B). Rab7 effectors such as RILP and FYCO1 mediate endosome motility, allowing late endosomes to interact with lysosomes (Wang et al., 2011). Although we find that RILP is recruited to enlarged $Rab7^{+}$ vacuoles in Vps34 KO cells (Fig. 13C), we did not explore the localization of FYCO1, which is also a PI(3)P binding protein (Pankiv et al., 2010). As such, endosome motility could be an interesting subject for future studies.

We also find that Vps34 deletion leads to a loss of Rab7 GAP Armus localization (Fig. 14D), suggesting that Vps34 regulates Rab7 activity through recruitment of Armus. Indeed, we confirm that the PH domain of Armus interacts with PI(3)P (Fig. 14F). These results identify a previously unappreciated connection between Vps34 and Rab7, and may help explain how Vps34 inhibition or deletion compromises late endosome functions.

Interestingly, knockdown of Rab7 or overexpression of Armus reverses vacuolization in Vps34 KO cells (Fig. 15A-C), suggesting that Rab7-mediated fusion reactions may be necessary for vacuolization. As Rab7 can control v-ATPase activity through RILP (De Luca et al., 2014), and as v-ATPase has been shown to play a role in vacuolization under other conditions (Genisset

et al., 2007), Rab7 may also regulate vacuolization through v-ATPase. We therefore investigated the role of v-ATPase in vacuolization of Vps34 KO cells. Indeed, specific inhibition of v-ATPase with Bafilomycin A1 or Concanamycin A (Fig. 15D), but not general lysosome inhibition (Fig. 15E), reverses vacuolization in knockout cells. This suggests that v-ATPase is required for vacuolization in Vps34 knockout cells, and that deletion of Vps34 may hyperactive v-ATPase. More work is required to determine the activity of v-ATPase in knockout cells and whether Vps34 may regulate v-ATPase through Rab7-RILP recruitment of V1G1.

Although v-ATPase inhibition reversed vacuolization, chloroquine (CQ) did not (Fig. 15E). Because chloroquine acts as a weak base to dissipate endosome pH, this suggests that the role of v-ATPase in vacuolization may extend beyond pH regulation. Interestingly, the endosome/lysosome contains multiple transporters and channels, and their activities can be co-regulated (Huotari and Helenius, 2011). Thus, it will be interesting to determine if flux of other ions such as Ca^{+2}, Na^{+} or K^{+} are affected by Vps34 deletion and are contributing to vacuolization.

It is important to note that the defects we observe in the Vps34-deficient MEFs are likely due in part to the loss of $PI(3,5)P_2$. Inhibition or genetic ablation of PIKfyve (which produces $PI(3,5)P_2$ from PI(3)P) also leads to vacuolization caused by enlargement of late endosomes, and decreases ILV formation (Shisheva, 2008). Importantly, expression of wild-type Vps34 in Vps34 knockout cells does not rescue vacuolization if PIKfyve is chemically inhibited, proving that PIKfyve loss is involved in vacuolization of Vps34 knockout cells (Ikonomov et al., 2015). Although the precise cellular mechanism of PIKfyve is not defined, it may control endosome fission and fusion reactions by regulating calcium release via TRPML channels (Dong et al., 2010; Ikonomov et al., 2006). Importantly, however, expression of kinase-dead PIKfyve does not alter EGFR degradation or cathepsin D maturation (Ikonomov et al., 2003), suggesting that the defects we observe in EGFR degradation and cathepsin D maturation in Vps34 knockout cells cannot be attributed to loss of $PI(3,5)P_2$.

Despite elevated Rab7 activity, lysosomal degradation remains compromised in Vps34 KO cells (Fig. 12D). Because we know that endocytic cargoes such as EGFR are able to reach late endosomes (Fig. 12C), we hypothesize that the defect lies either in late endosome-lysosome fusion or proteolytic degradation of the cargo. Although we do not know how Vps34 may mechanistically regulate fusion or degradation, there are a number of reasonable possibilities.

One possibility is that Rab7-GTP alone is not sufficient for fusion, and another signal is required. This second signal could potentially be regulated by PI(3)P or PI(3,5)P_2. Calcium is required for fusion processes (Pryor et al., 2000), which, as previously discussed, could be disrupted by Vps34 deletion and PI(3,5)P_2 loss. Another possibility is that elevated activities of Rab7 or v-ATPase in KO cells are inhibitive to fusion reactions.

Furthermore, we confirm that ILV formation is blocked in Vps34 knockout cells, causing EGFR to accumulate on the limiting membrane of endosomes (Fig. 12B, C). A major function of ILV formation is to prime endocytic cargoes for degradation because the limiting membrane of endosomes and lysosomes are protected from proteolytic cleavage by heavily glycosylated proteins such as Lamp1/2 (Huotari and Helenius, 2011; Wilke et al., 2012). Thus, the fact that EGFR accumulates on the limiting membrane suggests that even if late endosome-lysosome fusion occurred in Vps34 knockout cells, EGFR would not be degraded. It would be interesting to determine the degradation rate of a soluble endocytic cargo molecule.

Another possibility is that proteolytic degradation is not optimal in the Vps34 knockout cells due to abnormal v-ATPase activity, which regulates endosomal pH and thus hydrolase activity. Indeed, we find a defect in cathepsin D maturation in Vps34 KO MEFs (Fig. 12E); however, this could also represent a failure of cathepsin D delivery rather than processing in lysosomes. In sum, it is likely that a combination of these possibilities is at play in the Vps34 knockout cells. However, it will be important to determine the precise cause of blocked degradation to fully understand the role of Vps34 in endocytic trafficking.

While this work generated a brief characterization of endocytic trafficking in the context of Vps34 deletion, there are many questions still left to pursue. One such avenue is the consequence of blocked EGFR degradation in Vps34 knockout cells. Previous work demonstrates that a failure to sequester growth factor receptors into ILVs will result in inappropriate and persistent growth factor signaling, which often leads to detrimental consequences and cell death (Eden et al., 2009; Katzmann et al., 2002; Rush et al., 2012). Although we observe a growth defect in the Vps34 KO MEFs, suggesting that EGFR signaling does not result in proliferation, it would be interesting to investigate the kinetics of the EGFR signaling pathway in the KO cells.

In addition, the loss of ILV formation in Vps34-deficient cells may have more physiological consequences than we have identified thus far. For example, while amyloid

precursor protein (APP) is internalized to ILVs in wild-type cells, it is abnormally localized to the limiting membrane of endosomes upon Vps34 or Hrs knockdown. Vps34 knockdown also increases the amyloidogenic processing of APP, suggesting that the abnormal localization renders APP more susceptible to cleavage and processing (Morel et al., 2013). Of note, PI(3)P levels are dramatically reduced in mouse models of Alzheimer's disease as well as the brains of patients with Alzheimer's (Morel et al., 2013). Therefore, it would be interesting to characterize the physiological effects of Vps34-mediated endocytic trafficking.

V. The role of PI 3-kinase activity in Vps34 functions

Because kinase-independent functions have been identified for the Class I PI3K p110β (Ciraolo et al., 2008; Dou et al., 2010; Dou et al., 2013), we were interested to determine if Vps34 has kinase-independent functions as well. Reconstitution of a kinase-dead Vps34 mutant (K771A) did not rescue the defects in autophagy, endocytic degradation, endosome morphology or mTORC1 activity we observe in Vps34 KO cells (Fig. 16), suggesting that these functions of Vps34 are dependent on its lipid kinase activity.

Based on the crystal structure of Vps34, the K771A mutant will be unable to bind to its substrate phosphatidylinositol (PI) (Miller et al., 2010). However, Vps34 also possesses protein kinase activity, and although *in vivo* targets have not been identified (Backer, 2008), it would be interesting to determine if abolishment of the protein kinase activity of Vps34 produced a different phenotype.

5

Conclusions and Perspectives

In summary, the data generated by this dissertation (in collaboration with other scientists) provides a clearer understanding of the roles of mammalian Vps34 (Illustration 4). First, we confirm that like in yeast, mammalian Vps34 is required for autophagy. At the molecular level, we find that Vps34 is important for phagophore formation, and thus in the absence of Vps34 no mature autophagosomes or autophagic flux is detected. We also confirm that Vps34 is required for amino acid-induced mTORC1 activation, but not for steady state mTORC1 signaling.

A major contribution of this work is a better understanding of the role of Vps34 in the endocytic pathway. We find that the deletion of Vps34 does not compromise early endosome functions, but that this may represent a compensation mechanism through the enhancement of Rab5 activity. Furthermore, we find that Vps34 regulates Rab7 activity through regulation of the localization of the Rab7 GAP, Armus. Finally, we uncover some mechanistic details to explain the vacuolization observed upon Vps34 deletion or inhibition. We find that vacuolization is dependent on Rab7 and v-ATPase, suggesting that Vps34 may regulate v-ATPase activity. This suggests that a deregulation of Vps34 activity may be involved in certain physiological conditions where vacuolization is observed (Aki et al., 2012).

Since our generation and characterization of Vps34-deficient liver and heart (Jaber et al., 2012), many more Vps34 knockout mouse models have been created, which have uncovered more physiological roles of Vps34. For example, deletion of Vps34 in T cells found that it is required for T cell survival and autophagic flux (Parekh et al., 2013; Willinger and Flavell, 2012), and IL-7 signaling (McLeod et al., 2011).

Deletion of Vps34 in mouse podocytes, specialized kidney cells, also compromises autophagy flux, early endocytosis and cell viability (Bechtel et al., 2013). Likewise, deletion of Vps34 in cardiac and skeletal muscle leads to cardiac hypertrophy and muscular dystrophy, with phenotypes similar to that of myotubular myopathy (Reifler et al., 2014). Interestingly, deletion of the regulatory subunit Vps15 in skeletal muscle of mice leads to decreased Vps34 protein and PI(3)P levels, and phenocopies autophagic vacuolar myopathies such as Danon's disease. These diseases are caused by abnormal lysosome functioning, and overexpression of Vps34 and Vps15 in cells from patients of Danon's disease can partially rescue some of the characteristic defects (Nemazanyy et al., 2013). Likewise, deletion of the Vps34-binding partner Beclin 1 in neurons reduces Vps34 protein and activity levels, and also leads to severe neurodegeneration (McKnight et al., 2014). Thus, the disruption of Vps34 may be involved in multiple disease states.

Furthermore, an interest in pharmacological inhibition of autophagy for cancer treatment has lead to the recent discovery of multiple Vps34 inhibitors (Bago et al., 2014; Dowdle et al., 2014; Pasquier et al., 2015; Ronan et al., 2014). A screen for autophagy inhibitors identified a highly selective Vps34 inhibitor, SAR405, which does not inhibit class I or II PI3Ks or other protein kinases, including mTOR. Similar to our Vps34 knockout cells, treatment of cultured cells with SAR405 induces cytoplasmic vacuolization which are positive for lysosome marker Lamp1, and inhibits cathepsin D maturation. In addition, SAR405 was shown to synergize with the mTOR inhibitor everolimus to inhibit cell proliferation, suggesting its possible use for the treatment of cancer (Ronan et al., 2014). It will be interesting to see if these Vps34 inhibitors reach clinical trials and how they will fare. However, due to our understanding of the multiple functions of Vps34 and its role in promoting homeostasis, we predict that systemic inhibition of Vps34 will have serious side effects.

6

Figures, Tables and Illustrations

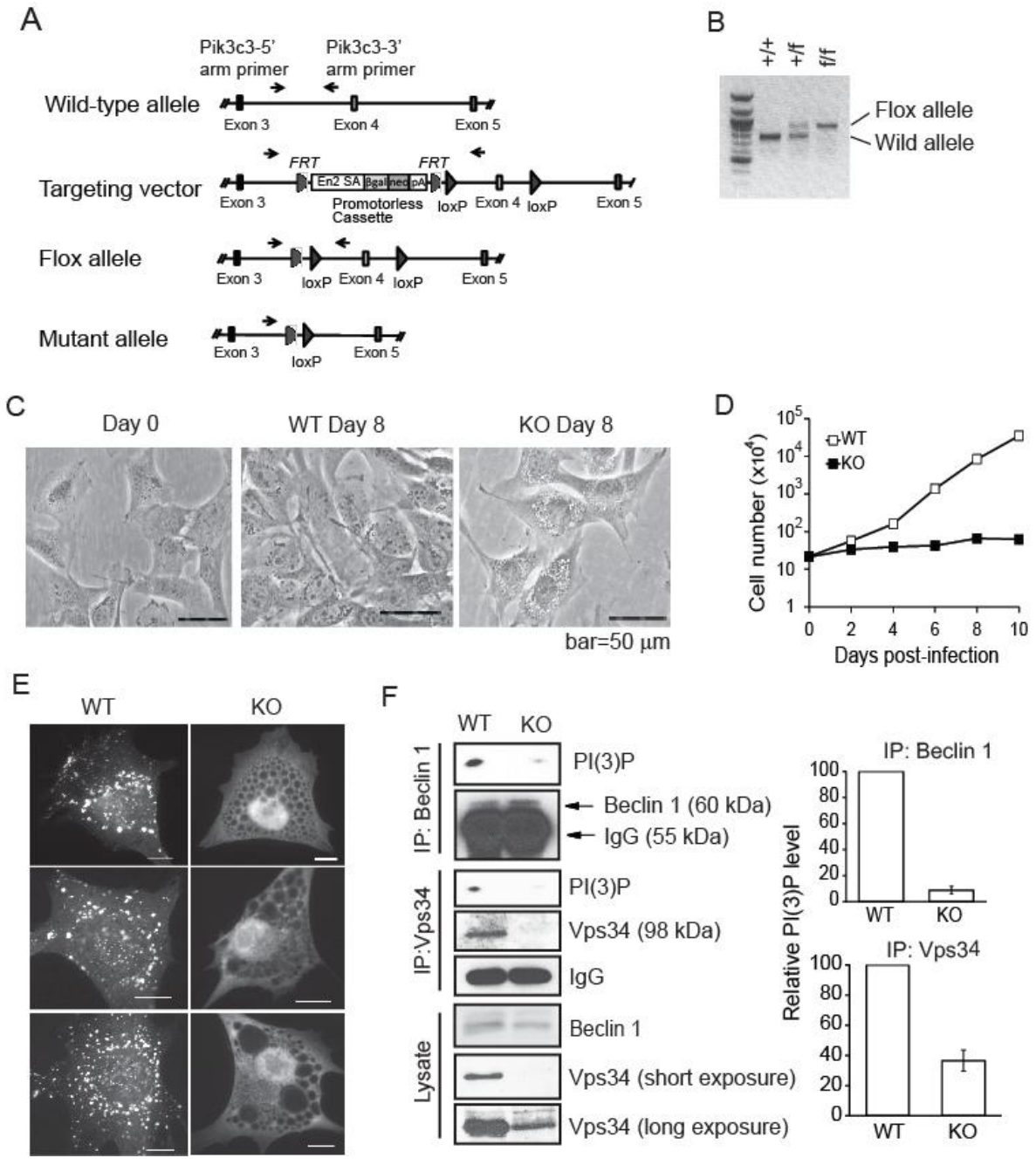

Figure 1. Knockout strategy and validation of Vps34 knockout MEFs. (A) Schematic representation of the Vps34 knockout strategy. Excision of exon 4 will produce a premature stop codon, leading to the deletion of 755 of the 887 amino acids of Vps34. (B) PCR analysis with the Pik3c3-5' and 3' arm primers (denoted in (A)) using genomic DNA isolated from MEFs generated from $Vps34^{+/f}$ breeding pairs. (C) Vps34 deletion leads to cytoplasmic vacuolization. Following addition of adenoviral control (WT) or adenoviral-Cre (KO) cells were imaged by phase-contrast microscope. (D) Vps34 deletion leads to a severe growth defect. Cells were counted via hemocytometer on the indicated days following adenovirus infection, and cell number is plotted. Data shown is an average of three countings +/- SEM. Error bars are too

narrow to be seen. (E) Deletion of Vps34 leads to ablation of PI(3)P. GFP-2xFYVE was stably expressed in Vps34f/f MEFs. Following adenoviral control (WT) or adenoviral-Cre (KO) cells were fixed and imaged by deconvolution microscope. Three representative images are shown. (F) Deletion of Vps34 reduces PI(3)P production. WT or KO cells were subjected to Beclin 1 or Vps34 immunoprecipitation and precipitates were analyzed for kinase activity. Western blots of the immunoprecipitates and cell lysates were probed with the indicated antibodies. Vps34 activity (indicated by the level of ^{32}P-labeled PI(3)P on the autoradiograms) was quantified by densitometry and normalized to that of the vector-infected cells. The average of three independent assays ± SEM is shown at right.

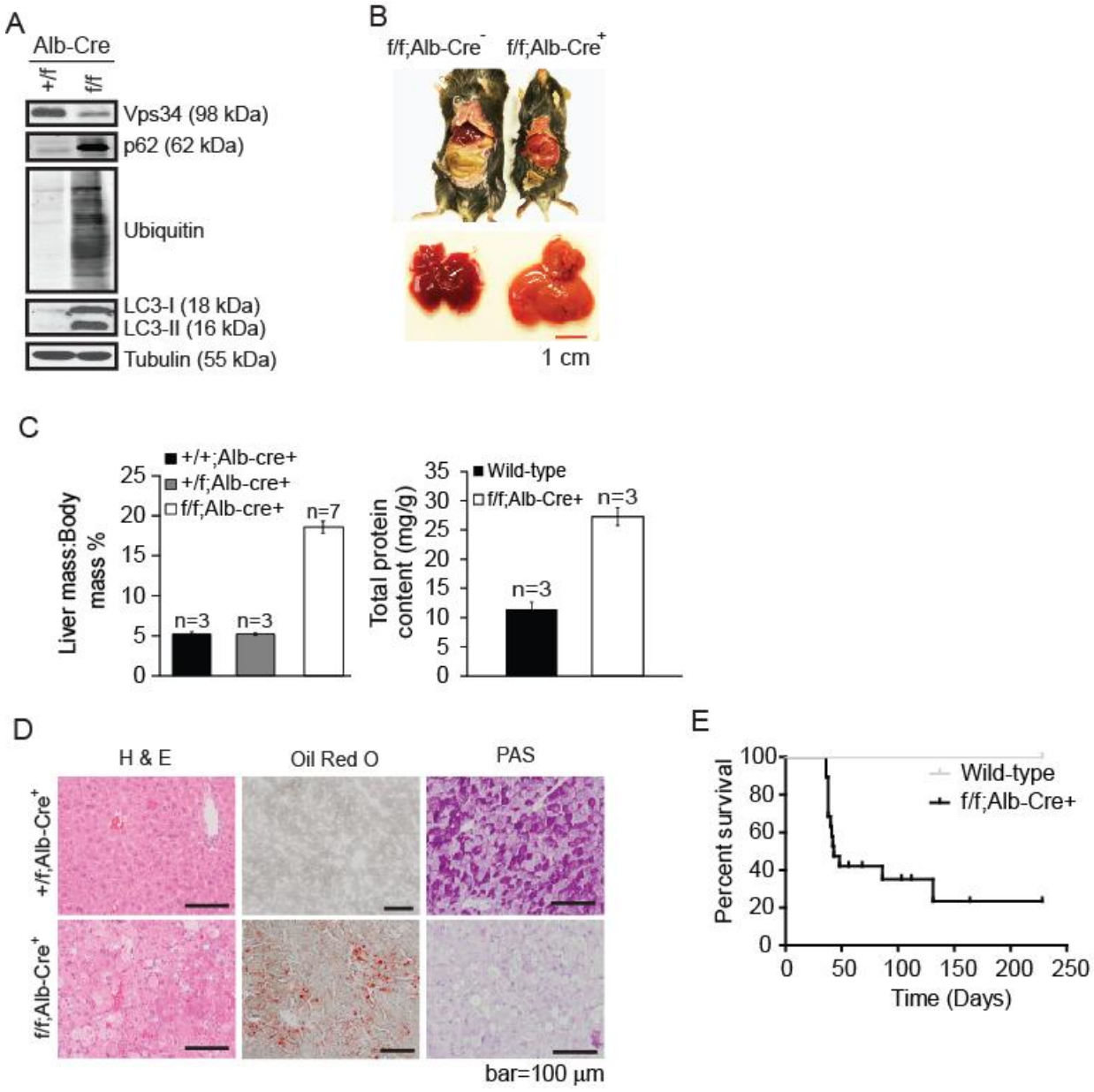

Figure 2. Deletion of Vps34 in the liver leads to hepatomegaly and hepatic steatosis. (A) Autophagy proteins p62, LC3-I/II, and poly-ubiquitinated proteins accumulate in Vps34-null hepatocytes. Lysates from primary hepatocytes with indicated genotypes were probed with indicated antibodies. (B) Vps34 deletion leads to hepatomegaly. Gross anatomical views of representative mice and livers with indicated genotypes. (C) Vps34 deletion leads to hepatomegaly and protein accumulation. The mass of livers with indicated genotypes was measured and expressed relative to body mass (left graph). Total protein content of wild-type and Vps34-null livers was quantified and expressed relative to the body weight (right graph). (D) Vps34 deletion leads to hepatic steatosis and a decrease in glycogen deposits. Livers isolated from mice with indicated genotypes were stained with hematoxylin and eosin (H&E), Oil Red O,

or periodic acid schiff (PAS). Representative images are shown. (E) Mice with Vps34-null livers have reduced viability. Kaplan-Meier survival curve of Alb-Cre;$Vps34^{f/f}$ mice.

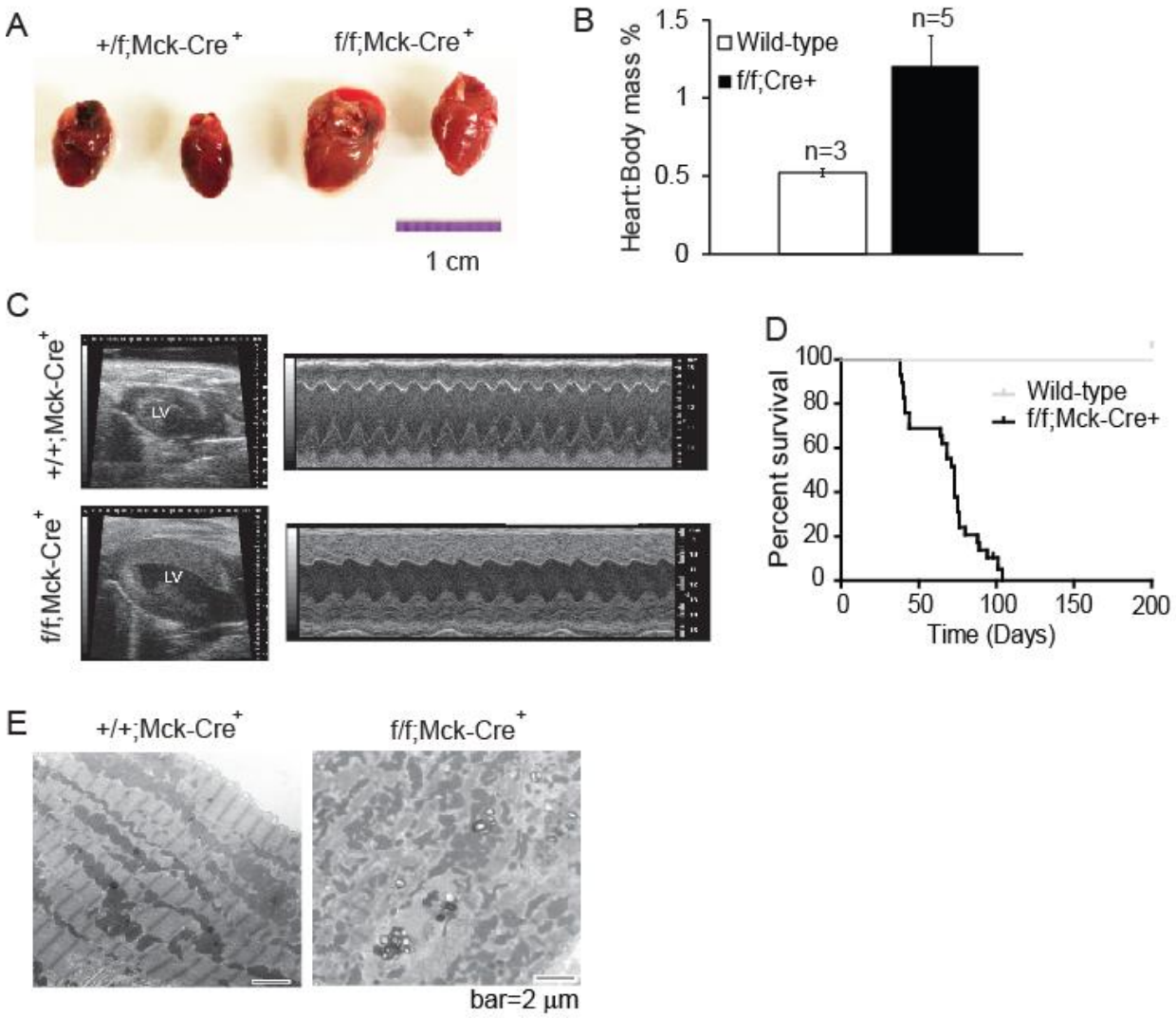

Figure 3. Deletion of Vps34 in the heart leads to cardiomegaly and cardiac dysfunction. (A) Deletion of Vps34 leads to cardiomegaly. Representative hearts isolated from 6 week old Mck-Cre;Vps34$^{+/f}$ and Mck-Cre;Vps34$^{f/f}$ mice were photographed. (B) Hearts were weighed and the heart mass is normalized to body mass. (C) Representative B-mode (left ventricle labeled) and M-mode echocardiographic images of control and Vps34$^{-/-}$ mice. (D) Mice with Vps34-null hearts have reduced viability. Kaplan-Meier survival curve of Mck-Cre;Vps34$^{f/f}$ mice. (E) Vps34-null heart tissue has disorganized mitochondria and Z-lines. Representative EM images of Vps34$^{+/+}$ and Vps34$^{-/-}$ hearts.

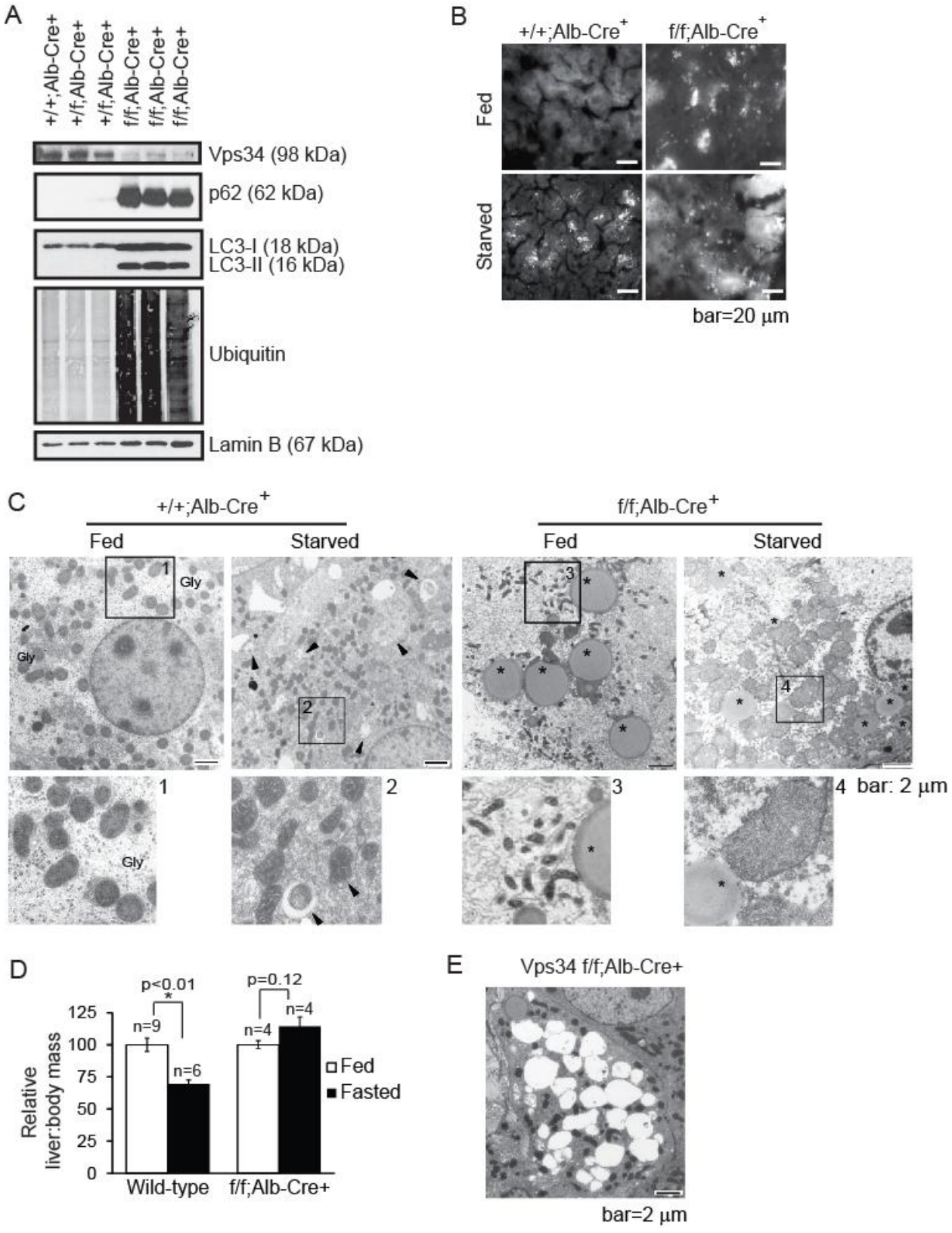
A
+/+;Alb-Cre+
+/f;Alb-Cre+
+/f;Alb-Cre+
f/f;Alb-Cre+
f/f;Alb-Cre+
f/f;Alb-Cre+
Vps34 (98 kDa)
p62 (62 kDa)
LC3-I (18 kDa)
LC3-II (16 kDa)
Ubiquitin
Lamin B (67 kDa)
B
+/+;Alb-Cre+
f/f;Alb-Cre+
Fed
Starved
bar=20 μm
C
+/+;Alb-Cre+
f/f;Alb-Cre+
Fed
Starved
Fed
Starved
Gly
bar: 2 μm
D
p<0.01
p=0.12
n=9
n=6
n=4
n=4
Relative liver:body mass
125
100
75
50
25
0
Fed
Fasted
Wild-type
f/f;Alb-Cre+
E
Vps34 f/f;Alb-Cre+
bar=2 μm

Figure 4. Autophagy is compromised by Vps34 deletion in the liver. (A) Autophagic proteins p62, LC3-II and poly-ubiquitinated proteins accumulate in the Vps34-null liver. Whole liver lysates were prepared from 6-13 week old mice with indicated genotypes, and were analyzed with indicated antibodies. (B) Vps34-null livers have LC3 aggregates which are not responsive to starvation. GFP-LC3 transgenic mice with indicated liver genotypes were fed or fasted for 24 h. Liver cryo-sections were observed and representative images are shown. Note that fasting resulted in increased GFP-LC3 puncta in wild-type liver, whereas Vps34-null liver showed large size GFP-LC3 aggregates in both fed and fasted conditions. (C) Vps34-null livers lack starvation-induced autophagosomes. Electron micrographic images of livers from fed and 24 h fasted $Vps34^{f/f}$; $Alb\text{-}Cre^{-}$ and $Vps34^{f/f}$; $Alb\text{-}Cre^{+}$ mice. Higher magnification views of boxed areas are numbered and shown in the bottom row. Gly: glycogen area; arrowheads point to autophagosomes; asterisks denote lipid droplets. (D) Vps34-null livers have reduced starvation-induced responses. Wild-type and $Vps34^{f/f}$;$Alb\text{-}Cre^{+}$ mice were fasted for 24 h. Liver/body mass ratio was determined, and expressed as normalized to that of respective fed animals. (E) Vps34-null livers accumulate cytoplasmic vacuoles. Representative electron micrographic images of livers from $Vps34^{f/f}$; $Alb\text{-}Cre^{+}$ mice are shown.

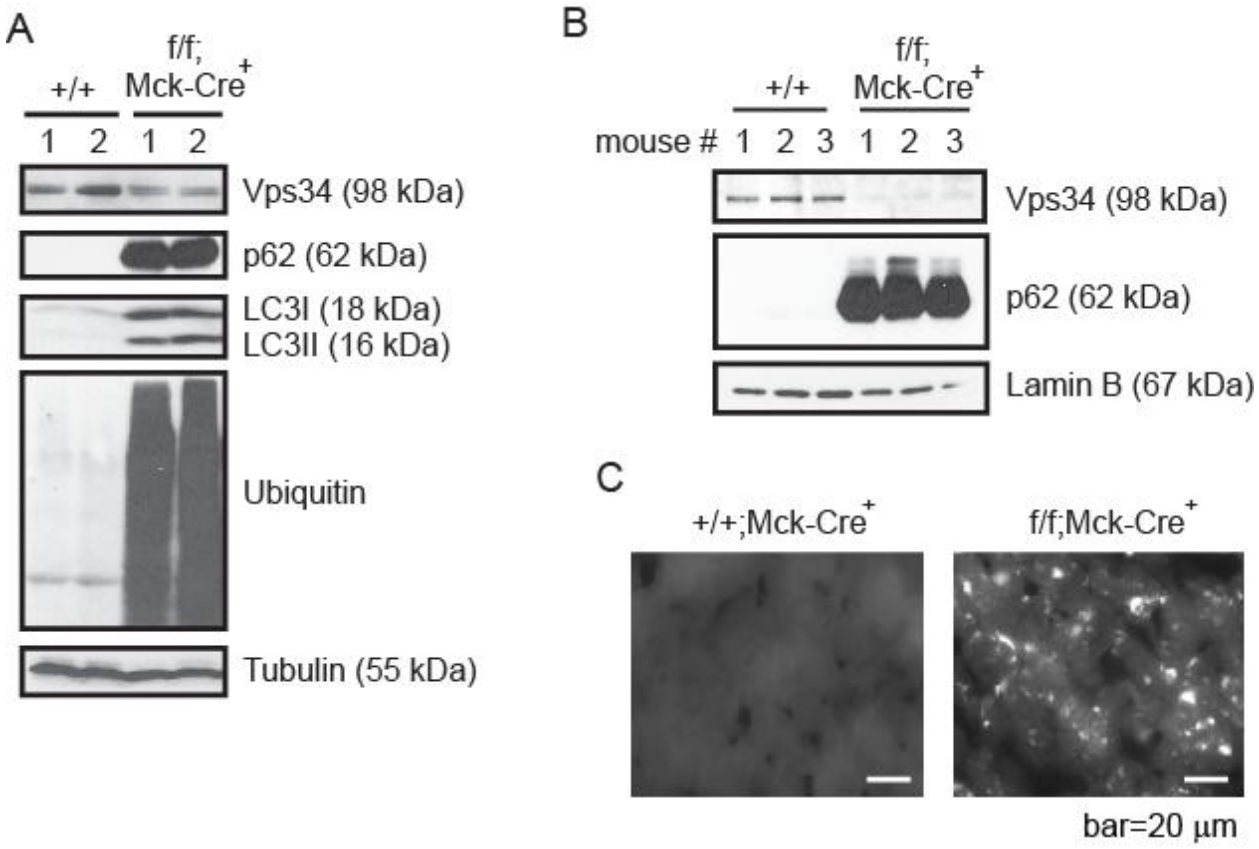

Figure 5. Autophagy is compromised by Vps34 deletion in the heart. Vps34-null hearts accumulate autophagic proteins p62, LC3-II and poly-ubiquitinated proteins. Whole heart lysates (A) and cardiomyocytes (B) were prepared from 6-13 week old mice with indicated genotypes, and were analyzed with indicated antibodies. (C) Vps34-null hearts accumulate large LC3 structures in the fed state. GFP-LC3 transgenic mice with indicated heart genotypes were subjected to heart cryo-section. Representative images are shown.

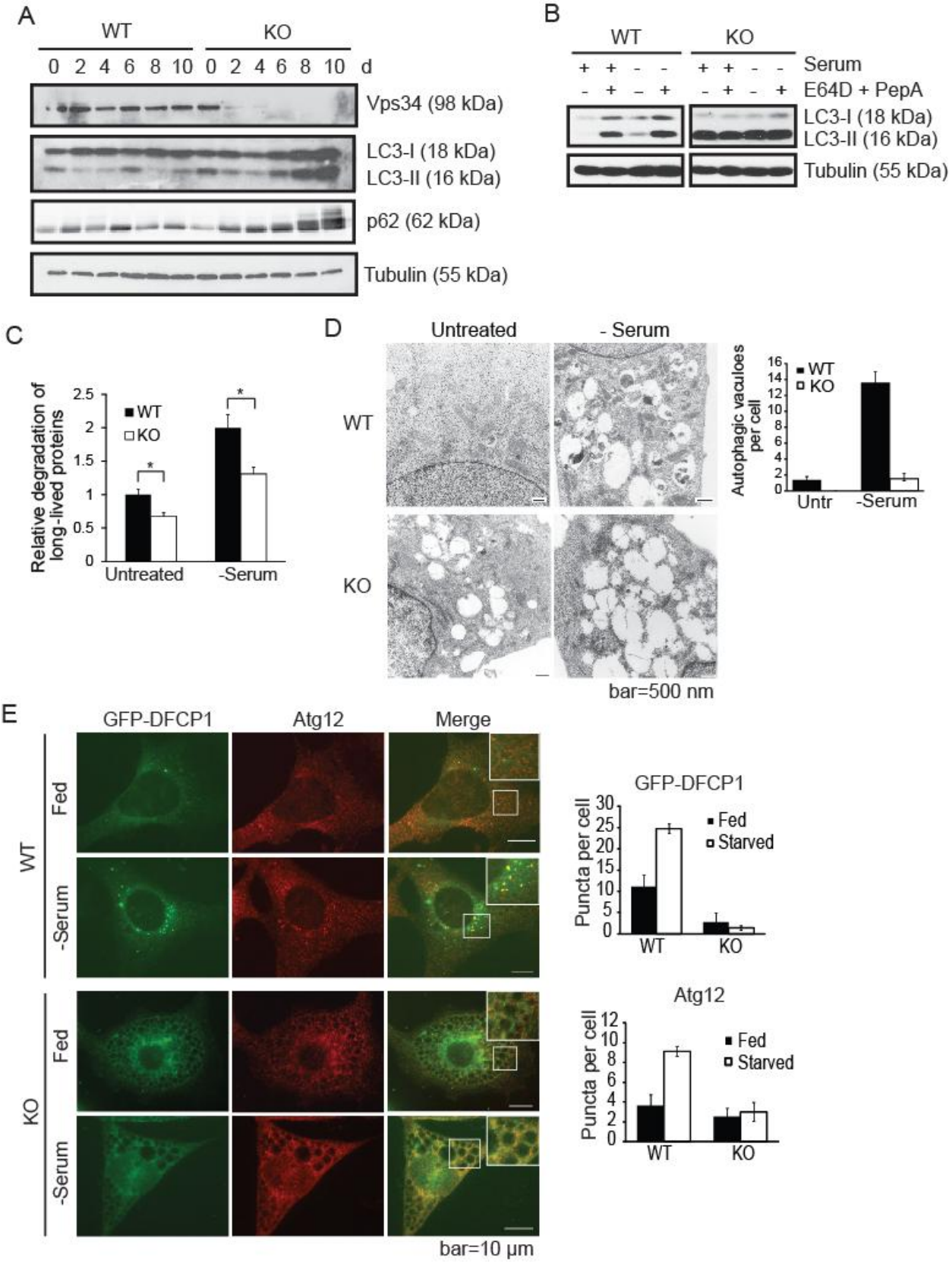
A
WT
KO
0 2 4 6 8 10 0 2 4 6 8 10 d
Vps34 (98 kDa)
LC3-I (18 kDa)
LC3-II (16 kDa)
p62 (62 kDa)
Tubulin (55 kDa)
B
WT
KO
Serum
E64D + PepA
LC3-I (18 kDa)
LC3-II (16 kDa)
Tubulin (55 kDa)
C
Relative degradation of long-lived proteins
WT
KO
Untreated
-Serum
D
Untreated
- Serum
WT
KO
Autophagic vaculoes per cell
Untr
-Serum
bar=500 nm
E
GFP-DFCP1
Atg12
Merge
WT
KO
Fed
-Serum
GFP-DFCP1
Puncta per cell
Fed
Starved
Atg12
bar=10 μm

Figure 6. Autophagy flux, autophagosome and phagophore formation are compromised in Vps34 knockout MEFs. (A) Vps34-null MEFs accumulate autophagic proteins. $Vps34^{f/f}$ MEFs were infected with adenoviral control virus (WT) or adenoviral Cre (KO). Cell lysates were collected at the indicated time points post infection and probed for Vps34, LC3 and p62. The fluctuation of the levels of LC3 and p62 in control cells may be due to the change of confluency during passaging. (B) Vps34 KO MEFs have blocked autophagic flux. WT and KO cells were left untreated or serum deprived for 6 h, with or without the addition of lysosomal protease inhibitors E64D (10 μg/ml) and PepA (10 μg/ml). Lysates were probed for the indicated proteins. Flux is determined by comparing the level of LC3-II in treated versus untreated conditions. (C) MEFs were labeled with ^{14}C-valine for 24 h and left untreated or cultured in serum-free media for 6 h. Degradation of long-lived proteins was measured. An average of three independent experiments +/- SEM is shown. *$p < 0.05$. (D) Vps34 knockout MEFs are devoid of autophagosomes. MEFs left in full media or serum starved for 6 h were observed by electron microscopy. Serum starvation induced the appearance of autophagosomes in wild-type, but not Vps34-null MEFs. Quantification of the number of autophagosomes was obtained by counting 10-20 cells and the averages +/- standard deviation (S.D.) are shown. (E) Phagophores are not formed in Vps34 knockout MEFs. MEFs expressing GFP-DFCP1 were left in full media or serum starved for 6 h, then fixed and immunostained for endogenous Atg12. The average number of puncta from eight countings is shown with SEM.

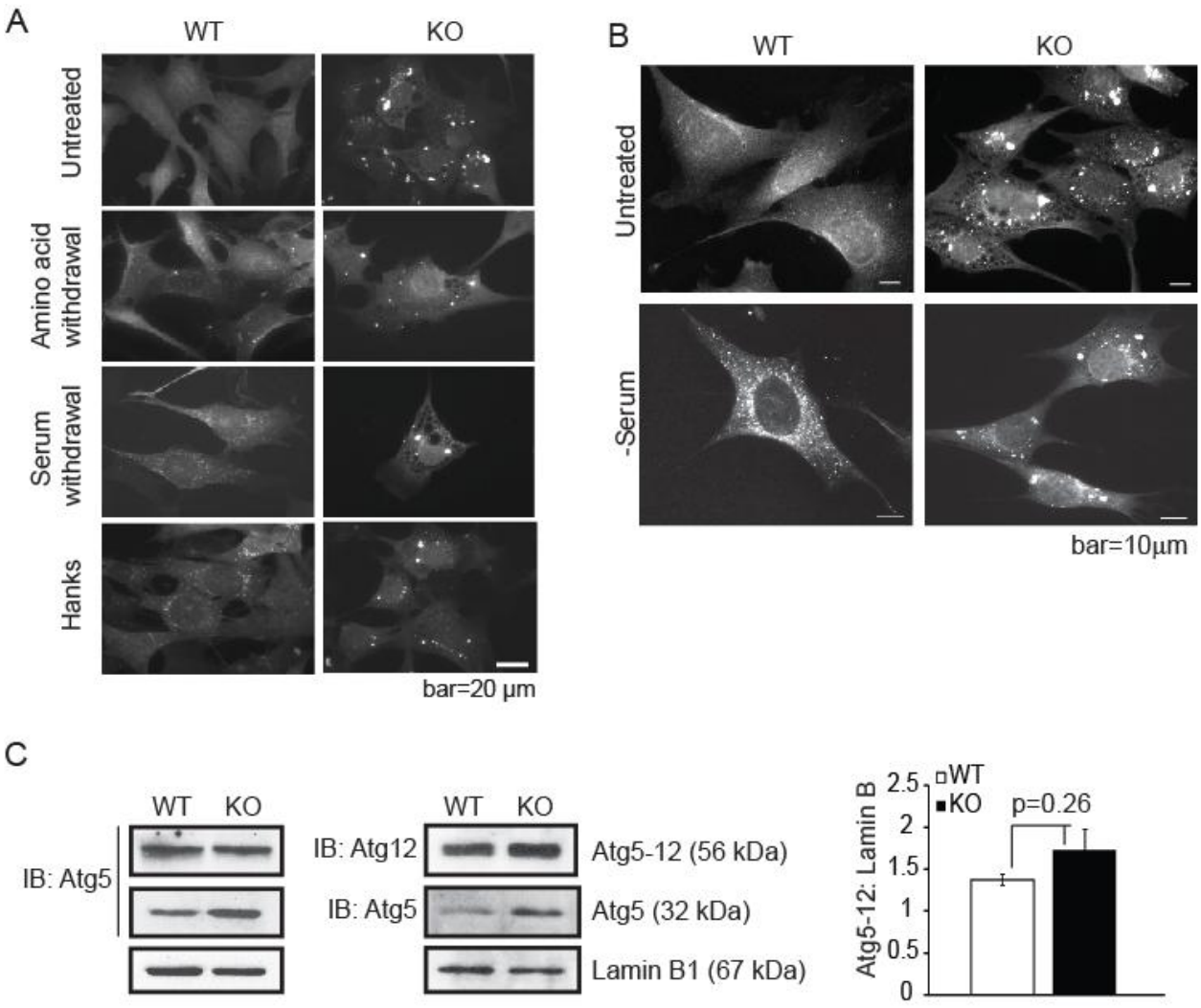

Figure 7. LC3 forms large aggregates in Vps34 knockout MEFs. (A) GFP-LC3 forms aggregates in Vps34 KO. MEFs stably expressing GFP-LC3 were starved in Hanks buffer for 2 h, serum-free media for 6 h, or amino acid-free media for 12 h. (B) Endogenous LC3 forms aggregates in KO. MEFs were serum starved for 6 h, then fixed and immunostained for endogenous LC3. (C) Atg5-12 conjugation is not affected by Vps34 deletion. Lysates from MEFs were probed with Atg5 or Atg12 antibodies to detect the Atg5-12 complex and free Atg5. The level of complexed Atg5-12 was normalized to Lamin B and shown on the right (n=4).

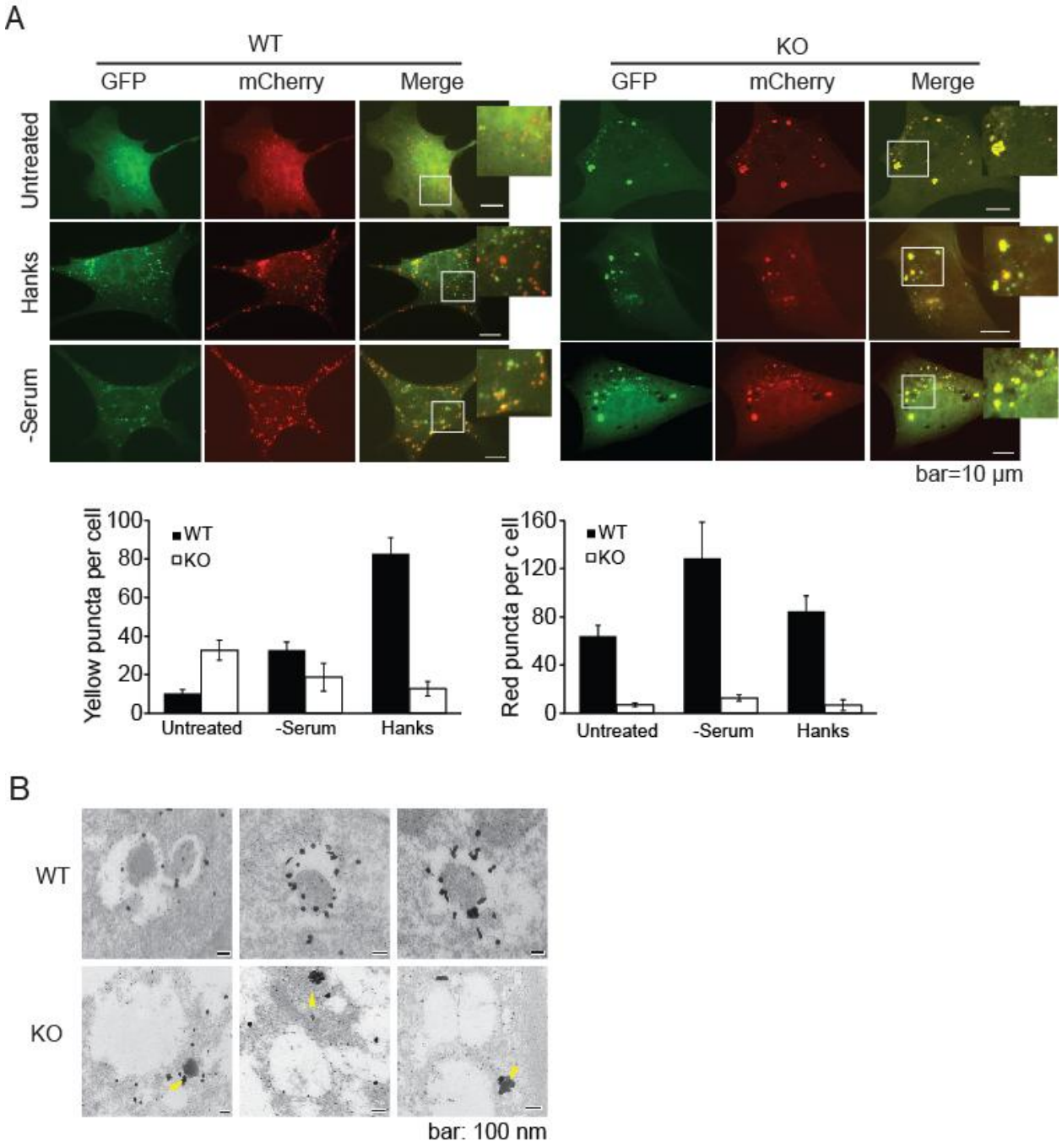

Figure 8. LC3 aggregates in KO MEFs are not functional autophagosomes. (A) LC3 aggregates in knockout cells are not functional autophagosomes. MEFs were transfected with mCherry-GFP-LC3. 48 h post-transfection, cells were starved in Hanks buffer or serum-free media. Cells were observed under a deconvolution microscope. Representative images are shown. The number of yellow or red puncta was counted from three countings, and the average is shown. (B) LC3 aggregates are not associated with any membrane structures. GFP-LC3 expressing MEFs were serum starved and subjected to immuno-gold EM analysis using

antibodies against GFP. Three representative images from each are shown. Yellow arrowheads point to aggregates.

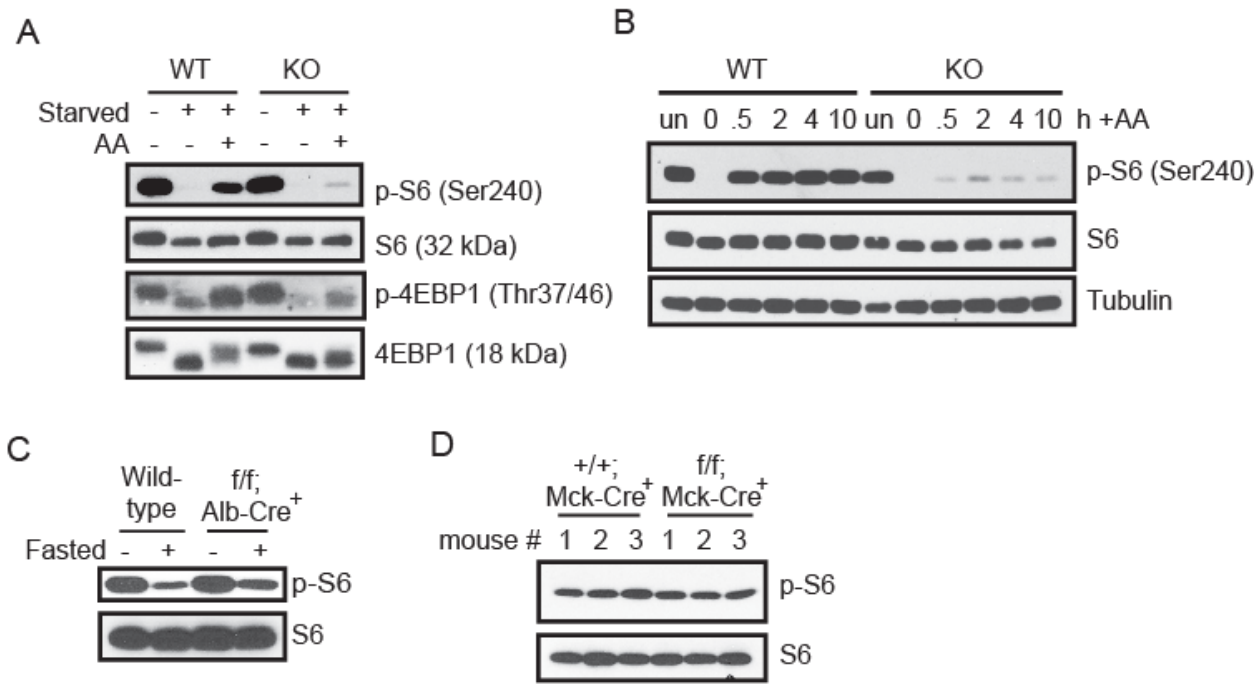

Figure 9. Amino acid-induced mTOR signaling is impaired in Vps34 knockout MEFs and mice. (A) Vps34 deletion severely reduces the amino acid-induced mTORC1 signaling response in MEFs. MEFs were left in full media, serum starved overnight plus amino acid starved for 2 h, or starved and restimulated with 2x MEM amino acids for 30 minutes. mTORC1 signaling was measured by the levels of phospho-S6 and phospho-4EBP1. (B) Amino acid-induced mTORC1 signaling is not slower in Vps34 knockout MEFs. MEFs were left in full media, serum starved overnight plus amino acid starved for 2 h, or starved and restimulated with 2x MEM amino acids for the indicated times. mTORC1 signaling was measured by the levels of phospho-S6 and phospho-4EBP1. (C) Steady state mTOR signaling is unaffected by Vps34 deletion in the liver. Wild-type or Vps34f/f/;Alb-Cre^{+} mice were fed or fasted for 24 h. Whole liver lysates were probed for the levels of phospho-S6. (D) Steady state mTOR signaling is unaffected by Vps34 deletion in the heart. Lysates from isolated cardiomyocytes were probed for the levels of phospho-S6.

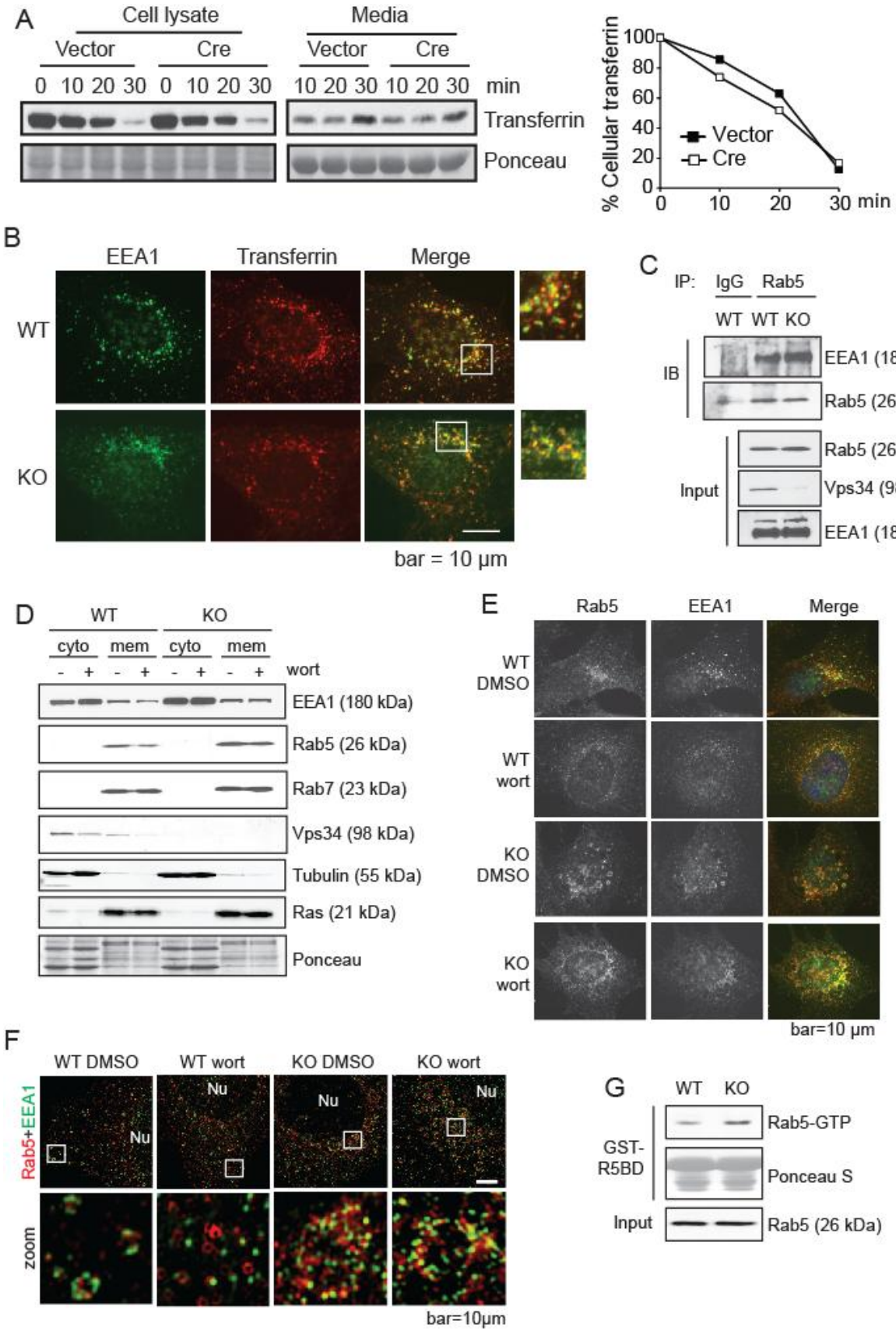
A
Cell lysate
Media
Vector
Cre
Vector
Cre
0 10 20 30 0 10 20 30
10 20 30 10 20 30
min
Transferrin
Ponceau
% Cellular transferrin
100
80
60
40
20
0
Vector
Cre
0 10 20 30 min
B
EEA1
Transferrin
Merge
WT
KO
bar = 10 μm
C
IP: IgG Rab5
WT WT KO
IB
EEA1 (180 kDa)
Rab5 (26 kDa)
Input
Rab5 (26 kDa)
Vps34 (98 kDa)
EEA1 (180 kDa)
D
WT
KO
cyto mem cyto mem
- + - + - + - +
wort
EEA1 (180 kDa)
Rab5 (26 kDa)
Rab7 (23 kDa)
Vps34 (98 kDa)
Tubulin (55 kDa)
Ras (21 kDa)
Ponceau
E
Rab5
EEA1
Merge
WT DMSO
WT wort
KO DMSO
KO wort
bar=10 μm
F
WT DMSO
WT wort
KO DMSO
KO wort
Rab5+EEA1
Nu
zoom
bar=10μm
G
WT KO
GST-R5BD
Rab5-GTP
Ponceau S
Input
Rab5 (26 kDa)

Figure 10. Vps34 deletion enhances Rab5 activity but does not compromise early endosome functions. (A) The rate of transferrin recycling is not affected by Vps34 deletion. MEFs were serum starved for 4 h and incubated with biotinylated-transferrin, then stripped and chased with unlabeled transferrin for indicated time points. Cells and culture media were collected and analyzed for biotinylated-transferrin levels. Relative amounts of intracellular transferrin at each time point was quantified by densitometry and normalized to that of time 0. (B) EEA1-positive early endosomes in Vps34 KO MEFs can receive transferrin cargo. Cells were loaded with Transferrin-AF-594, fixed, and immunostained for EEA1. Cells were observed under deconvolution microscope. Note that colocalization between EEA1 and transferrin was observed in both WT and KO cells. (C) Rab5-EEA1 interaction is not disrupted in Vps34 KO cells. Vps34 WT and KO MEFs were immunoprecipitated for endogenous Rab5 then probed for EEA1. (D) EEA1 is membrane localized and is refractory to wortmannin treatment in Vps34 KO cells. Subcellular fractionation was performed in Vps34 WT and KO MEFs in the presence or absence of wortmannin (wort, 1 μM for 1 h). Cytoplasmic (cyto) and membrane (mem) fractions were analyzed by immunoblotting. Note that wortmannin treatment leads to decreased EEA1 membrane localization in WT but not in KO cells. (E and F) Rab5 and EEAl colocalize on enlarged early endosomes in Vps34 KO MEFs. Vps34 WT and KO MEFs were treated with DMSO or wortmannin (wort, 1 μM) for 1 h. Cells were immunostained for endogenous Rab5 and EEA1, counterstained with DAPI, and observed under deconvolution microscope (E) or with a super resolution Structured Illumination Microscope (SIM) (F). The boxed areas are further zoomed in. Nu: nucleus. Note that in WT cells, Rab5 and EEA1 colocalize on endosomes, while wortmannin treatment disrupts the punctate staining pattern and Rab5-EEA1 colocalization. In Vps34 KO cells, Rab5 and EEA1 colocalize on enlarged endosomes and the colocalization is not affected by wortmannin. (G) Rab5-GTP level is enhanced in Vps34 KO cells. Rab5 activity assay was performed using a Rab5 binding domain (R5BD) fused to GST, which pulls down GTP-bound Rab5.

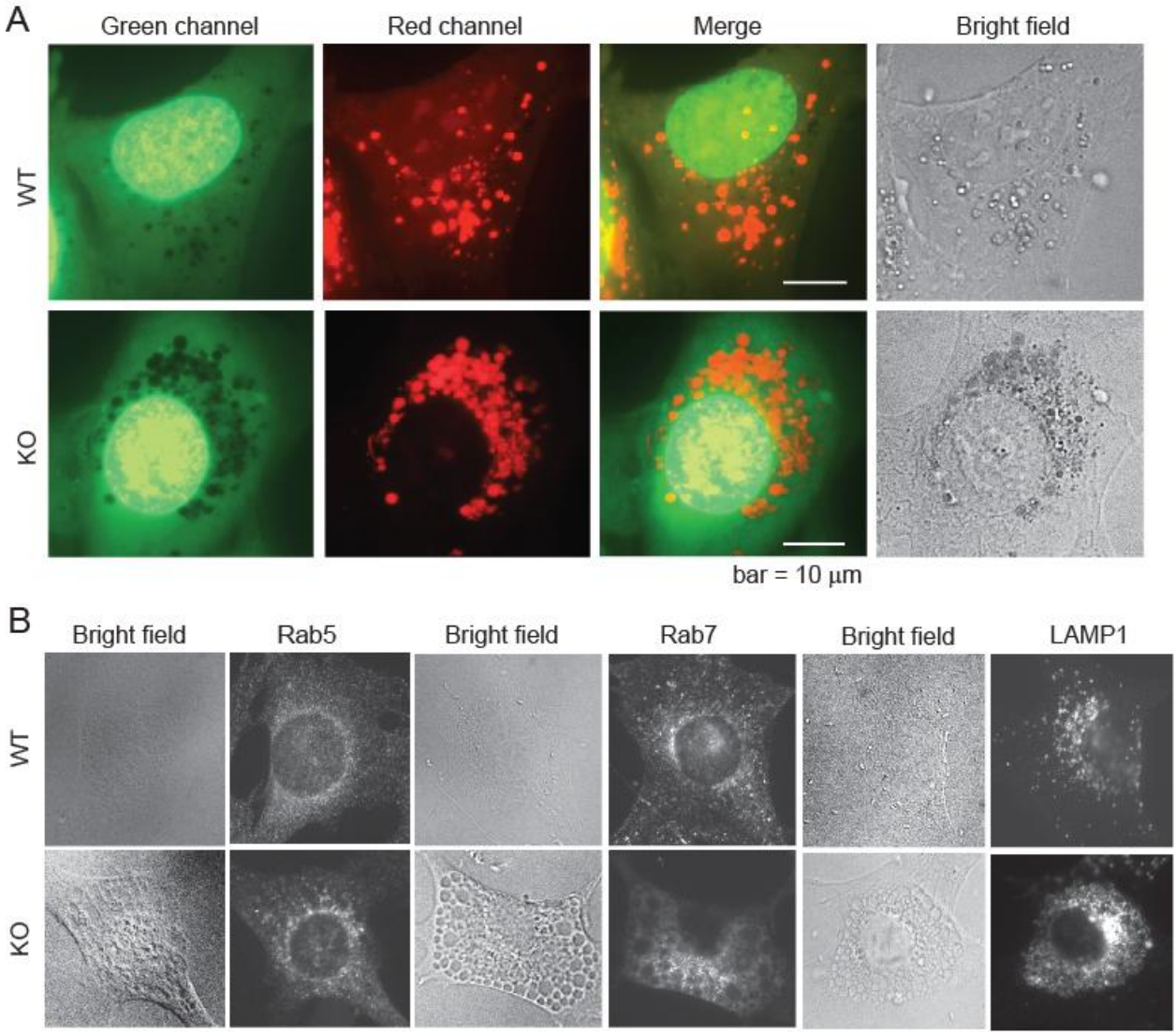

Figure 11. Vps34 deletion leads to the dramatic enlargement of late endosomes. (A) Cells were incubated with Acridine Orange (AO) staining solution in full media for 30 minutes at 37^{o}C. Live cells were immediately observed. While neutral AO emits green fluorescence, protonated AO emits red fluorescence, indicative of acidic environment. Note that Vps34-null cells exhibited an accumulation of acidic structures, which colocalized with the large-sized translucent vacuoles (see bright field). (B) MEFs were stained with early endosome marker Rab5, late endosome marker Rab7, and lysosomal protein LAPM1. Fluorescence and phase contrast images were taken.

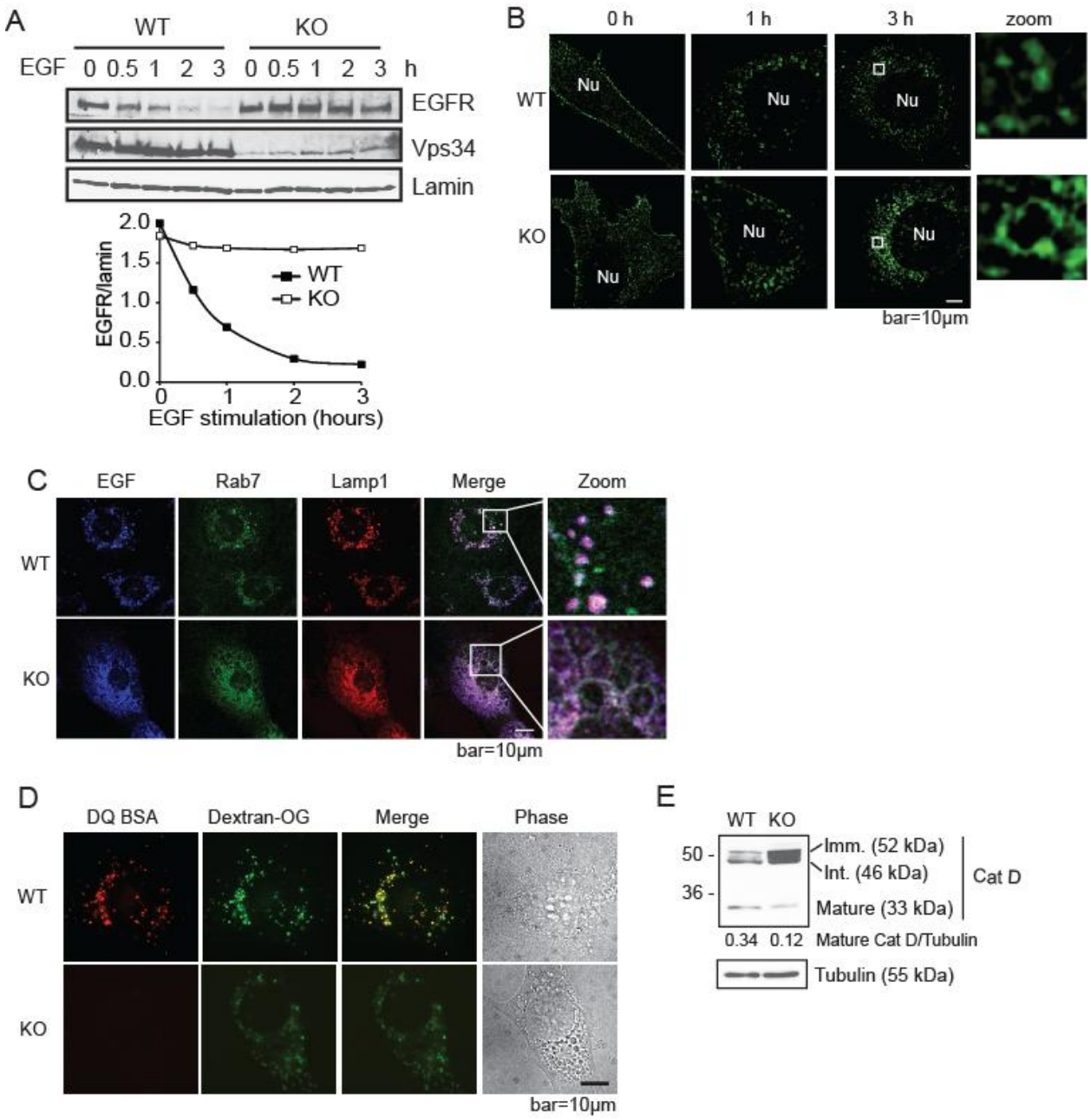

Figure 12. EGFR degradation, ILV formation and degradative capacity are abrogated in Vps34 knockout MEFs. (A) MEFs were serum starved overnight and stimulated with EGF (100 ng/ml) for indicated time points. EGFR protein level is quantified relative to Lamin. (B) Internalized EGFR localizes to the limiting membrane of enlarged endosomes in Vps34 KO cells. GFP-EGFR expressing MEFs were serum starved and stimulated with 100 ng/mL EGF for the indicated times, then fixed and analyzed by super resolution SIM. The boxed areas are further zoomed in. Nu: nucleus. (C) EGF accumulates on the limiting membrane of enlarged late endosomes in Vps34 KO cells. Vps34 WT and KO MEFs were stimulated with EGF-AF-647 for 45 min. Cells were stained for endogenous Rab7 and Lamp1, and analyzed by confocal microscopy. (D) Lysosomal protease activity is diminished in Vps34 KO MEFs. Cells were

loaded with 10 μg/mL Dextran-Oregon Green for 16 h plus 4 h chase, then loaded with DQ-BSA for 1 h. Cells were washed extensively and the fluorescence pattern was analyzed in live cells using deconvolution microscope. (E) Vps34 deletion disrupts cathepsin D maturation. The steady-state levels of immature (imm), intermediate (int), and mature cathepsin D were analyzed by immunoblotting.

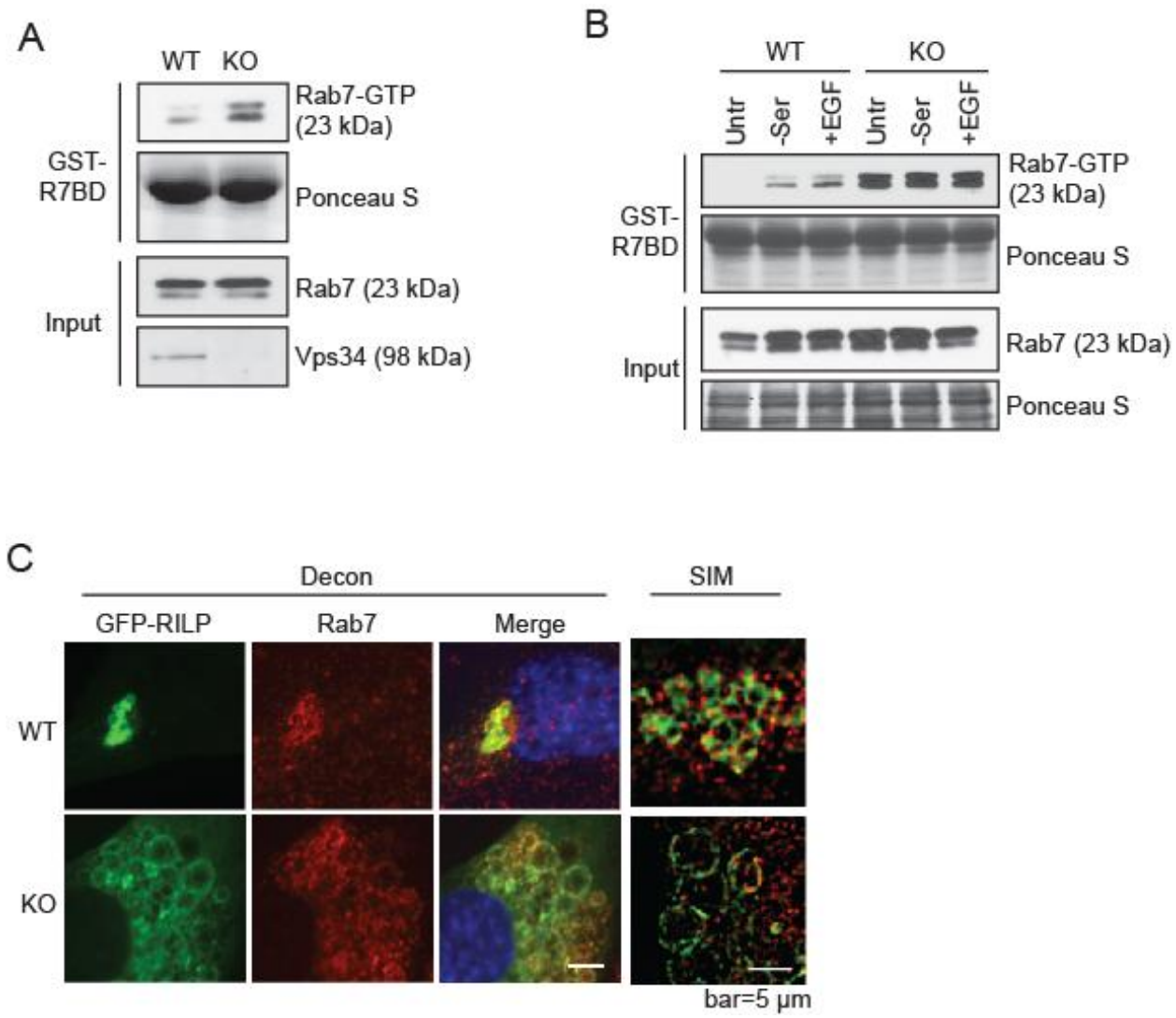

Figure 13. Rab7 activity is elevated by Vps34 deletion. (A) Rab7-GTP levels are increased in KO MEFs. A Rab7 activity assay was performed using a Rab7 binding domain (R7BD) fused to GST (GST-R7BD), which pulls down GTP-bound Rab7. (B) Rab7 activity is refractory to starvation and EGF stimulation in Vps34 KO cells. WT and KO MEFs were left untreated (untr), serum starved (-ser), or starved plus 100 ng/mL EGF stimulation (+EGF). A Rab7 activity assay was performed using GST-R7BD. (C) Rab7 effector RILP localizes on the limiting membrane of enlarged late endosomes in Vps34 KO cells. GFP-RILP was transfected in Vps34 WT and KO cells. Cells were fixed and immunostained for endogenous Rab7. Cells were observed under deconvolution or SIM (right) microscopes.

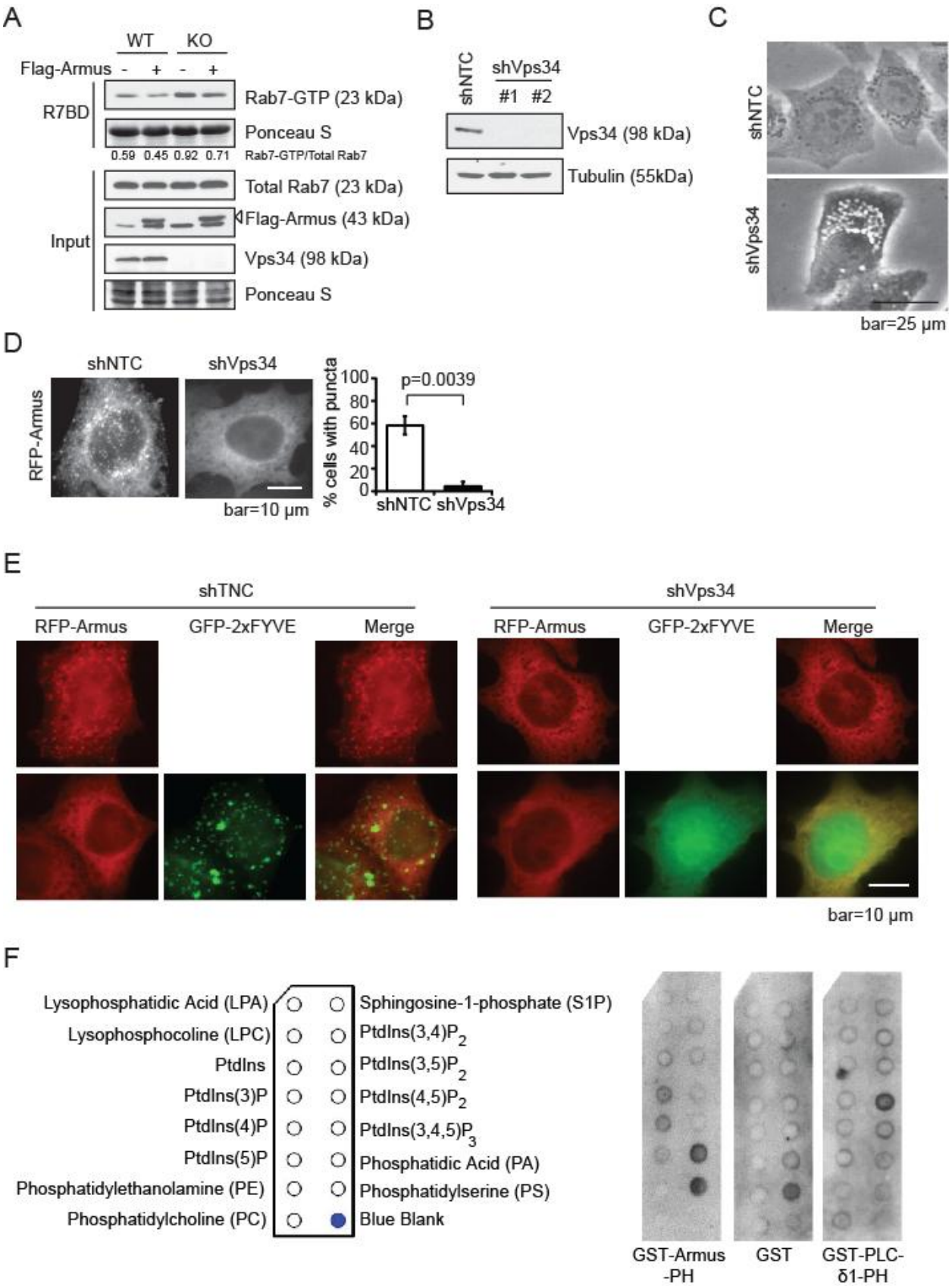
A
WT
KO
Flag-Armus - + - +
R7BD
Rab7-GTP (23 kDa)
Ponceau S
0.59 0.45 0.92 0.71
Rab7-GTP/Total Rab7
Input
Total Rab7 (23 kDa)
Flag-Armus (43 kDa)
Vps34 (98 kDa)
Ponceau S
B
shNTC
shVps34
#1 #2
Vps34 (98 kDa)
Tubulin (55kDa)
C
shNTC
shVps34
bar=25 μm
D
shNTC
shVps34
RFP-Armus
bar=10 μm
% cells with puncta
p=0.0039
shNTC shVps34
E
shTNC
shVps34
RFP-Armus
GFP-2xFYVE
Merge
bar=10 μm
F
Lysophosphatidic Acid (LPA)
Lysophosphocoline (LPC)
PtdIns
PtdIns(3)P
PtdIns(4)P
PtdIns(5)P
Phosphatidylethanolamine (PE)
Phosphatidylcholine (PC)
Sphingosine-1-phosphate (S1P)
PtdIns(3,4)P2
PtdIns(3,5)P2
PtdIns(4,5)P2
PtdIns(3,4,5)P3
Phosphatidic Acid (PA)
Phosphatidylserine (PS)
Blue Blank
GST-Armus -PH
GST
GST-PLC-δ1-PH

Figure 14. Vps34 recruits Rab7 GAP Armus via PI(3)P production. (A) Armus overexpression reduces the enahnced Rab7-GTP levels in Vps34 KO cells. Flag-Armus (547-928) was expressed in Vps34 WT and KO MEFs, then a Rab7 activity assay was performed. (B) HeLa cells were lentivirally infected with non-targeting control shRNA (shNTC) or two independent Vps34 shRNAs (shVps34), and analyzed for Vps34 protein level by immunoblotting. (C) Cell morphology of HeLa cells expressing Vps34 shRNA was observed by phase contrast microscopy. Note that Vps34 silencing leads to vacuolization. (D) Vps34 silencing abolishes punctate Armus localization. RFP-Armus was expressed in shNTC or shVps34-expressing HeLa cells. Cells were observed under fluorescence microscope. The average numbers of cells with punctate RFP-Armus localization were obtained by 3 blind countings of 100 cells each, and are shown on the right. (E) PI(3)P sequestration abolishes punctate Armus localization. GFP-2xFYVE and RFP-Armus were expressed in shNTC or shVps34 expressing HeLa cells. Cells were observed under deconvolution microscope. (F) Armus is a PI(3)P-binding protein. 0.5 μg/ml of Armus-PH-GST, GST only, or PLC-δ1-PH-GST was added to PIP strips and detected by anti-GST antibody. PLC-δ1-PH-GST binding to $PI(4,5)P_2$ was used as a positive control.

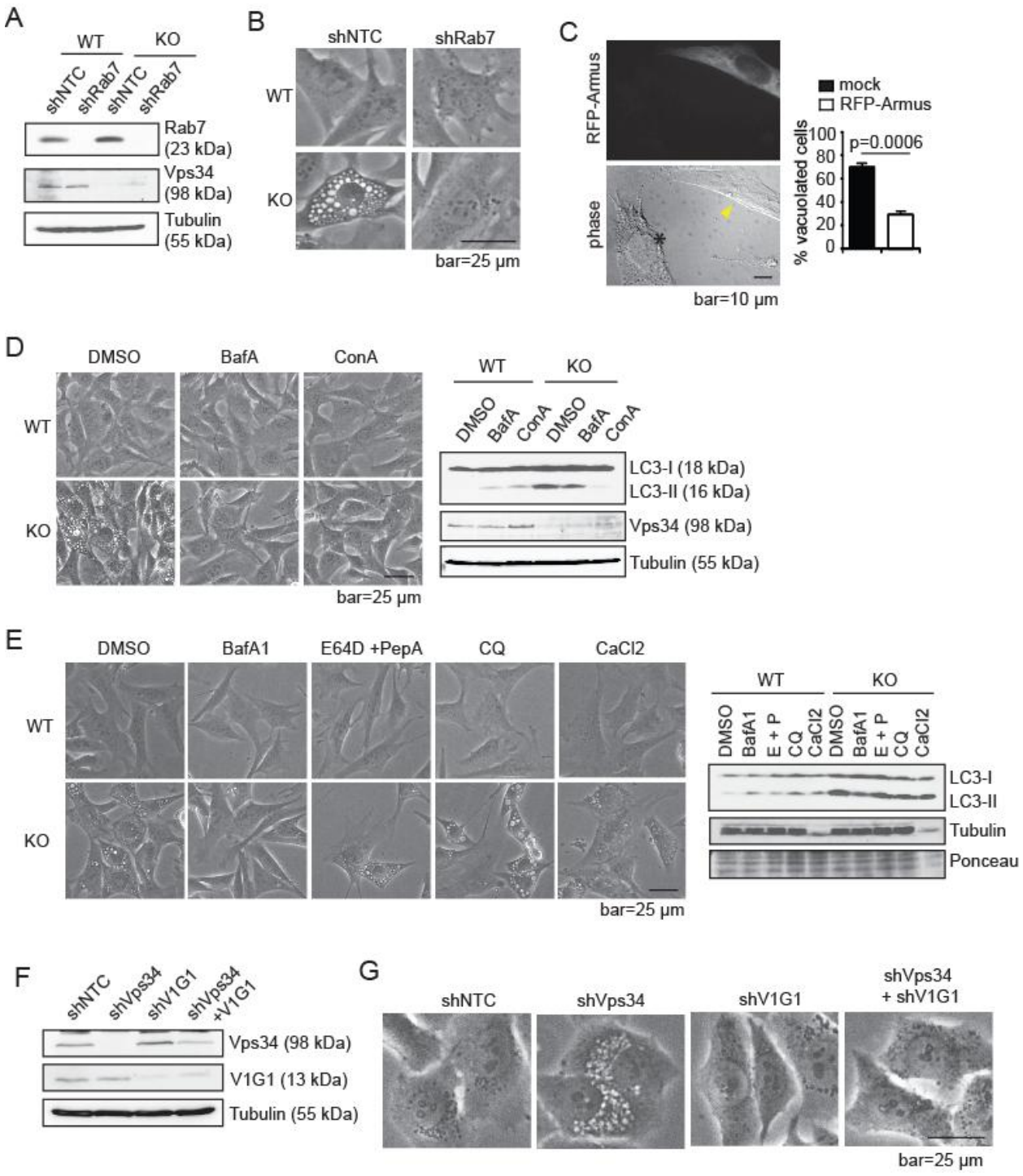

Figure 15. Rab7 and v-ATPase mediate vacuolization in Vps34-deficient cells. (A) Non-targeting (shNTC) and Rab7 shRNA were lentivirally expressed in Vps34 WT and KO MEFs. Cell lysates were probed for indicated proteins. (B) Rab7 knockdown prevents vacuolization in Vps34 KO cells. MEFs expressing shNTC or shRab7 were infected with adenoviral control or adenoviral cre to generate Vps34 WT and KO, respectively. Cell morphology was observed under phase-contrast microscope 6 d after infection. (C) Armus overexpression reverses

vacuolization in Vps34 knockout MEFs. Full-length RFP-Armus was expressed in Vps34 KO MEFs. Cells were observed under deconvolution microscope. Asterisk denotes vacuolated cell, arrowhead points to transfected cell. Cells with enlarged vacuoles were quantified in mock or RFP-Armus transfected cells. Shown is the average of 3 countings of over 100 cells plus S.D. **(**D) v-ATPase inhibitors reverse vacuolization in KO MEFs. Vps34 WT and KO MEFs were treated with DMSO, 20 nM Bafilomycin A1 (Baf A1) or 500 nM Concanamycin A (ConA) for 6 h. Cells were observed by phase contrast microscope. An immunoblot for LC3-II is shown as a positive control for inhibitor activity. (E) Vacuolization reversal is specific to v-ATPase inhibition. Vps34 WT and KO MEFs were treated with DMSO, Baf A1, E64D and PepA, chloroquine (CQ) or calcium chloride ($CaCl_2$). An immunoblot for LC3-II is shown as a positive control for lysosomal inhibition. (F and G) V1G1 is required for vacuolation of Vps34 KD cells. (F) shNTC or shRNA to Vps34, V1G1 or both were lentivirally expressed in HeLa cells. Respective proteins were probed by immunoblotting. (G) Cell morphology was observed under phase-contrast microscope. Note that knockdown of V1G1 prevents vacuolization induced by Vps34 knockdown alone.

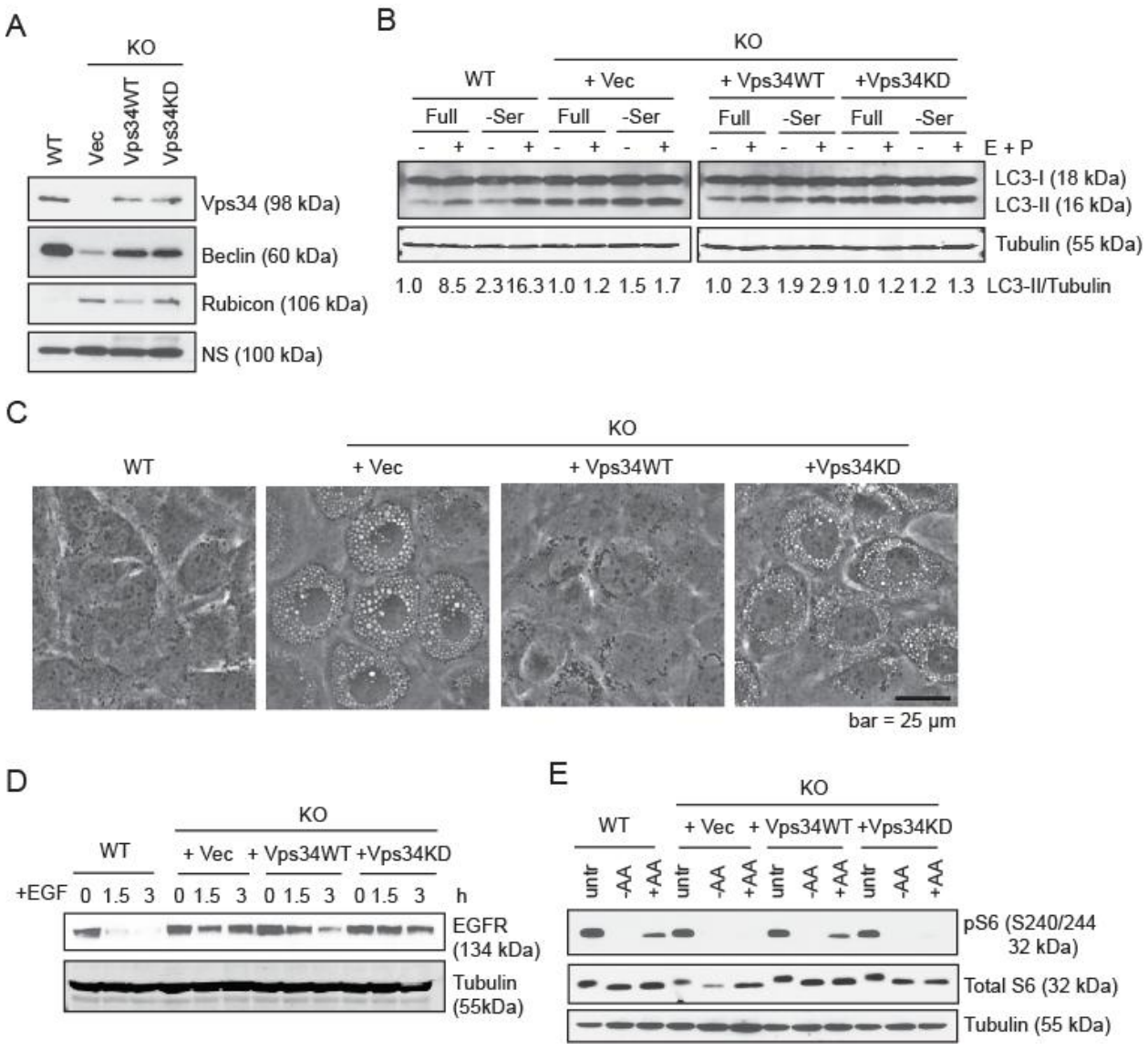

Figure 16. The functions of Vps34 are dependent on its catalytic activity. (A) Empty vector (Vec), HA-tagged Vps34 wild-type (Vps34WT) or Vps34 kinase-dead mutant K771A (Vps34KD) were stably expressed in Vps34 KO MEFs. Indicated proteins were probed via immunoblotting. NS, non-specific band. (B) Vps34 wild-type, but not kinase-dead, rescues autophagy flux. Indicated MEFs were cultured in full or serum-free media for 6 h, with or without 10 μg/mL E64D and 10 μg/mL Pepstatin A (E + P) to block lysosomal degradation. Autophagy flux is evaluated by comparing LC3-II/tubulin levels in the presence and absence of the protease inhibitors using ImageJ. (C) Intracellular vacuolization induced by Vps34 ablation is rescued by wild-type but not kinase-dead Vps34. Indicated cells were photographed and representative images are shown. (D) EGFR degradation is rescued by wild-type but not kinase-dead Vps34. Indicated cells were serum-starved overnight and then stimulated with 100 ng/mL EGF for indicated times. The level of EGF receptor was analyzed by immunoblotting. (E) Amino acid-induced mTOR signaling is rescued by wild-type but not kinase-dead Vps34. Indicated cells were left untreated (untr), amino acid starved (-AA), or starved and re-stimulated

with 2x amino acids for 30 min (+AA). Cell lysates were probed with indicated antibodies by immunoblotting.

Table 1. Echocardiographic measurements

	Wild-type	Vps34f/f;Cre^{+}
LVEDD (mm)	3.17 ± 0.06	2.93 ± 0.18
LVESD (mm)	1.58 ± 0.03	2.03 ± 0.14
SWT (mm)	0.13 ± 0.01	0.43 ± 0.13
PWT (mm)	0.96 ± 0.03	0.94 ± 0.16
FS (%)	50.0 ± 3.4	30.1 ± 3.4*
EF (%)	82.3 ± 3.2	57.7 ± 5.2*
LV mass (mg)	34.8 ± 4.5	49.8 ± 6.4*

LV, Left ventricular; LVEDD, LV end-diastolic diameter; LVESD, LV end-systolic diameter; SWT, septal wall thickness; PWT, posterior wall thickness; FS, fractional shortening; EF, ejection fraction; Values are mean ± SEM. *Significantly different from the control group, $P < 0.05$, *t*-test. $n = 4$ for control; $n = 6$ for Vps34f/f;Cre^{+}.

Table 1. Electrocardiographic measurements. Vps34-deficient hearts have increased left ventricular wall mass (LV mass), lower ejection fraction (EF) and fractional shortening (FS). Ejection fraction and fractional shortening measure contractility, and low ejection fraction denotes heart failure.

Class	Catalytic Subunit	Regulatory Subunit	Preferred Substrate	Distribution
IA	p110α		$PI(4,5)P_2$	Ubiquitous
	p110β			Ubiquitous
	p110δ			High in leukocytes
		p85α		Ubiquitous
		p55α		High in brain and muscle
		p50α		High in liver
		p85β		Ubiquitous
		p55γ		High in brain and testis
IB	p110γ		$PI(4,5)P_2$	High in leukocytes
		p101		High in leukocytes
		p84/p87		High in leukocytes and heart
II	PI3K-C2α		PI	Ubiquitous
	PI3K-C2β		PI(4)P	Ubiquitous
	PI3K-C2γ		PI(5)P	High in liver and prostate
III	Vps34	Vps15	PI	Ubiquitous
	(the only PI3K in yeast)			Ubiquitous

Illustration 1. Chart of the PI3K family. Mammals have a large PI3K gene family, which is grouped into three classes based on substrate specificity and sequence homology. Class I is further separated into class IA and class IB based on regulatory subunit binding and regulation.

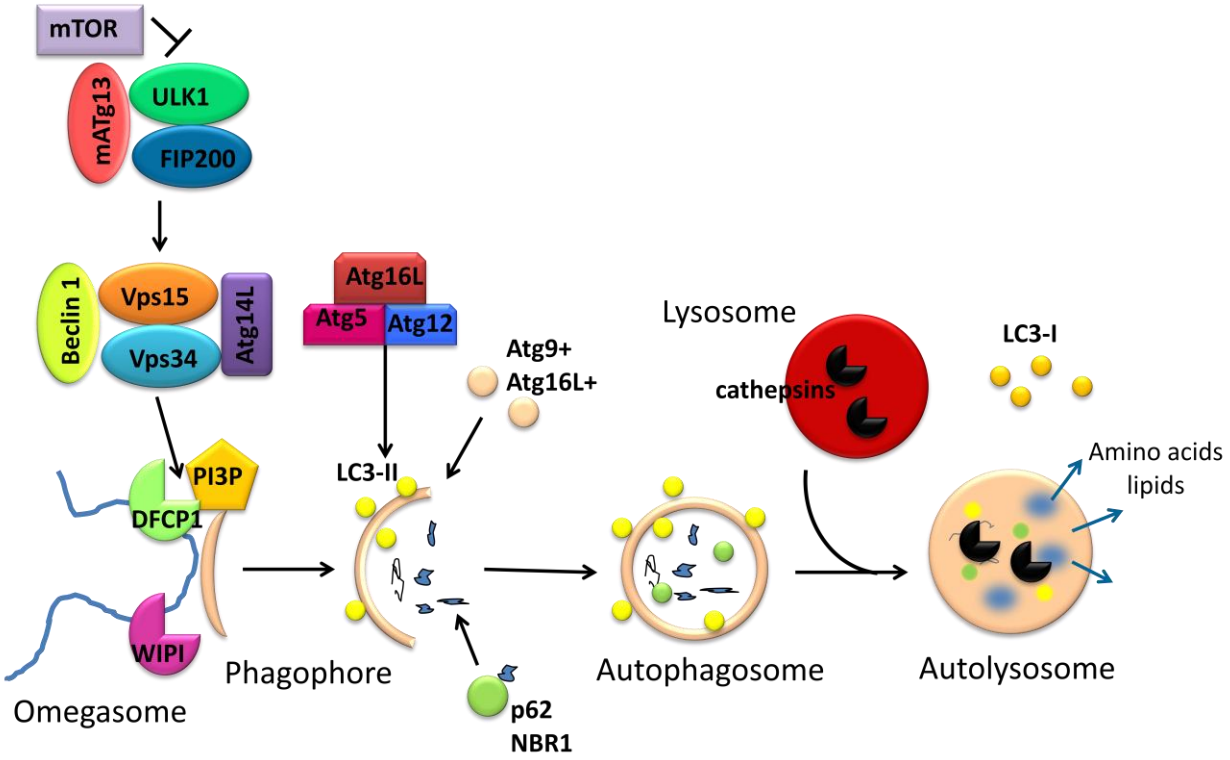

Illustration 2. Molecular mechanisms of autophagy. mTOR regulates starvation-induced autophagy by binding and inhibiting the ULK1 complex, which consists of ULK1, FIP200 and mAtg13. The ULK1 complex is upstream of the Vps34-Vps15-Beclin 1-Atg14L complex. Through the production of PI(3)P, Vps34 recruits DFCP1 and WIPI1-4 to the omegasome, the site of autophagosome formation. At the omegasome, the phagophore is nucleated and expands via addition of $Atg9^{+}$ and $Atg16L1^{+}$ vesicles. NBR1 and p62 bring ubiquitinated cargo to the expanding phagophore. The Atg5-12-16L1 regulates lipidation of LC3 to PE on the inner and outer membranes. Closure of the membrane produces a mature autophagosome, which then fuses with early/late endosomes and lysosomes to generate amphisomes and autolysosomes, respectively (for simplicity only fusion with lysosomes is pictured). This facilitates degradation of autophagic cargo, and the macromolecules are returned to the cytoplasm for re-use.

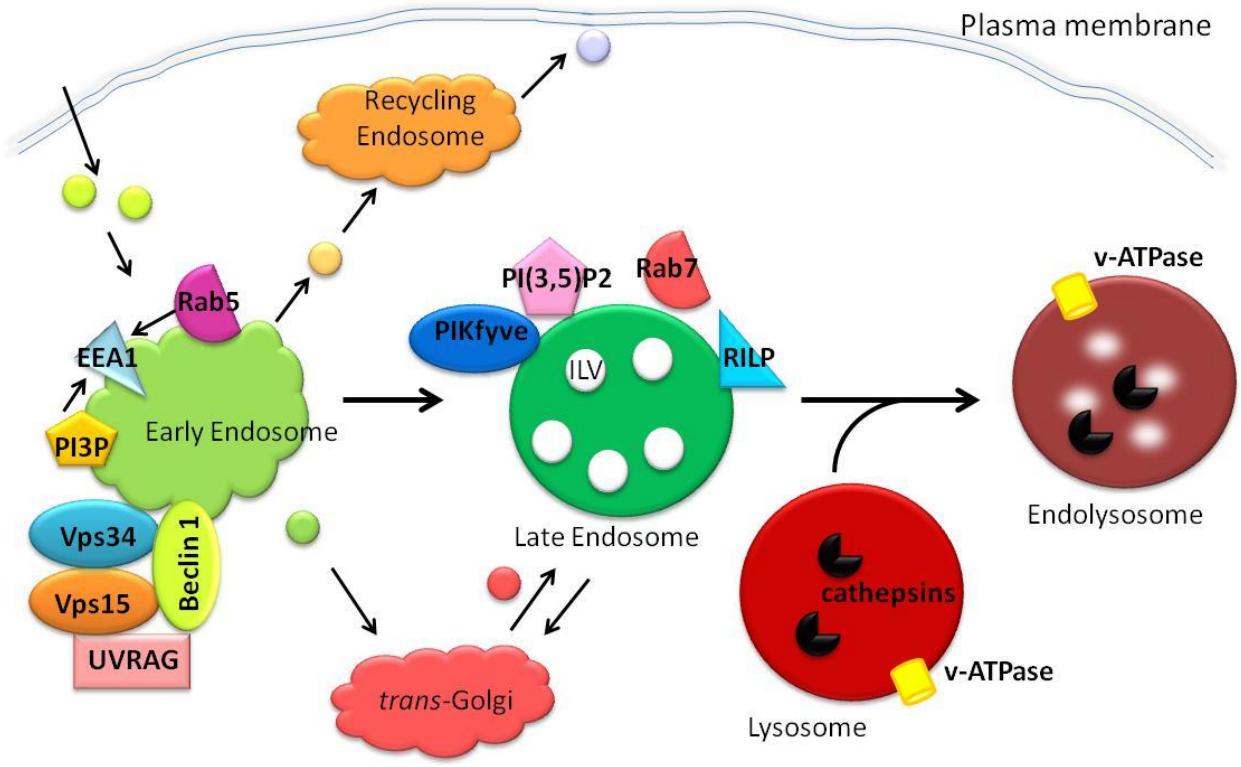

Illustration 3. Molecular mechanisms of endocytosis. Transmembrane receptors, ligands, lipids, and solutes are internalized into vesicles at the plasma membrane and delivered to the early endosome. Active Rab5-GTP and PI(3)P produced by Vps34 co-recruit effectors such as EEA1 and Hrs which mediate docking and fusion of vesicles and sorting of the enclosed cargo, respectively. Cargo can be recycled via the recycling endosome, delivered to the trans-Golgi or remain in the endosome as it matures into a late endosome. As it matures the endosome loses Rab5, gains Rab7, acquires more intraluminal vesicles (ILVs), converts PI(3)P to PI(3,5)P_2, and translocates to the perinuclear space. The late endosome then fuses with the lysosome, which contains hydrolases such as cathepsins to degrade the endocytic cargo. v-ATPase on the endosome and lysosome membranes maintains an acidic pH.

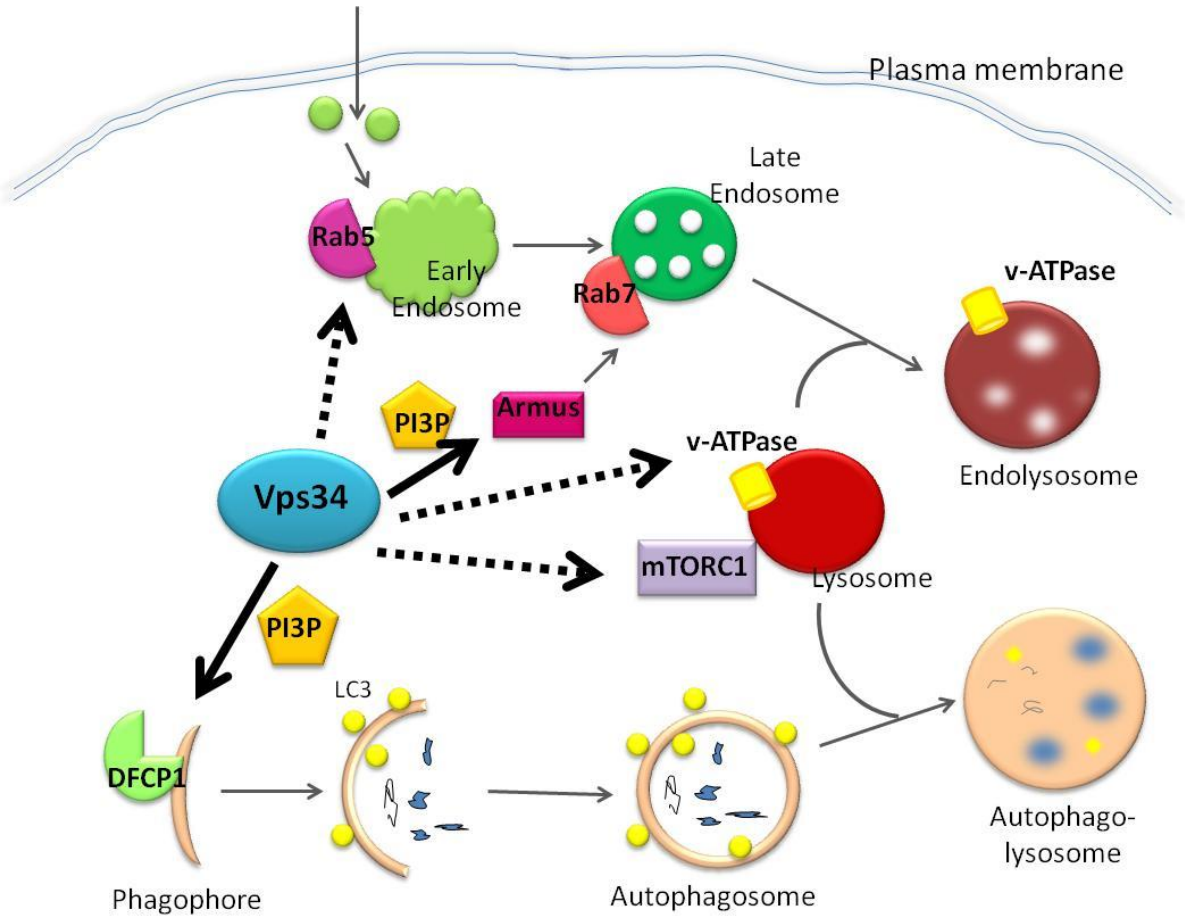

Illustration 4. Model of the roles of mammalian Vps34. This work provides evidence that Vps34 regulates phagophore formation through recruitment of PI(3)P-binding proteins such as DFCP1. Through an unknown mechanism, possibly a compensation mechanism, Vps34 regulates Rab5 activity to sustain early endosome functions. Vps34 also modulates Rab7 activity via PI(3)P-mediated regulation of intracellular localization of the Rab7 GAP, Armus. In addition, Vps34 regulates the activity of v-ATPase on endosomes and lysosomes. Finally, through an unknown mechanism, Vps34 mediates amino acid-stimulated mTORC1 activity.

7

Materials and Methods

Generation of Vps34$^{f/f}$ mice

Vps34 (Pik3c3) gene conditional knockout ES cells in C57BL/6 background were purchased from Sanger Institute, in which LoxP sequences were inserted flanking exon 4. A promotorless cassette encoding β-galactosidase and neomycin resistance flanked by FRT sequences was inserted. Blastocyst injection was performed in the University of Alabama at Birmingham transgenic core, followed by breeding to germline. The β-galactosidase and neomycin resistance cassette was deleted by breeding to FLP mice. Genotyping was carried out by tail clips and PCR to distinguish the floxed and wild-type alleles, as well as the existence of the cre gene. Genotyping was performed with the following primers:
(Pik3C3-5'arm) 5'-CCTGTTTCCTATCCCTGGCATTCC-3' and
(Pik3C3-3'arm) 5'-GGTTTGTGCAACAGAGAGCTAAGC-3'.

GFP-LC3 transgenic mice were a gift from Dr. Noboru Mizushima (Mizushima et al., 2004) . Alb-Cre and Mck-Cre mice were purchased from the Jackson Laboratory. For fasting studies, mice were deprived of food while having free access to water. All mice were experimented in compliance with the Stony Brook University and University of Alabama at Birmingham Institutional Animal Care and Use Committee guidelines.

MEF preparation

Early passage MEFs were immortalized by transfection with SV40 large T-antigen. Immortalized MEFs were infected with adenoviral GFP for Vps34$^{+/+}$ (WT) or adenoviral Cre-GFP for Vps34$^{-/-}$ (KO), for 24 h. experiments were performed 4-8 d after infection to allow sufficient knockout and vacuole formation. Immunofluorescent experiments were performed at a minimum of 6 d post infection to allow for loss of adenoviral GFP expression.

Cell culture

MEFs and HeLa were cultured in DMEM supplemented with 10% fetal bovine serum (HyClone Fetal Clone III), 100 units/ml penicillin, 100 μg/ml streptomycin and 2 mM glutamine. For starvation assays, cells were cultured in serum-free media for 6 h, amino acid-free media (Hanks buffer supplemented with 10% dialyzed serum, 100 units/ml penicillin, 100 μg/ml streptomycin, 4.5 g/L glucose) for 12 h, or Hanks buffer (with 10 mM HEPES) for 2 h. Mouse ventricular

myocytes were isolated from wild type and Vps34$^{-/-}$ hearts, and cultured as previously described (Lu et al., 2009).

Hepatocyte isolation

Hepatocytes were isolated by anesthetizing the mice with ketamine/zylazine and the livers were perfused through the inferior vena cava. Buffers used for the perfusion were heated to 37°C and aerated with 5% CO_2/95% O_2. The livers were perfused first with approximately 40 ml of Krebs Ringer buffer (122 mM NaCl, 5.6 mM KCl, 5.5 mM glucose, 25 mM $NaHCO_3$, and 20 mM HEPES, pH 7.4) containing 10 U/ml heparin, followed by the same volume of Krebs Ringer buffer with 20 mg collagenase type I (Worthington). The digested livers were removed and the cells were washed out with DMEM/F12 medium (Sigma) supplemented with 5% FBS, 1 g/L fatty-acid free BSA, and 1% antibiotic/antimycotic. The cells were pelleted by gentle centrifugation and washed with hepatocyte wash buffer (Invitrogen) containing 1 g/L fatty acid-free BSA. The cells were suspended in DMEM supplemented with 5% FBS and antibiotics and plated on collagen-coated dishes. After incubation at 37°C in 5% CO_2 for 3-4 h, the attached cells were rinsed with PBS and then incubated overnight in medium 199 (Invitrogen) supplemented with 100 nM dexamethasone, 1 nM insulin, 100 nM 3,3,5-triiodo-L-thyronine, and antibiotics.

Plasmids

GFP-LC3 constructs were described previously (Ullman et al., 2008). mCherry-GFP-LC3 is a gift from Dr. Terje Johanson (Pankiv et al., 2007). GFP-FYVE is a gift from Dr. Deborah Brown. GST-R5BD was described previously (Liu et al., 2007). GST-R7BD, GFP-RILP and GFP-Rab7 plasmids were described previously (Peralta et al., 2010). Rab7 shRNA lentiviral plasmid was purchased from Sigma-Aldrich. V1G1 lentiviral plasmid (TRCN0000038615) was purchased from Dharmacon GE Healthcare. Myc-Armus$^{547\text{-}928}$, Flag-Armus$^{547\text{-}928}$, Myc-Armus$^{1\text{-}550}$ and RFP-Armus (full-length) are described elsewhere (Carroll et al., 2013; Frasa et al., 2010). We cloned human Vps34 from a bicistronic Myc-Vps34-V5-Vps15 plasmid (Yan et al., 2009) into the retroviral LPC vector, and added an HA tag. The Vps34 KD mutant K771A (Miller et al., 2010) was generated by point mutagenesis and was confirmed by PCR.

Antibodies

We used the following antibodies: p62/SQSTM1 (Abnova, 1:200,000), Atg5 (to detect free form, 1:500, Abgent; to detect conjugated form, 1:1,000, Sigma), Atg12 (Cell Signaling Technology, 1:500 for WB; 1:200 for IF), WIPI2 (Santa Cruz Biotechnology, 1:200 for IF), S6 (1:1,000, Cell Signaling Technology), Phospho-S6 Serine 240 (1:1,000, Cell Signaling Technology), 4-EBP1 and phospho-4EBP1 (1:1,000, Cell Signaling Technology), Rab5 (D11, Santa Cruz Biotechnology, 1:300 for IF; Cell Signaling Technology, 1:5,000 for WB), EEA1 (Cell Signaling Technology, 1:5,000 for WB; 1:400 for IF), Vps34 (Cell Signaling Technology, 1:1,000 for WB), Rab7 (Cell Signaling Technology, 1:5,000 for WB; 1:300 for IF), β-tubulin (Sigma-Aldrich, 1:10,000 for WB), Ras (Invitrogen, 1:10,000 for WB), Flag (M2, Sigma-Aldrich, 1:1,000 for WB), LC3 (MBL, 1:3,000 for WB), V1G1 (H-80, Santa Cruz Biotechnology, 1:100 for WB), Lamin B (M-20, Santa Cruz Biotechnology, 1:500 for WB), Beclin 1 (D-18, Santa Cruz Biotechnology, 1:1,000 for WB), EGFR (Abcam, 1:500 for WB), Cathepsin D (C-20, Santa Cruz Biotechnology, 1:250 for WB), and LAMP1 (Developmental Studies Hybridoma Bank, 1:300 for IF). Alexa-Fluor secondary antibodies (1:500) were purchased from Life Technologies.

Reagents

DMEM and Hank's buffer was purchased from Invitrogen, E64D (10 μg/mL) from EMD, Pepstatin A (10 μg/mL) from Sigma, wortmannin (1.0 or 0.1 μM) from EMD Millipore, Bafilomycin A1 (20 nM) from Enzo, Concanamycin (500 nM) from Santa Cruz Biotechnology, Transferrin-Alexa Fluor-594 (1.5 μg/mL) from Life Technologies, Ponceau from Sigma-Aldrich, DQ Red BSA (10 μg/mL) from Life Technologies, Dextran Oregon Green MW 10,000 (10 μg/mL) from Molecular Probes, DAPI (4',6'-diamidino-2-phenylindole; 1 μg/ml) from Sigma, chloroquine (CQ; used at 10 μM) from Sigma, Prote-CEASE-M (1:100) from GBiosciences, and Pierce BCA Protein Assay from Thermo Scientific. The following reagents were used for the transferrin recycling assay: deferoxamine mesylate (100 μM, Sigma-Aldrich), mouse transferrin (Rockland), mouse transferrin biotin-conjugated (Rockland) and VECTASTAIN ABC-AmP Western Blotting Immunodetection Kit (Vector Laboratories).

Immunofluorescence

Cells were plated at 3–5 × 10^4 cells per well on gelatin-coated glass coverslips in 24-well plates. After treatment, cells were fixed in 4% (wt/vol) paraformaldehyde (PFA) in PBS for 20 min at room temperature. Cells were washed twice with PBS and permeabilized with 0.1% Triton X-100 in PBS for 10 min. Cells were washed three times with PBS and blocked in 5% (wt/vol) goat serum in PBS for 1 h. Primary antibodies were added in 5% (wt/vol) BSA in PBS plus 0.1% Tween-20 (PBST) overnight at 4°C. Cells were washed four times with PBS. Fluorophore-conjugated secondary antibodies were added (1:500) in 5% BSA in PBST for 1 h at room temperature with gentle shaking. Cells were washed three times with PBST, twice with PBS, and then mounted with Immuno-Mount.

Immunoprecipitation

Cells were lysed in general lysis buffer (30 mM Tris [pH 7.5], 150 mM NaCl, 10% glycerol, 1% Triton X-100) plus protease inhibitor cocktail (1:100) and phenylmethylsulfonyl fluoride (PMSF, 200 μM) on ice for 20 minutes with frequent vortexing. Lysates were cleared by centrifuging at 14,000 xg for 10 min at 4°C. After protein quantitation 4 μg IgG or 2 μg Rab5 antibody (D-11, Santa Cruz Biotechnology) were added to lysates and incubated on a rotator at 4°C overnight. The following day, equal volumes of protein G and A (Roche) were aliquoted and washed with general lysis buffer four times. Washed beads were added to the lysates and incubated on a rotator at 4°C for 4 h. The precipitates were washed six times with general lysis buffer, before displacing the precipitated proteins with SDS loading dye.

Transfection, retroviral and lentiviral infection

MEFs were transfected with Lipofectamine 2000 (Invitrogen) or TransIT X2 (Mirus) 2-3 days after adenoviral infection, following manufacturer's protocol that is optimized for MEFs.

For retroviral or lentiviral infections 293T cells were transfected with the experimental plasmid, ΔR8.91 and VSV-G with Lipofectamine 2000 (Invitrogen). Virus-containing supernatant was collected at 24, 48 and 72 h post-transfection. Filtered virus-containing supernatant was added to $Vps34^{f/f}$ MEFs in suspension for 5 min before plating the cells. Fresh aliquots of virus were added to the cells every 8 to 12 h. Following a 24 h recovery, the cells were selected with 2 μg/mL puromycin for 2 to 3 days or until uninfected control cells were dead.

Echocardiograms

Echocardiography was performed as previously described (Lu et al., 2009). M-mode images were used for ventricular measurements that were obtained from 9 cardiac cycles for each animal.

Measurement of long-lived protein degradation

MEFs (2×104) were plated into 12-well plate. After overnight recovery, cells were labeled with 0.5 μCi/ml 14C-L-valine in L-valine free medium (Invitrogen). 24 h post labeling, cells were washed three times with PBS, and incubated in complete medium plus 10 mM unlabeled L-valine for 24 h to chase out short-lived proteins. Cells were washed again for three times with PBS, and cultured either in complete media or in serum-free media, both containing 10 mM unlabeled L-valine. The supernatant was collected and precipitated with ice cold trichloroacetic acid (TCA) at a final concentration of 10%. The TCA-soluble radioactivity was measured by liquid scintillation counting. At the end of the experiments, cells were precipitated with 10% ice old TCA, washed with 10% TCA, and dissolved in 0.2 N NaOH, and the radioactivity was measured. The degradation of long-lived protein was calculated by the radioactivity in TCA-soluble supernatant normalized against the total 14C-radioactivity present in supernatants and cell pellets.

Vps34 kinase activity assays

Vps34f/f MEFs were infected with vector or Cre virus. Upon reaching confluence, cell layers on 10 cm tissue culture plates were washed with 5 ml of ice-cold PBS and 5 ml of ice-cold wash buffer (20 mM Tris, pH 7.5, 137 mM NaCl, 1 mM MgCl2, 1 mM CaCl2, 100 mM NaF and 10 mM sodium pyrophosphate). The cells were then scraped into lysis buffer (wash buffer containing 100 μM orthovanadate, 1% NP-40, 10% glycerol and 200 μM phenylmethylsulfonyl fluoride), and the lysates were incubated on ice for 15-20 min with frequent vortexing. The lysates were centrifuged at 18,000 g for 15 min at 4°C, and protein concentration of the supernatants was determined by Bradford assay (Bio-Rad Laboratories). Equal amounts of supernatant protein were mixed with antibody to Vps34 (Cell Signaling Technology) or Beclin 1 (Santa Cruz Biotechnology) and kept on ice overnight, then the immunocomplexes were pulled

down with protein A-agarose. The beads were washed, divided, and used for Vps34 assays and western blotting as previously described (1). Briefly, the kinase assays were initiated by the addition of γ-[32P]ATP (PerkinElmer) and L-α-phosphatidylinositol (Sigma-Aldrich). The reaction product was isolated by thin layer chromatography and visualized by autoradiography.

Histological studies

For cryosections, the tissue was embedded directly in O.C.T. compound (Sakura Finetek USA), stored at -80°C, and sectioned into 6 μm sections. For paraffin-embedded sections, tissue was fixed in 10% neutral buffered formalin overnight, dehydrated in gradually increasing concentrations of ethanol, perfused in paraffin at 60°C overnight, and embedded in paraffin the next day. Tissue was sectioned into 6-μm sections, and paraffin tissue was dewaxed and rehydrated in decreasing concentrations of ethanol solutions. Immunohistochemistry was performed according to standard protocol unless otherwise noted. Briefly, for PAS staining, a Periodic Acid-Schiff kit (Sigma) was used and counterstained with hematoxylin. For Oil Red O staining, cryosections were brought to room temperature, fixed in 10% neutral buffered formalin, washed in running tap water, rinsed with 60% isopropanol, and stained with Oil Red O solution (Sigma). Sections were then rinsed with 60% isopropanol, washed with distilled water, and mounted in glycerin jelly. Tissue sections were observed and imaged under Zeiss inverted Axiovert 200M microscope.

Electron microscopy

Tissue samples were collected freshly and fixed in 4.0% PFA, 2.5% EM grade glutaraldehyde in 0.1 M PBS (pH 7.4). Cell samples were fixed in 2.5% EM grade glutaraldehyde in 0.1 M PBS (pH 7.4). After fixation, samples were placed in 2% osmium tetroxide for tissues and 1% for cells in 0.1 M PBS (pH 7.4), dehydrated in a graded series of ethyl alcohol, and embedded in Epon resin for tissues and Durcupan resin for cells. Ultra-thin sections of 80 nm were cut with a Reichert-Jung UltracutE ultramicrotome and placed on formvar coated slot copper grids. Sections were counterstained with uranyl acetate and lead citrate, and viewed with a FEI Tecnai12 BioTwinG2 electron microscope. Images were acquired with an AMT XR-60 CCD Digital Camera System.

mTOR stimulation

Cells were plated at 2.5x105 cells/well in a 6-well plate. Once adherent, cells were starved overnight in serum-free media. Cells were then incubated in high-salt glucose buffer (10 mM HEPES, pH 7.4, 140 mM NaCl, 4 mM KCl, 2 mM MgSO4, 1 mM KH2PO4, 10 mM glucose) for 2 h, and re-stimulated with 2x MEM amino acids (Sigma) for 30 min. Cell lysates were collected in general lysis buffer (1:100 ProteCEASE-M, 0.2 mM PMSF, 0.1 mM Na3VO4, 20 mM β-glycerol phosphate disodium, 10 mM NaF, 1 mM Na4P2O7).

Transferrin internalization

For transferrin internalization assays, cells were serum starved for 4 h, loaded with 1.5 μg/mL Alexa Fluor-594 conjugated transferrin (Life Technologies) at 4 °C for 40 min, and then incubated for 2 or 5 min at 37 °C. At the end of each time point, cells were subjected to acid wash (10 mM acetic acid and 150 mM NaCl, pH 3.5) for 5 min at 4 °C, and then fixed with 4% paraformaldehyde. Immunofluorescence for EEA1 was then performed.

GST-R5BD and GST-R7BD pulldowns

The preparation of GST-R5BD and GST-R7BD linked to glutathione agarose beads has been described elsewhere (Dou et al., 2013; Peralta et al., 2010). We followed the published protocol with slight modifications. Glutathione agarose beads (Invitrogen) were washed twice with wash buffer (30 mM Tris [pH 7.5], 150 mM NaCl, 10% glycerol, 1% Triton X-100, 10 mM NaF, 100 μM orthovanadate, 200 μM phenylmethylsulfonyl fluoride [PMSF]). Glutathione agarose beads were incubated with GST-R7BD-expressing bacterial lysates for 2-3 h at 4°C on a rotator. The beads were washed four times, 10 minutes each, with wash buffer at 4°C on a rotator. Cells were lysed in Rab7 buffer (20mM HEPES, 100mM NaCl, 5mM MgCl2, 1% triton x-100; plus PMSF (200 μM) and Prote-CEASE-M (1:100). Lysates were cleared by centrifuging at 14,000 xg at 4°C. After protein quantitation equal amounts of protein were added to the washed GST-R7BD beads and incubated at 4°C on a rotator overnight. The beads were washed with Rab7 buffer plus DTT (1 μM) 4 times, 5 min each. After the final wash the samples were boiled in 1X SDS loading dye.

Acridine Orange Staining

MEFs (1.5x105) were plated on glass-bottomed dishes. After overnight recovery, cells were incubated with 0.3 ml Acridine Orange Staining solution (Invitrogen) in 0.7ml full media for 30 minutes at 37^{o}C. Cells were then immediately observed by deconvolution microscope.

EGF transport and EGFR degradation assays

For EGF transport, cells were serum starved overnight then stimulated with 100 ng/mL EGF-Alexa Fluor-647 (Life Technologies) in cold serum-free media for 1 h at 4°C. Cells were then incubated in pre-warmed serum-free DMEM at 10 or 45 min before fixing with 4% paraformaldehyde and performing immunofluorescence. For EGFR degradation, cells were serum-starved overnight then stimulated with 100 ng/mL EGF in serum-free medium for the indicated time points. Cells were rinsed twice with PBS and lysed in RIPA buffer plus 1% SDS, protease inhibitor cocktail (1:100) and EDTA (5 mM).

DQ-BSA assay

Cells were plated on 30 mm glass-bottomed dishes (MatTek). After overnight recovery cells were loaded with 0.5 mg/mL Dextran-Oregon Green for 16 h plus 4 h chase, then loaded with 10 μg/mL DQ-BSA for 1 h. Cells were washed 3 times with PBS, then incubated in fresh media for 30 min. Live cells were imaged by taking pictures of 5-10 randomly chosen areas.

Protein-lipid overlay assay

PIP strips (Echelon Biosciences, Utah, USA) spotted with 15 different lipids were blocked with blocking buffer (phosphate-buffered saline (PBS), 0.1% Tween-20, 3% fatty-acid free BSA (PBS-T 3% BSA)) and gently agitated overnight at 4°C. GST-Armus$^{31-147}$ was incubated with the membrane at a concentration of 0.5 μg/ml in PBS-T 3% BSA for 1 h at room temperature with gentle agitation. 0.5 μg/ml of GST only was used as a negative control and 0.5 μg/ml of PLC-δ1-PH-GST (provided with PIP strip when purchased) as a positive control. Bound protein on lipids was detected using mouse anti-GST antibody in PBS-T 3% BSA followed by HRP-coupled anti-mouse IgG in PBS-T 3% BSA, both for 1 h at room temperature with gentle agitation. Membranes were washed three times for 5 min in PBST in between incubations with protein and antibodies. Positive binding on membranes were visualized with ECL detection kit (GE Healthcare) and exposed to Hyperfilm ECL (GE Healthcare).

Statistics

Student's t-test was used to compare the differences between two groups. Significance was judged when $p<0.05$. Kaplan-Meier curves for mouse survival were constructed using the Log-rank (Mantel-Cox) test.

Image processing and densitometry measurement

Fluorescence and immunofluorescence was analyzed by Zeiss Deconvolution Microscope with AxioCam HRM (Zeiss), Zeiss LSM 510 META NLO Laser Scanning Confocal Microscope system, or Nikon N-SIM super Resolution Microscope system with EMCCD camera iXon3 DU-897E (Andor Technology Ltd.). Images taken from deconvolution and confocal microscopes were viewed and processed by AxioVision LE and Zeiss LSM image browser, respectively. Images were processed in Adobe Photoshop to enhance the brightness and contrast. Densitometry of immunoblot bands was determined by ImageJ software. Background was subtracted from respective measurements for the protein of interest and loading control. Values are expressed as measurement for protein of interest divided by loading control.

8

References

Aki, S., K. Yoshioka, Y. Okamoto, N. Takuwa, and Y. Takuwa. 2015. Phosphatidylinositol 3-kinase class II alpha-isoform PI3K-C2alpha is required for transforming growth factor beta-induced Smad signaling in endothelial cells. *The Journal of biological chemistry*. 290:6086-6105.

Aki, T., A. Nara, and K. Uemura. 2012. Cytoplasmic vacuolization during exposure to drugs and other substances. *Cell biology and toxicology*. 28:125-131.

Axe, E.L., S.A. Walker, M. Manifava, P. Chandra, H.L. Roderick, A. Habermann, G. Griffiths, and N.T. Ktistakis. 2008. Autophagosome formation from membrane compartments enriched in phosphatidylinositol 3-phosphate and dynamically connected to the endoplasmic reticulum. *The Journal of cell biology*. 182:685-701.

Baars, T.L., S. Petri, C. Peters, and A. Mayer. 2007. Role of the V-ATPase in regulation of the vacuolar fission-fusion equilibrium. *Molecular biology of the cell*. 18:3873-3882.

Backer, J.M. 2008. The regulation and function of Class III PI3Ks: novel roles for Vps34. *The Biochemical journal*. 410:1-17.

Bago, R., N. Malik, M.J. Munson, A.R. Prescott, P. Davies, E. Sommer, N. Shpiro, R. Ward, D. Cross, I.G. Ganley, and D.R. Alessi. 2014. Characterization of VPS34-IN1, a selective inhibitor of Vps34, reveals that the phosphatidylinositol 3-phosphate-binding SGK3 protein kinase is a downstream target of class III phosphoinositide 3-kinase. *The Biochemical journal*. 463:413-427.

Balderhaar, H.J., and C. Ungermann. 2013. CORVET and HOPS tethering complexes - coordinators of endosome and lysosome fusion. *Journal of cell science*. 126:1307-1316.

Bechtel, W., M. Helmstadter, J. Balica, B. Hartleben, B. Kiefer, F. Hrnjic, C. Schell, O. Kretz, S. Liu, F. Geist, D. Kerjaschki, G. Walz, and T.B. Huber. 2013. Vps34 deficiency reveals the importance of endocytosis for podocyte homeostasis. *Journal of the American Society of Nephrology : JASN*. 24:727-743.

Beyenbach, K.W., and H. Wieczorek. 2006. The V-type H+ ATPase: molecular structure and function, physiological roles and regulation. *The Journal of experimental biology*. 209:577-589.

Blajecka, K., M. Marinov, L. Leitner, K. Uth, G. Posern, and A. Arcaro. 2012. Phosphoinositide 3-kinase C2beta regulates RhoA and the actin cytoskeleton through an interaction with Dbl. *PloS one*. 7:e44945.

Blommaart, E.F., U. Krause, J.P. Schellens, H. Vreeling-Sindelarova, and A.J. Meijer. 1997. The phosphatidylinositol 3-kinase inhibitors wortmannin and LY294002 inhibit autophagy in isolated rat hepatocytes. *European journal of biochemistry / FEBS*. 243:240-246.

Bohdanowicz, M., and S. Grinstein. 2010. Vesicular traffic: a Rab SANDwich. *Current biology : CB*. 20:R311-314.

Boll, M., H. Daniel, and B. Gasnier. 2004. The SLC36 family: proton-coupled transporters for the absorption of selected amino acids from extracellular and intracellular proteolysis. *Pflugers Archiv : European journal of physiology*. 447:776-779.

Breton, S., and D. Brown. 2007. New insights into the regulation of V-ATPase-dependent proton secretion. *American journal of physiology. Renal physiology*. 292:F1-10.

Bright, N.A., M.J. Gratian, and J.P. Luzio. 2005. Endocytic delivery to lysosomes mediated by concurrent fusion and kissing events in living cells. *Current biology : CB*. 15:360-365.

Byfield, M.P., J.T. Murray, and J.M. Backer. 2005. hVps34 is a nutrient-regulated lipid kinase required for activation of p70 S6 kinase. *The Journal of biological chemistry*. 280:33076-33082.

Cabrera, M., M. Nordmann, A. Perz, D. Schmedt, A. Gerondopoulos, F. Barr, J. Piehler, S. Engelbrecht-Vandre, and C. Ungermann. 2014. The Mon1-Ccz1 GEF activates the Rab7 GTPase Ypt7 via a longin-fold-Rab interface and association with PI3P-positive membranes. *Journal of cell science*. 127:1043-1051.

Carpentier, S., F. N'Kuli, G. Grieco, P. Van Der Smissen, V. Janssens, H. Emonard, B. Bilanges, B. Vanhaesebroeck, H.P. Gaide Chevronnay, C.E. Pierreux, D. Tyteca, and P.J. Courtoy. 2013. Class III phosphoinositide 3-kinase/VPS34 and dynamin are critical for apical endocytic recycling. *Traffic*. 14:933-948.

Carroll, B., N. Mohd-Naim, F. Maximiano, M.A. Frasa, J. McCormack, M. Finelli, S.B. Thoresen, L. Perdios, R. Daigaku, R.E. Francis, C. Futter, I. Dikic, and V.M. Braga. 2013. The TBC/RabGAP Armus coordinates Rac1 and Rab7 functions during autophagy. *Developmental cell*. 25:15-28.

Chotard, L., A.K. Mishra, M.A. Sylvain, S. Tuck, D.G. Lambright, and C.E. Rocheleau. 2010. TBC-2 regulates RAB-5/RAB-7-mediated endosomal trafficking in Caenorhabditis elegans. *Molecular biology of the cell*. 21:2285-2296.

Christoforidis, S., H.M. McBride, R.D. Burgoyne, and M. Zerial. 1999a. The Rab5 effector EEA1 is a core component of endosome docking. *Nature*. 397:621-625.

Christoforidis, S., M. Miaczynska, K. Ashman, M. Wilm, L. Zhao, S.C. Yip, M.D. Waterfield, J.M. Backer, and M. Zerial. 1999b. Phosphatidylinositol-3-OH kinases are Rab5 effectors. *Nature cell biology*. 1:249-252.

Ciraolo, E., M. Iezzi, R. Marone, S. Marengo, C. Curcio, C. Costa, O. Azzolino, C. Gonella, C. Rubinetto, H. Wu, W. Dastru, E.L. Martin, L. Silengo, F. Altruda, E. Turco, L. Lanzetti, P. Musiani, T. Ruckle, C. Rommel, J.M. Backer, G. Forni, M.P. Wymann, and E. Hirsch. 2008. Phosphoinositide 3-kinase p110beta activity: key role in metabolism and mammary gland cancer but not development. *Science signaling*. 1:ra3.

Codogno, P., M. Mehrpour, and T. Proikas-Cezanne. 2012. Canonical and non-canonical autophagy: variations on a common theme of self-eating? *Nature reviews. Molecular cell biology*. 13:7-12.

Cogli, L., F. Piro, and C. Bucci. 2009. Rab7 and the CMT2B disease. *Biochemical Society transactions*. 37:1027-1031.

Dai, S., Y. Zhang, T. Weimbs, M.B. Yaffe, and D. Zhou. 2007. Bacteria-generated PtdIns(3)P recruits VAMP8 to facilitate phagocytosis. *Traffic*. 8:1365-1374.

De Luca, M., L. Cogli, C. Progida, V. Nisi, R. Pascolutti, S. Sigismund, P.P. Di Fiore, and C. Bucci. 2014. RILP regulates vacuolar ATPase through interaction with the V1G1 subunit. *Journal of cell science*. 127:2697-2708.

Deretic, V. 2006. Autophagy as an immune defense mechanism. *Current opinion in immunology*. 18:375-382.

Devereaux, K., C. Dall'Armi, A. Alcazar-Roman, Y. Ogasawara, X. Zhou, F. Wang, A. Yamamoto, P. De Camilli, and G. Di Paolo. 2013. Regulation of mammalian autophagy by class II and III PI 3-kinases through PI3P synthesis. *PloS one*. 8:e76405.

Dong, X.P., D. Shen, X. Wang, T. Dawson, X. Li, Q. Zhang, X. Cheng, Y. Zhang, L.S. Weisman, M. Delling, and H. Xu. 2010. PI(3,5)P(2) controls membrane trafficking by

direct activation of mucolipin Ca(2+) release channels in the endolysosome. *Nature communications*. 1:38.

Dou, Z., M. Chattopadhyay, J.A. Pan, J.L. Guerriero, Y.P. Jiang, L.M. Ballou, Z. Yue, R.Z. Lin, and W.X. Zong. 2010. The class IA phosphatidylinositol 3-kinase p110-beta subunit is a positive regulator of autophagy. *The Journal of cell biology*. 191:827-843.

Dou, Z., J.A. Pan, H.A. Dbouk, L.M. Ballou, J.L. DeLeon, Y. Fan, J.S. Chen, Z. Liang, G. Li, J.M. Backer, R.Z. Lin, and W.X. Zong. 2013. Class IA PI3K p110beta subunit promotes autophagy through Rab5 small GTPase in response to growth factor limitation. *Molecular cell*. 50:29-42.

Dowdle, W.E., B. Nyfeler, J. Nagel, R.A. Elling, S. Liu, E. Triantafellow, S. Menon, Z. Wang, A. Honda, G. Pardee, J. Cantwell, C. Luu, I. Cornella-Taracido, E. Harrington, P. Fekkes, H. Lei, Q. Fang, M.E. Digan, D. Burdick, A.F. Powers, S.B. Helliwell, S. D'Aquin, J. Bastien, H. Wang, D. Wiederschain, J. Kuerth, P. Bergman, D. Schwalb, J. Thomas, S. Ugwonali, F. Harbinski, J. Tallarico, C.J. Wilson, V.E. Myer, J.A. Porter, D.E. Bussiere, P.M. Finan, M.A. Labow, X. Mao, L.G. Hamann, B.D. Manning, R.A. Valdez, T. Nicholson, M. Schirle, M.S. Knapp, E.P. Keaney, and L.O. Murphy. 2014. Selective VPS34 inhibitor blocks autophagy and uncovers a role for NCOA4 in ferritin degradation and iron homeostasis in vivo. *Nature cell biology*. 16:1069-1079.

Eden, E.R., I.J. White, and C.E. Futter. 2009. Down-regulation of epidermal growth factor receptor signalling within multivesicular bodies. *Biochemical Society transactions*. 37:173-177.

Eskelinen, E.L. 2005. Maturation of autophagic vacuoles in Mammalian cells. *Autophagy*. 1:1-10.

Falasca, M., and T. Maffucci. 2012. Regulation and cellular functions of class II phosphoinositide 3-kinases. *The Biochemical journal*. 443:587-601.

Fang, Y., M. Vilella-Bach, R. Bachmann, A. Flanigan, and J. Chen. 2001. Phosphatidic acid-mediated mitogenic activation of mTOR signaling. *Science*. 294:1942-1945.

Fili, N., V. Calleja, R. Woscholski, P.J. Parker, and B. Larijani. 2006. Compartmental signal modulation: Endosomal phosphatidylinositol 3-phosphate controls endosome morphology and selective cargo sorting. *Proceedings of the National Academy of Sciences of the United States of America*. 103:15473-15478.

Flinn, R.J., Y. Yan, S. Goswami, P.J. Parker, and J.M. Backer. 2010. The late endosome is essential for mTORC1 signaling. *Molecular biology of the cell*. 21:833-841.

Florey, O., N. Gammoh, S.E. Kim, X. Jiang, and M. Overholtzer. 2015. V-ATPase and osmotic imbalances activate endolysosomal LC3 lipidation. *Autophagy*. 11:88-99.

Frasa, M.A., F.C. Maximiano, K. Smolarczyk, R.E. Francis, M.E. Betson, E. Lozano, J. Goldenring, M.C. Seabra, A. Rak, M.R. Ahmadian, and V.M. Braga. 2010. Armus is a Rac1 effector that inactivates Rab7 and regulates E-cadherin degradation. *Current biology : CB*. 20:198-208.

Fujita, N., M. Hayashi-Nishino, H. Fukumoto, H. Omori, A. Yamamoto, T. Noda, and T. Yoshimori. 2008. An Atg4B mutant hampers the lipidation of LC3 paralogues and causes defects in autophagosome closure. *Molecular biology of the cell*. 19:4651-4659.

Funderburk, S.F., Q.J. Wang, and Z. Yue. 2010. The Beclin 1-VPS34 complex--at the crossroads of autophagy and beyond. *Trends in cell biology*. 20:355-362.

Furuya, T., M. Kim, M. Lipinski, J. Li, D. Kim, T. Lu, Y. Shen, L. Rameh, B. Yankner, L.H. Tsai, and J. Yuan. 2010. Negative regulation of Vps34 by Cdk mediated phosphorylation. *Molecular cell*. 38:500-511.

Gaidarov, I., M.E. Smith, J. Domin, and J.H. Keen. 2001. The class II phosphoinositide 3-kinase C2alpha is activated by clathrin and regulates clathrin-mediated membrane trafficking. *Molecular cell*. 7:443-449.

Genisset, C., A. Puhar, F. Calore, M. de Bernard, P. Dell'Antone, and C. Montecucco. 2007. The concerted action of the Helicobacter pylori cytotoxin VacA and of the v-ATPase proton pump induces swelling of isolated endosomes. *Cellular microbiology*. 9:1481-1490.

Haas, A., D. Scheglmann, T. Lazar, D. Gallwitz, and W. Wickner. 1995. The GTPase Ypt7p of Saccharomyces cerevisiae is required on both partner vacuoles for the homotypic fusion step of vacuole inheritance. *The EMBO journal*. 14:5258-5270.

Harrison, R.E., C. Bucci, O.V. Vieira, T.A. Schroer, and S. Grinstein. 2003. Phagosomes fuse with late endosomes and/or lysosomes by extension of membrane protrusions along microtubules: role of Rab7 and RILP. *Molecular and cellular biology*. 23:6494-6506.

He, C., and D.J. Klionsky. 2009. Regulation mechanisms and signaling pathways of autophagy. *Annual review of genetics*. 43:67-93.

Heenan, E.J., J.L. Vanhooke, B.R. Temple, L. Betts, J.E. Sondek, and H.G. Dohlman. 2009. Structure and function of Vps15 in the endosomal G protein signaling pathway. *Biochemistry*. 48:6390-6401.

Herman, P.K., and S.D. Emr. 1990. Characterization of VPS34, a gene required for vacuolar protein sorting and vacuole segregation in Saccharomyces cerevisiae. *Molecular and cellular biology*. 10:6742-6754.

Hosokawa, N., T. Hara, T. Kaizuka, C. Kishi, A. Takamura, Y. Miura, S. Iemura, T. Natsume, K. Takehana, N. Yamada, J.L. Guan, N. Oshiro, and N. Mizushima. 2009. Nutrient-dependent mTORC1 association with the ULK1-Atg13-FIP200 complex required for autophagy. *Molecular biology of the cell*. 20:1981-1991.

Huotari, J., and A. Helenius. 2011. Endosome maturation. *The EMBO journal*. 30:3481-3500.

Ichimura, Y., Y. Imamura, K. Emoto, M. Umeda, T. Noda, and Y. Ohsumi. 2004. In vivo and in vitro reconstitution of Atg8 conjugation essential for autophagy. *The Journal of biological chemistry*. 279:40584-40592.

Ikonomov, O.C., D. Sbrissa, M. Foti, J.L. Carpentier, and A. Shisheva. 2003. PIKfyve controls fluid phase endocytosis but not recycling/degradation of endocytosed receptors or sorting of procathepsin D by regulating multivesicular body morphogenesis. *Molecular biology of the cell*. 14:4581-4591.

Ikonomov, O.C., D. Sbrissa, and A. Shisheva. 2006. Localized PtdIns 3,5-P2 synthesis to regulate early endosome dynamics and fusion. *American journal of physiology. Cell physiology*. 291:C393-404.

Ikonomov, O.C., D. Sbrissa, M. Venkatareddy, E. Tisdale, P. Garg, and A. Shisheva. 2015. Class III PI 3-kinase is the main source of PtdIns3P substrate and membrane recruitment signal for PIKfyve constitutive function in podocyte endomembrane homeostasis. *Biochimica et biophysica acta*. 1853:1240-1250.

Itakura, E., C. Kishi, K. Inoue, and N. Mizushima. 2008. Beclin 1 forms two distinct phosphatidylinositol 3-kinase complexes with mammalian Atg14 and UVRAG. *Molecular biology of the cell*. 19:5360-5372.

Itakura, E., and N. Mizushima. 2010. Characterization of autophagosome formation site by a hierarchical analysis of mammalian Atg proteins. *Autophagy*. 6:764-776.
Jaber, N., Z. Dou, J.S. Chen, J. Catanzaro, Y.P. Jiang, L.M. Ballou, E. Selinger, X. Ouyang, R.Z. Lin, J. Zhang, and W.X. Zong. 2012. Class III PI3K Vps34 plays an essential role in autophagy and in heart and liver function. *Proceedings of the National Academy of Sciences of the United States of America*. 109:2003-2008.
Johnson, E.E., J.H. Overmeyer, W.T. Gunning, and W.A. Maltese. 2006. Gene silencing reveals a specific function of hVps34 phosphatidylinositol 3-kinase in late versus early endosomes. *Journal of cell science*. 119:1219-1232.
Jovic, M., M. Sharma, J. Rahajeng, and S. Caplan. 2010. The early endosome: a busy sorting station for proteins at the crossroads. *Histology and histopathology*. 25:99-112.
Katzmann, D.J., G. Odorizzi, and S.D. Emr. 2002. Receptor downregulation and multivesicular-body sorting. *Nature reviews. Molecular cell biology*. 3:893-905.
Kaushik, S., A.C. Massey, N. Mizushima, and A.M. Cuervo. 2008. Constitutive activation of chaperone-mediated autophagy in cells with impaired macroautophagy. *Molecular biology of the cell*. 19:2179-2192.
Kawai, A., H. Uchiyama, S. Takano, N. Nakamura, and S. Ohkuma. 2007. Autophagosome-lysosome fusion depends on the pH in acidic compartments in CHO cells. *Autophagy*. 3:154-157.
Kim, J., M. Kundu, B. Viollet, and K.L. Guan. 2011. AMPK and mTOR regulate autophagy through direct phosphorylation of Ulk1. *Nature cell biology*. 13:132-141.
Kirkin, V., D.G. McEwan, I. Novak, and I. Dikic. 2009. A role for ubiquitin in selective autophagy. *Molecular cell*. 34:259-269.
Klionsky, D.J., Z. Elazar, P.O. Seglen, and D.C. Rubinsztein. 2008. Does bafilomycin A1 block the fusion of autophagosomes with lysosomes? *Autophagy*. 4:849-850.
Komatsu, M., S. Waguri, T. Chiba, S. Murata, J. Iwata, I. Tanida, T. Ueno, M. Koike, Y. Uchiyama, E. Kominami, and K. Tanaka. 2006. Loss of autophagy in the central nervous system causes neurodegeneration in mice. *Nature*. 441:880-884.
Komatsu, M., S. Waguri, T. Ueno, J. Iwata, S. Murata, I. Tanida, J. Ezaki, N. Mizushima, Y. Ohsumi, Y. Uchiyama, E. Kominami, K. Tanaka, and T. Chiba. 2005. Impairment of starvation-induced and constitutive autophagy in Atg7-deficient mice. *The Journal of cell biology*. 169:425-434.
Korolchuk, V.I., S. Saiki, M. Lichtenberg, F.H. Siddiqi, E.A. Roberts, S. Imarisio, L. Jahreiss, S. Sarkar, M. Futter, F.M. Menzies, C.J. O'Kane, V. Deretic, and D.C. Rubinsztein. 2011. Lysosomal positioning coordinates cellular nutrient responses. *Nature cell biology*. 13:453-460.
Ktistakis, N.T., M. Manifava, P. Schoenfelder, and S. Rotondo. 2012. How phosphoinositide 3-phosphate controls growth downstream of amino acids and autophagy downstream of amino acid withdrawal. *Biochemical Society transactions*. 40:37-43.
Kuma, A., M. Hatano, M. Matsui, A. Yamamoto, H. Nakaya, T. Yoshimori, Y. Ohsumi, T. Tokuhisa, and N. Mizushima. 2004. The role of autophagy during the early neonatal starvation period. *Nature*. 432:1032-1036.
Kummel, D., and C. Ungermann. 2014. Principles of membrane tethering and fusion in endosome and lysosome biogenesis. *Current opinion in cell biology*. 29:61-66.
Laplante, M., and D.M. Sabatini. 2009. mTOR signaling at a glance. *Journal of cell science*. 122:3589-3594.

Lawrence, G., C.C. Brown, B.A. Flood, S. Karunakaran, M. Cabrera, M. Nordmann, C. Ungermann, and R.A. Fratti. 2014. Dynamic association of the PI3P-interacting Mon1-Ccz1 GEF with vacuoles is controlled through its phosphorylation by the type 1 casein kinase Yck3. *Molecular biology of the cell*. 25:1608-1619.

Lebrand, C., M. Corti, H. Goodson, P. Cosson, V. Cavalli, N. Mayran, J. Faure, and J. Gruenberg. 2002. Late endosome motility depends on lipids via the small GTPase Rab7. *The EMBO journal*. 21:1289-1300.

Lemmon, M.A. 2003. Phosphoinositide recognition domains. *Traffic*. 4:201-213.

Li, G., C. D'Souza-Schorey, M.A. Barbieri, R.L. Roberts, A. Klippel, L.T. Williams, and P.D. Stahl. 1995. Evidence for phosphatidylinositol 3-kinase as a regulator of endocytosis via activation of Rab5. *Proceedings of the National Academy of Sciences of the United States of America*. 92:10207-10211.

Liang, C., J.S. Lee, K.S. Inn, M.U. Gack, Q. Li, E.A. Roberts, I. Vergne, V. Deretic, P. Feng, C. Akazawa, and J.U. Jung. 2008a. Beclin1-binding UVRAG targets the class C Vps complex to coordinate autophagosome maturation and endocytic trafficking. *Nature cell biology*. 10:776-787.

Liang, C., D. Sir, S. Lee, J.H. Ou, and J.U. Jung. 2008b. Beyond autophagy: the role of UVRAG in membrane trafficking. *Autophagy*. 4:817-820.

Lindmo, K., and H. Stenmark. 2006. Regulation of membrane traffic by phosphoinositide 3-kinases. *Journal of cell science*. 119:605-614.

Lipinski, M.M., G. Hoffman, A. Ng, W. Zhou, B.F. Py, E. Hsu, X. Liu, J. Eisenberg, J. Liu, J. Blenis, R.J. Xavier, and J. Yuan. 2010a. A genome-wide siRNA screen reveals multiple mTORC1 independent signaling pathways regulating autophagy under normal nutritional conditions. *Developmental cell*. 18:1041-1052.

Lipinski, M.M., B. Zheng, T. Lu, Z. Yan, B.F. Py, A. Ng, R.J. Xavier, C. Li, B.A. Yankner, C.R. Scherzer, and J. Yuan. 2010b. Genome-wide analysis reveals mechanisms modulating autophagy in normal brain aging and in Alzheimer's disease. *Proceedings of the National Academy of Sciences of the United States of America*. 107:14164-14169.

Liu, J., D. Lamb, M.M. Chou, Y.J. Liu, and G. Li. 2007. Nerve growth factor-mediated neurite outgrowth via regulation of Rab5. *Molecular biology of the cell*. 18:1375-1384.

Lu, Q., P. Yang, X. Huang, W. Hu, B. Guo, F. Wu, L. Lin, A.L. Kovacs, L. Yu, and H. Zhang. 2011. The WD40 repeat PtdIns(3)P-binding protein EPG-6 regulates progression of omegasomes to autophagosomes. *Developmental cell*. 21:343-357.

Lu, Z., Y.P. Jiang, W. Wang, X.H. Xu, R.T. Mathias, E. Entcheva, L.M. Ballou, I.S. Cohen, and R.Z. Lin. 2009. Loss of cardiac phosphoinositide 3-kinase p110 alpha results in contractile dysfunction. *Circulation*. 120:318-325.

Luzio, J.P., N.A. Bright, and P.R. Pryor. 2007a. The role of calcium and other ions in sorting and delivery in the late endocytic pathway. *Biochemical Society transactions*. 35:1088-1091.

Luzio, J.P., P.R. Pryor, and N.A. Bright. 2007b. Lysosomes: fusion and function. *Nature reviews. Molecular cell biology*. 8:622-632.

Luzio, J.P., B.A. Rous, N.A. Bright, P.R. Pryor, B.M. Mullock, and R.C. Piper. 2000. Lysosome-endosome fusion and lysosome biogenesis. *Journal of cell science*. 113 (Pt 9):1515-1524.

Majeski, A.E., and J.F. Dice. 2004. Mechanisms of chaperone-mediated autophagy. *The international journal of biochemistry & cell biology*. 36:2435-2444.

Martys, J.L., C. Wjasow, D.M. Gangi, M.C. Kielian, T.E. McGraw, and J.M. Backer. 1996. Wortmannin-sensitive trafficking pathways in Chinese hamster ovary cells. Differential effects on endocytosis and lysosomal sorting. *The Journal of biological chemistry*. 271:10953-10962.

Mathew, R., and E. White. 2007. Why sick cells produce tumors: the protective role of autophagy. *Autophagy*. 3:502-505.

McKnight, N.C., and Y. Zhenyu. 2013. Beclin 1, an Essential Component and Master Regulator of PI3K-III in Health and Disease. *Current pathobiology reports*. 1:231-238.

McKnight, N.C., Y. Zhong, M.S. Wold, S. Gong, G.R. Phillips, Z. Dou, Y. Zhao, N. Heintz, W.X. Zong, and Z. Yue. 2014. Beclin 1 is required for neuron viability and regulates endosome pathways via the UVRAG-VPS34 complex. *PLoS genetics*. 10:e1004626.

McLeod, I.X., X. Zhou, Q.J. Li, F. Wang, and Y.W. He. 2011. The class III kinase Vps34 promotes T lymphocyte survival through regulating IL-7Ralpha surface expression. *J Immunol*. 187:5051-5061.

Miller, S., B. Tavshanjian, A. Oleksy, O. Perisic, B.T. Houseman, K.M. Shokat, and R.L. Williams. 2010. Shaping development of autophagy inhibitors with the structure of the lipid kinase Vps34. *Science*. 327:1638-1642.

Mizushima, N., B. Levine, A.M. Cuervo, and D.J. Klionsky. 2008. Autophagy fights disease through cellular self-digestion. *Nature*. 451:1069-1075.

Mizushima, N., A. Yamamoto, M. Matsui, T. Yoshimori, and Y. Ohsumi. 2004. In vivo analysis of autophagy in response to nutrient starvation using transgenic mice expressing a fluorescent autophagosome marker. *Molecular biology of the cell*. 15:1101-1111.

Mizushima, N., T. Yoshimori, and B. Levine. 2010. Methods in mammalian autophagy research. *Cell*. 140:313-326.

Moreau, K., C. Puri, and D.C. Rubinsztein. 2015. Methods to analyze SNARE-dependent vesicular fusion events that regulate autophagosome biogenesis. *Methods*. 75:19-24.

Moreau, K., B. Ravikumar, M. Renna, C. Puri, and D.C. Rubinsztein. 2011. Autophagosome precursor maturation requires homotypic fusion. *Cell*. 146:303-317.

Moreau, K., M. Renna, and D.C. Rubinsztein. 2013. Connections between SNAREs and autophagy. *Trends in biochemical sciences*. 38:57-63.

Morel, E., Z. Chamoun, Z.M. Lasiecka, R.B. Chan, R.L. Williamson, C. Vetanovetz, C. Dall'Armi, S. Simoes, K.S. Point Du Jour, B.D. McCabe, S.A. Small, and G. Di Paolo. 2013. Phosphatidylinositol-3-phosphate regulates sorting and processing of amyloid precursor protein through the endosomal system. *Nature communications*. 4:2250.

Mousavi, S.A., A. Brech, T. Berg, and R. Kjeken. 2003. Phosphoinositide 3-kinase regulates maturation of lysosomes in rat hepatocytes. *The Biochemical journal*. 372:861-869.

Mullock, B.M., N.A. Bright, C.W. Fearon, S.R. Gray, and J.P. Luzio. 1998. Fusion of lysosomes with late endosomes produces a hybrid organelle of intermediate density and is NSF dependent. *The Journal of cell biology*. 140:591-601.

Nair, U., and D.J. Klionsky. 2005. Molecular mechanisms and regulation of specific and nonspecific autophagy pathways in yeast. *The Journal of biological chemistry*. 280:41785-41788.

Nakai, A., O. Yamaguchi, T. Takeda, Y. Higuchi, S. Hikoso, M. Taniike, S. Omiya, I. Mizote, Y. Matsumura, M. Asahi, K. Nishida, M. Hori, N. Mizushima, and K. Otsu. 2007. The role of autophagy in cardiomyocytes in the basal state and in response to hemodynamic stress. *Nature medicine*. 13:619-624.

Nakatogawa, H., Y. Ichimura, and Y. Ohsumi. 2007. Atg8, a ubiquitin-like protein required for autophagosome formation, mediates membrane tethering and hemifusion. *Cell*. 130:165-178.

Nemazanyy, I., B. Blaauw, C. Paolini, C. Caillaud, F. Protasi, A. Mueller, T. Proikas-Cezanne, R.C. Russell, K.L. Guan, I. Nishino, M. Sandri, M. Pende, and G. Panasyuk. 2013. Defects of Vps15 in skeletal muscles lead to autophagic vacuolar myopathy and lysosomal disease. *EMBO molecular medicine*. 5:870-890.

Nobukuni, T., M. Joaquin, M. Roccio, S.G. Dann, S.Y. Kim, P. Gulati, M.P. Byfield, J.M. Backer, F. Natt, J.L. Bos, F.J. Zwartkruis, and G. Thomas. 2005. Amino acids mediate mTOR/raptor signaling through activation of class 3 phosphatidylinositol 3OH-kinase. *Proceedings of the National Academy of Sciences of the United States of America*. 102:14238-14243.

Obara, K., T. Noda, K. Niimi, and Y. Ohsumi. 2008. Transport of phosphatidylinositol 3-phosphate into the vacuole via autophagic membranes in Saccharomyces cerevisiae. *Genes to cells : devoted to molecular & cellular mechanisms*. 13:537-547.

Olkkonen, V.M., and E. Ikonen. 2006. When intracellular logistics fails--genetic defects in membrane trafficking. *Journal of cell science*. 119:5031-5045.

Pankiv, S., E.A. Alemu, A. Brech, J.A. Bruun, T. Lamark, A. Overvatn, G. Bjorkoy, and T. Johansen. 2010. FYCO1 is a Rab7 effector that binds to LC3 and PI3P to mediate microtubule plus end-directed vesicle transport. *The Journal of cell biology*. 188:253-269.

Pankiv, S., T.H. Clausen, T. Lamark, A. Brech, J.A. Bruun, H. Outzen, A. Overvatn, G. Bjorkoy, and T. Johansen. 2007. p62/SQSTM1 binds directly to Atg8/LC3 to facilitate degradation of ubiquitinated protein aggregates by autophagy. *The Journal of biological chemistry*. 282:24131-24145.

Papini, E., E. Gottardi, B. Satin, M. de Bernard, P. Massari, J. Telford, R. Rappuoli, S.B. Sato, and C. Montecucco. 1996. The vacuolar ATPase proton pump is present on intracellular vacuoles induced by Helicobacter pylori. *Journal of medical microbiology*. 45:84-89.

Papini, E., B. Satin, C. Bucci, M. de Bernard, J.L. Telford, R. Manetti, R. Rappuoli, M. Zerial, and C. Montecucco. 1997. The small GTP binding protein rab7 is essential for cellular vacuolation induced by Helicobacter pylori cytotoxin. *The EMBO journal*. 16:15-24.

Parekh, V.V., L. Wu, K.L. Boyd, J.A. Williams, J.A. Gaddy, D. Olivares-Villagomez, T.L. Cover, W.X. Zong, J. Zhang, and L. Van Kaer. 2013. Impaired autophagy, defective T cell homeostasis, and a wasting syndrome in mice with a T cell-specific deletion of Vps34. *J Immunol*. 190:5086-5101.

Pasquier, B., Y. El-Ahmad, B. Filoche-Romme, C. Dureuil, F. Fassy, P.Y. Abecassis, M. Mathieu, T. Bertrand, T. Benard, C. Barriere, S. El Batti, J.P. Letallec, V. Sonnefraud, M. Brollo, L. Delbarre, V. Loyau, F. Pilorge, L. Bertin, P. Richepin, J. Arigon, J.R. Labrosse, J. Clement, F. Durand, R. Combet, P. Perraut, V. Leroy, F. Gay, D. Lefrancois, F. Bretin, J.P. Marquette, N. Michot, A. Caron, C. Castell, L. Schio, G. McCort, H. Goulaouic, C. Garcia-Echeverria, and B. Ronan. 2015. Discovery of (2S)-8-[(3R)-3-methylmorpholin-4-yl]-1-(3-methyl-2-oxobutyl)-2-(trifluoromethyl)- 3,4-dihydro-2H-pyrimido[1,2-a]pyrimidin-6-one: a novel potent and selective inhibitor of Vps34 for the treatment of solid tumors. *Journal of medicinal chemistry*. 58:376-400.

Pena-Llopis, S., and J. Brugarolas. 2011. TFEB, a novel mTORC1 effector implicated in lysosome biogenesis, endocytosis and autophagy. *Cell Cycle*. 10:3987-3988.

Peralta, E.R., B.C. Martin, and A.L. Edinger. 2010. Differential effects of TBC1D15 and mammalian Vps39 on Rab7 activation state, lysosomal morphology, and growth factor dependence. *The Journal of biological chemistry*. 285:16814-16821.

Peters, C., M.J. Bayer, S. Buhler, J.S. Andersen, M. Mann, and A. Mayer. 2001. Trans-complex formation by proteolipid channels in the terminal phase of membrane fusion. *Nature*. 409:581-588.

Petiot, A., E. Ogier-Denis, E.F. Blommaart, A.J. Meijer, and P. Codogno. 2000. Distinct classes of phosphatidylinositol 3'-kinases are involved in signaling pathways that control macroautophagy in HT-29 cells. *The Journal of biological chemistry*. 275:992-998.

Platt, F.M., B. Boland, and A.C. van der Spoel. 2012. The cell biology of disease: lysosomal storage disorders: the cellular impact of lysosomal dysfunction. *The Journal of cell biology*. 199:723-734.

Polson, H.E., J. de Lartigue, D.J. Rigden, M. Reedijk, S. Urbe, M.J. Clague, and S.A. Tooze. 2010. Mammalian Atg18 (WIPI2) localizes to omegasome-anchored phagophores and positively regulates LC3 lipidation. *Autophagy*. 6:506-522.

Posor, Y., M. Eichhorn-Gruenig, D. Puchkov, J. Schoneberg, A. Ullrich, A. Lampe, R. Muller, S. Zarbakhsh, F. Gulluni, E. Hirsch, M. Krauss, C. Schultz, J. Schmoranzer, F. Noe, and V. Haucke. 2013. Spatiotemporal control of endocytosis by phosphatidylinositol-3,4-bisphosphate. *Nature*. 499:233-237.

Posor, Y., M. Eichhorn-Grunig, and V. Haucke. 2015. Phosphoinositides in endocytosis. *Biochimica et biophysica acta*. 1851:794-804.

Poteryaev, D., S. Datta, K. Ackema, M. Zerial, and A. Spang. 2010. Identification of the switch in early-to-late endosome transition. *Cell*. 141:497-508.

Proikas-Cezanne, T., S. Waddell, A. Gaugel, T. Frickey, A. Lupas, and A. Nordheim. 2004. WIPI-1alpha (WIPI49), a member of the novel 7-bladed WIPI protein family, is aberrantly expressed in human cancer and is linked to starvation-induced autophagy. *Oncogene*. 23:9314-9325.

Pryor, P.R., B.M. Mullock, N.A. Bright, S.R. Gray, and J.P. Luzio. 2000. The role of intraorganellar Ca(2+) in late endosome-lysosome heterotypic fusion and in the reformation of lysosomes from hybrid organelles. *The Journal of cell biology*. 149:1053-1062.

Pryor, P.R., B.M. Mullock, N.A. Bright, M.R. Lindsay, S.R. Gray, S.C. Richardson, A. Stewart, D.E. James, R.C. Piper, and J.P. Luzio. 2004. Combinatorial SNARE complexes with VAMP7 or VAMP8 define different late endocytic fusion events. *EMBO reports*. 5:590-595.

Puri, C., M. Renna, C.F. Bento, K. Moreau, and D.C. Rubinsztein. 2014. ATG16L1 meets ATG9 in recycling endosomes: additional roles for the plasma membrane and endocytosis in autophagosome biogenesis. *Autophagy*. 10:182-184.

Ravikumar, B., S. Imarisio, S. Sarkar, C.J. O'Kane, and D.C. Rubinsztein. 2008. Rab5 modulates aggregation and toxicity of mutant huntingtin through macroautophagy in cell and fly models of Huntington disease. *Journal of cell science*. 121:1649-1660.

Ravikumar, B., C. Vacher, Z. Berger, J.E. Davies, S. Luo, L.G. Oroz, F. Scaravilli, D.F. Easton, R. Duden, C.J. O'Kane, and D.C. Rubinsztein. 2004. Inhibition of mTOR induces autophagy and reduces toxicity of polyglutamine expansions in fly and mouse models of Huntington disease. *Nature genetics*. 36:585-595.

Reaves, B.J., N.A. Bright, B.M. Mullock, and J.P. Luzio. 1996. The effect of wortmannin on the localisation of lysosomal type I integral membrane glycoproteins suggests a role for phosphoinositide 3-kinase activity in regulating membrane traffic late in the endocytic pathway. *Journal of cell science*. 109 (Pt 4):749-762.

Reifler, A., X. Li, A.J. Archambeau, J.R. McDade, N. Sabha, D.E. Michele, and J.J. Dowling. 2014. Conditional knockout of pik3c3 causes a murine muscular dystrophy. *The American journal of pathology*. 184:1819-1830.

Rink, J., E. Ghigo, Y. Kalaidzidis, and M. Zerial. 2005. Rab conversion as a mechanism of progression from early to late endosomes. *Cell*. 122:735-749.

Robinson, J.S., D.J. Klionsky, L.M. Banta, and S.D. Emr. 1988. Protein sorting in Saccharomyces cerevisiae: isolation of mutants defective in the delivery and processing of multiple vacuolar hydrolases. *Molecular and cellular biology*. 8:4936-4948.

Ronan, B., O. Flamand, L. Vescovi, C. Dureuil, L. Durand, F. Fassy, M.F. Bachelot, A. Lamberton, M. Mathieu, T. Bertrand, J.P. Marquette, Y. El-Ahmad, B. Filoche-Romme, L. Schio, C. Garcia-Echeverria, H. Goulaouic, and B. Pasquier. 2014. A highly potent and selective Vps34 inhibitor alters vesicle trafficking and autophagy. *Nature chemical biology*. 10:1013-1019.

Rush, J.S., L.M. Quinalty, L. Engelman, D.M. Sherry, and B.P. Ceresa. 2012. Endosomal accumulation of the activated epidermal growth factor receptor (EGFR) induces apoptosis. *The Journal of biological chemistry*. 287:712-722.

Saito, K., Y. Araki, K. Kontani, H. Nishina, and T. Katada. 2005. Novel role of the small GTPase Rheb: its implication in endocytic pathway independent of the activation of mammalian target of rapamycin. *Journal of biochemistry*. 137:423-430.

Sancak, Y., L. Bar-Peled, R. Zoncu, A.L. Markhard, S. Nada, and D.M. Sabatini. 2010. Ragulator-Rag complex targets mTORC1 to the lysosomal surface and is necessary for its activation by amino acids. *Cell*. 141:290-303.

Sancak, Y., T.R. Peterson, Y.D. Shaul, R.A. Lindquist, C.C. Thoreen, L. Bar-Peled, and D.M. Sabatini. 2008. The Rag GTPases bind raptor and mediate amino acid signaling to mTORC1. *Science*. 320:1496-1501.

Sato, T.K., M. Overduin, and S.D. Emr. 2001. Location, location, location: membrane targeting directed by PX domains. *Science*. 294:1881-1885.

Schimmoller, F., and H. Riezman. 1993. Involvement of Ypt7p, a small GTPase, in traffic from late endosome to the vacuole in yeast. *Journal of cell science*. 106 (Pt 3):823-830.

Seglen, P.O., and P.B. Gordon. 1982. 3-Methyladenine: specific inhibitor of autophagic/lysosomal protein degradation in isolated rat hepatocytes. *Proceedings of the National Academy of Sciences of the United States of America*. 79:1889-1892.

Shin, H.W., M. Hayashi, S. Christoforidis, S. Lacas-Gervais, S. Hoepfner, M.R. Wenk, J. Modregger, S. Uttenweiler-Joseph, M. Wilm, A. Nystuen, W.N. Frankel, M. Solimena, P. De Camilli, and M. Zerial. 2005. An enzymatic cascade of Rab5 effectors regulates phosphoinositide turnover in the endocytic pathway. *The Journal of cell biology*. 170:607-618.

Shisheva, A. 2008. PIKfyve: Partners, significance, debates and paradoxes. *Cell biology international*. 32:591-604.

Simonsen, A., R. Lippe, S. Christoforidis, J.M. Gaullier, A. Brech, J. Callaghan, B.H. Toh, C. Murphy, M. Zerial, and H. Stenmark. 1998. EEA1 links PI(3)K function to Rab5 regulation of endosome fusion. *Nature*. 394:494-498.

Simonsen, A., and S.A. Tooze. 2009. Coordination of membrane events during autophagy by multiple class III PI3-kinase complexes. *The Journal of cell biology*. 186:773-782.

Singh, R., S. Kaushik, Y. Wang, Y. Xiang, I. Novak, M. Komatsu, K. Tanaka, A.M. Cuervo, and M.J. Czaja. 2009. Autophagy regulates lipid metabolism. *Nature*. 458:1131-1135.

Sou, Y.S., S. Waguri, J. Iwata, T. Ueno, T. Fujimura, T. Hara, N. Sawada, A. Yamada, N. Mizushima, Y. Uchiyama, E. Kominami, K. Tanaka, and M. Komatsu. 2008. The Atg8 conjugation system is indispensable for proper development of autophagic isolation membranes in mice. *Molecular biology of the cell*. 19:4762-4775.

Spiro, D.J., W. Boll, T. Kirchhausen, and M. Wessling-Resnick. 1996. Wortmannin alters the transferrin receptor endocytic pathway in vivo and in vitro. *Molecular biology of the cell*. 7:355-367.

Stack, J.H., and S.D. Emr. 1994. Vps34p required for yeast vacuolar protein sorting is a multiple specificity kinase that exhibits both protein kinase and phosphatidylinositol-specific PI 3-kinase activities. *The Journal of biological chemistry*. 269:31552-31562.

Starai, V.J., C.M. Hickey, and W. Wickner. 2008. HOPS proofreads the trans-SNARE complex for yeast vacuole fusion. *Molecular biology of the cell*. 19:2500-2508.

Stroupe, C., K.M. Collins, R.A. Fratti, and W. Wickner. 2006. Purification of active HOPS complex reveals its affinities for phosphoinositides and the SNARE Vam7p. *The EMBO journal*. 25:1579-1589.

Sun, Q., W. Westphal, K.N. Wong, I. Tan, and Q. Zhong. 2010. Rubicon controls endosome maturation as a Rab7 effector. *Proceedings of the National Academy of Sciences of the United States of America*. 107:19338-19343.

Sun, Y., Y. Fang, M.S. Yoon, C. Zhang, M. Roccio, F.J. Zwartkruis, M. Armstrong, H.A. Brown, and J. Chen. 2008. Phospholipase D1 is an effector of Rheb in the mTOR pathway. *Proceedings of the National Academy of Sciences of the United States of America*. 105:8286-8291.

Takamura, A., M. Komatsu, T. Hara, A. Sakamoto, C. Kishi, S. Waguri, Y. Eishi, O. Hino, K. Tanaka, and N. Mizushima. 2011. Autophagy-deficient mice develop multiple liver tumors. *Genes & development*. 25:795-800.

Ullman, E., Y. Fan, M. Stawowczyk, H.M. Chen, Z. Yue, and W.X. Zong. 2008. Autophagy promotes necrosis in apoptosis-deficient cells in response to ER stress. *Cell death and differentiation*. 15:422-425.

van Weert, A.W., K.W. Dunn, H.J. Geuze, F.R. Maxfield, and W. Stoorvogel. 1995. Transport from late endosomes to lysosomes, but not sorting of integral membrane proteins in endosomes, depends on the vacuolar proton pump. *The Journal of cell biology*. 130:821-834.

Vanhaesebroeck, B., J. Guillermet-Guibert, M. Graupera, and B. Bilanges. 2010. The emerging mechanisms of isoform-specific PI3K signalling. *Nature reviews. Molecular cell biology*. 11:329-341.

Wang, T., Z. Ming, W. Xiaochun, and W. Hong. 2011. Rab7: role of its protein interaction cascades in endo-lysosomal traffic. *Cellular signalling*. 23:516-521.

Wang, X., X. Zhang, X.P. Dong, M. Samie, X. Li, X. Cheng, A. Goschka, D. Shen, Y. Zhou, J. Harlow, M.X. Zhu, D.E. Clapham, D. Ren, and H. Xu. 2012. TPC proteins are phosphoinositide- activated sodium-selective ion channels in endosomes and lysosomes. *Cell*. 151:372-383.

Webber, J.L., A.R. Young, and S.A. Tooze. 2007. Atg9 trafficking in Mammalian cells. *Autophagy*. 3:54-56.
Weidberg, H., E. Shvets, T. Shpilka, F. Shimron, V. Shinder, and Z. Elazar. 2010. LC3 and GATE-16/GABARAP subfamilies are both essential yet act differently in autophagosome biogenesis. *The EMBO journal*. 29:1792-1802.
Wiczer, B.M., and G. Thomas. 2012. Phospholipase D and mTORC1: nutrients are what bring them together. *Science signaling*. 5:pe13.
Wilke, S., J. Krausze, and K. Bussow. 2012. Crystal structure of the conserved domain of the DC lysosomal associated membrane protein: implications for the lysosomal glycocalyx. *BMC biology*. 10:62.
Willinger, T., and R.A. Flavell. 2012. Canonical autophagy dependent on the class III phosphoinositide-3 kinase Vps34 is required for naive T-cell homeostasis. *Proceedings of the National Academy of Sciences of the United States of America*. 109:8670-8675.
Woodman, P.G. 2000. Biogenesis of the sorting endosome: the role of Rab5. *Traffic*. 1:695-701.
Wu, Y.T., H.L. Tan, G. Shui, C. Bauvy, Q. Huang, M.R. Wenk, C.N. Ong, P. Codogno, and H.M. Shen. 2010. Dual role of 3-methyladenine in modulation of autophagy via different temporal patterns of inhibition on class I and III phosphoinositide 3-kinase. *The Journal of biological chemistry*. 285:10850-10861.
Yan, Y., R.J. Flinn, H. Wu, R.S. Schnur, and J.M. Backer. 2009. hVps15, but not Ca2+/CaM, is required for the activity and regulation of hVps34 in mammalian cells. *The Biochemical journal*. 417:747-755.
Yang, Z., and D.J. Klionsky. 2010. Mammalian autophagy: core molecular machinery and signaling regulation. *Current opinion in cell biology*. 22:124-131.
Yoon, M.S., G. Du, J.M. Backer, M.A. Frohman, and J. Chen. 2011. Class III PI-3-kinase activates phospholipase D in an amino acid-sensing mTORC1 pathway. *The Journal of cell biology*. 195:435-447.
Yu, L., C.K. McPhee, L. Zheng, G.A. Mardones, Y. Rong, J. Peng, N. Mi, Y. Zhao, Z. Liu, F. Wan, D.W. Hailey, V. Oorschot, J. Klumperman, E.H. Baehrecke, and M.J. Lenardo. 2010. Termination of autophagy and reformation of lysosomes regulated by mTOR. *Nature*. 465:942-946.
Yue, Z., S. Jin, C. Yang, A.J. Levine, and N. Heintz. 2003. Beclin 1, an autophagy gene essential for early embryonic development, is a haploinsufficient tumor suppressor. *Proceedings of the National Academy of Sciences of the United States of America*. 100:15077-15082.
Zaidi, N., A. Maurer, S. Nieke, and H. Kalbacher. 2008. Cathepsin D: a cellular roadmap. *Biochemical and biophysical research communications*. 376:5-9.
Zhong, Y., Q.J. Wang, X. Li, Y. Yan, J.M. Backer, B.T. Chait, N. Heintz, and Z. Yue. 2009. Distinct regulation of autophagic activity by Atg14L and Rubicon associated with Beclin 1-phosphatidylinositol-3-kinase complex. *Nature cell biology*. 11:468-476.
Zhou, X., J. Takatoh, and F. Wang. 2011. The mammalian class 3 PI3K (PIK3C3) is required for early embryogenesis and cell proliferation. *PloS one*. 6:e16358.
Zhou, X., L. Wang, H. Hasegawa, P. Amin, B.X. Han, S. Kaneko, Y. He, and F. Wang. 2010. Deletion of PIK3C3/Vps34 in sensory neurons causes rapid neurodegeneration by disrupting the endosomal but not the autophagic pathway. *Proceedings of the National Academy of Sciences of the United States of America*. 107:9424-9429.

Zoncu, R., L. Bar-Peled, A. Efeyan, S. Wang, Y. Sancak, and D.M. Sabatini. 2011. mTORC1 senses lysosomal amino acids through an inside-out mechanism that requires the vacuolar H(+)-ATPase. *Science*. 334:678-683.